AD

USAAVLABS TECHNICAL REPORT 66-62

MICROMECHANICAL BEHAVIOR OF FIBER REINFORCED PLASTICS

By

Juan Haener

September 1966

U. S. ARMY AVIATION MATERIEL LABORATORIES
FORT EUSTIS, VIRGINIA

CONTRACT DA 44-177-AMC-320(T)
WHITTAKER CORPORATION
SAN DIEGO, CALIFORNIA

U S ARMY MATERIEL COMMAND

Disclaimers

The findings in this report are not to be construed as an official Department of the Army position unless so designated by other authorized documents.

When Government drawings, specifications, or other data are used for any purpose other than in connection with a definitely related Government procurement operation, the United States Government thereby incurs no responsibility nor any obligation whatsoever; and the fact that the Government may have formulated, furnished, or in any way supplied the said drawings, specifications, or other data is not to be regarded by implication or otherwise as in any manner licensing the holder or any other person or corporation, or conveying any rights or permission, to manufacture, use, or sell any patented invention that may in any way be related thereto.

Trade names cited in this report do not constitute an official endorsement or approval of the use of such commercial hardware or software.

Disposition Instructions

Destroy this report when no longer needed. Do not return it to originator.

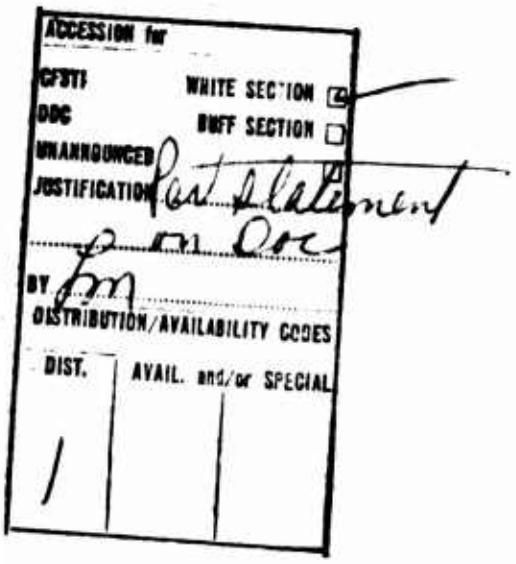

DEPARTMENT OF THE ARMY
U. S. ARMY AVIATION MATERIEL LABORATORIES
FORT EUSTIS, VIRGINIA 23604

This program was carried out under Contract DA 44-177-AMC-320(T) with Whittaker Corporation, Narmco Research and Development Division.

The data contained in this report are the result of research conducted to determine the mechanism of load transfer through a composite material consisting of fibers embedded in a matrix under consideration of internal stresses caused by polymerization and temperature shrinkage of the matrix as well as externally imposed loads.

The report has been reviewed by the U.S. Army Aviation Materiel Laboratories and is considered to be technically sound. It is published for the exchange of information and the stimulation of future research.

Project 1P121401A14176
Contract DA 44-177-AMC-320(T)
USAAVLABS Technical Report 66-62
September 1966

MICROMECHANICAL BEHAVIOR OF FIBER REINFORCED PLASTICS

Final Report

by

Juan Haener

Prepared by
WHITTAKER CORPORATION
Narmco Research & Development Division
San Diego, California

for

U.S. ARMY AVIATION MATERIEL LABORATORIES
FORT EUSTIS, VIRGINIA

Distribution of this document is unlimited

ABSTRACT

The distribution of stresses in a unidirectionally oriented, multi-fiber composite as a result of process shrinkage and external loads has been analyzed after assuming continuity boundary conditions at the interface and certain hexagonal boundary conditions in the space between the reinforcements. Selected model specimens have been numerically analyzed by computer, and the results have been compared with photoelastic experimental studies.

FOREWORD

This report was prepared by Whittaker Corporation, Narmco Research & Development Division, San Diego, California, under Contract DA 44-177-AMC-320(T), entitled "Micromechanical Behavior of Fiber Reinforced Plastics." The work was accomplished under the technical supervision of Dr. R. Echols, Chief, Physical Sciences Laboratories Division, US Army Aviation Materiel Laboratories (USAAVLABS), Fort Eustis, Virginia.

This report covers work conducted from 14 June 1965 to 14 May 1966.

The principal technical investigator on this project was Dr. Juan Haener. Dr. Gerhard Nowak contributed as a consultant, and Dr. George Burgin was responsible for computer work. Other contributors to this program were Messrs. Krishna Naik, Ming-Yuan Feng, Noel Ashbaugh, and Curt Thompson. The program was conducted by Narmco's Engineering Department under the supervision of Mr. B. L. Duft, Engineering Department Manager. The program management responsibility resided with Mr. B. Levenetz, Research Engineering, and the administrative responsibility with Mr. R. Hidde, Project Engineering.

BLANK PAGE

TABLE OF CONTENTS

LIST OF ILLUSTRATIONS

LIST OF ILLUSTRATIONS (Continued)

LIST OF SYMBOLS

a_o, a	radius of fiber before and after stress develops respectively
A, A_i	constants
b_o, b	radius of resin cylinder in the single-fiber model before and after stress develops
B_i, B_{ik}	constants
$2C_o$	distance of the fibers in the multifiber model before shrinkage
C_i	constants
D_i	constants
D_{ij}, D^{ij}	physical components of the strain tensor
D_{kk}, D_{ii}	volumetric change, or dilation, or trace of the strain tensor
E	Young's modulus of elasticity
F	functions defined in (A100) to (A119) Appendix A
I_n	modified Bessel function of n^{th} order and first kind
J_n	Bessel function of n^{th} order and first kind
k	integers
K_n	modified Bessel function of n^{th} order and second kind
$2\ell_o$	length of specimen before stress develops
2ℓ	length after shrinkage
m	integers, eigenvalues

LIST OF SYMBOLS (Continued)

n	integers, eigenvalues
P_i	Papkovitch potentials in cylindrical coordinates
$\overline{P}_i$	Papkovitch potentials in rectangular coordinates
q	index referring to q^{th} eigenvalue
r	cylindrical coordinate in the radial direction
t	time
T	temperature
u_j	general Cartesian coordinates of original position of particles
x_i	Cartesian coordinates in direction i
X_k	body forces
Y_n	Neumann functions of n^{th} order; Bessel function of second kind
Z, z	cylindrical coordinates in axial direction
α^I, α^{II}	coefficients of thermal expansion of reinforcement and matrix respectively
α_{nk}	constants
β^I, β^{II}	coefficient of shrinkage of reinforcements and matrix, respectively
γ_{nk}	integration constants
δ_{ij}	Kronecker delta
δ_{nk}	integration constants
ϵ	total shrinkage of a composite

LIST OF SYMBOLS (Continued)

ϵ_{nk}	integration constants
λ_{nk}	eigenvalue
μ_{nk}	eigenvalues connected with the boundary of the hexagon
ν	Poisson's ratio
ξ_i	displacements in direction i
ρ	mass per volume
σ_{ij}	stress tensor component
$\sigma(\ell)$	stress at $Z = \ell$
σ_{11}	stress in radial direction
σ_{12}, σ_{32}	shear in tangential direction
σ_{13}, σ_{23}	shear in axial direction
σ_{21}, σ_{31}	shear in radial direction
σ_{22}	stress in tangential direction
σ_{33}	stress in axial direction
φ	cylindrical coordinate
Φ	potential function
∇	Laplace operator
L	Love functions

LIST OF SYMBOLS (Continued)

Superscripts

I	refers to reinforcement
II	refers to matrix

Subscripts

i,j,k,ℓ,r, or s	free index

BLANK PAGE

SUMMARY

This program was initiated as a continuation of analytical research on composite materials which had been reported in USAAVLABS Technical Report 65-58. The objective is to improve the understanding of the mechanism of load transfer through the composite material consisting of fibers embedded in a matrix under consideration of internal stresses caused by polymerization and temperature shrinkage of the matrix as well as externally imposed loads. It is anticipated that this research will lead to more reliable methods of predicting mechanical behavior of fiber reinforced plastic composites under load in order that the structural integrity of airframe components from this material can be improved.

During the program reported here, the boundary conditions at the interface and at the hexagon boundary have been analytically investigated and a tridimensional stress and strain analysis on a unidirectionally oriented multifiber bundle has been performed. The developed analytical expressions have been checked on a special case of a single fiber and then applied to analyze the distribution of stresses within a multifiber composite. The solutions were checked by computer analysis, which also provided numerical results for stress distribution in selected model specimens. The analytical work has been compared with results of microphotoelastic studies conducted on similar experimental model specimens.

INTRODUCTION

The high strength-to-weight ratio of oriented-filament composites can be most fully realized only if the optimization of these materials is based on accurate stress analysis. Test results have shown that present stress equations do not accurately reflect the true stress-strain distribution in matrices reinforced with oriented filaments. At present, there is incomplete understanding of the three-dimensional mechanical load transfer between reinforcements and matrix in a composite subjected to externally imposed stresses combined with internal residual stresses. The influence of these combined stress conditions on composite characteristics must be resolved by these fundamental steps:

1. Study of the solutions to the differential equations of distortions

2. Expression of the physical problem in terms of restricted numbers of these solutions

3. Examination of mathematical implications of the solutions

4. Comparison of the solutions with test results

5. Derivation of practical design formulas from the theoretical solutions

During the process of the previous contract [DA 44-177-AMC-208(T)], mathematical relationships were derived for a single fiber embedded in a resin cylinder for the case of shrinkage and static loading with general boundary conditions. Efforts on the multifiber case have led to the point of obtaining solutions to the differential equations; however, boundary conditions which would relegate these solutions to a specific physical problem were not yet applied.

During the present contract, the general boundary conditions have been specialized to correspond with the experimental specimens. This provided the possibility of programming the equations for a computer analysis and of obtaining numerical results for stress distribution within the composite models.

The question of so-called "potentials" present in the anaysis of the multifiber case has also been resolved. The solutions of the short and very long multifiber case have been obtained in three dimensions. They have been programmed for the very long fiber bundle.

As a special case of the multifiber problem, the stress distributions for the single-fiber problem have been established for any fiber length.

Because the theoretical analysis is applicable for any combination of elastic properties of the constituent materials, specific properties which correspond to those of the selected specimen materials have been used in the computer analysis to establish the diagrams for stress distributions. This now makes it possible to relate the theoretical results with results of the microphotoelastic studies.

TECHNICAL DISCUSSION

METHOD OF APPROACH

There are two generally known methods for reducing the fifteen linear field equations. One method leads to three equations for the displacements

$$\nabla^2 \xi_i + \frac{1}{1 - 2\nu} \frac{\partial^2 \xi_j}{\partial x_i \partial x_j} + \frac{X_i}{G} = \frac{\rho}{G} \frac{\partial^2 \xi_i}{\partial t^2} \qquad (1)$$

$$i = 1,2,3$$

$$j = 1,2,3$$

and the other leads to six equations for stresses.

In the present work, the displacement method expressed in equation (1) was utilized. This equation covers completely the linear three-dimensional elastomechanics, including the mechanics of elastic wave propagations (References 1 through 5).

One of the reasons for this decision was the existence of extensive literature (chapters on basic equations in References 1 through 5) showing how facts must be arranged to obtain solutions in terms of a restricted number of elementary solutions. Further, it was believed that the obtained solutions of the displacement equations for the static case can later be more readily extended for dynamic considerations such as acoustical and shock-wave propagation (Reference 4) than it would be by utilization of stress equations.

Another reason for selecting the approach of displacement functions was that in three-dimensional elasticity, this approach is the only one that has been used effectively in obtaining solutions of practical problems.

For the static case and by neglecting the body forces and assuming rectangular coordinates, the equation for displacements becomes

$$\nabla^2 \nabla^2 \bar{\xi}_i = 0 . \qquad (2)$$

There are two classical approaches often used (see Reference 2) to find expressions for displacement and stresses from equation (2): the Galerkin-Westergaard approach and that of Boussinesg-Papkovitch and Neuber. Here, the second method was selected, because the stresses appear as second and not as third derivatives of a potential P defined as Papkovitch functions. This fact facilitates considerably the transformation into cylindrical coordinates as well as the numerical calculations.

The displacements expressed in Papkovitch functions are

$$\bar{\xi}_i = \bar{P}_i - \frac{1}{4(1-\nu)} \frac{\partial}{\partial x_i} \left(x_j \bar{P}_j + \bar{P}_o \right) \qquad (3)$$

$$i = 1,2,3$$

$$j = 1,2,3 .$$

The four Papkovitch potentials in equation (3) are solutions of the harmonic equations.

$$\nabla^2 \bar{P}_i = 0 \qquad i = 0,1,2,3 . \qquad (4)$$

The completeness of the Papkovitch functions is shown in Reference (6) and also in Reference (2).

Transformation of the equations into cylindrical coordinates, a process which is shown in Appendix A, equations (A1) through (A25), enables us to express the internal elastic condition in the composite. Without going into further details of transforming the basic equations, (1) and (2), and equation (4), we transform directly the solutions $\bar{\xi}_i$ and the $\bar{P}_i$ into cylindrical coordinates, obtaining

$$P_j(r,\phi,z) = \sum_{n=0}^{\infty} \left\{ \sum_{k=1}^{\infty} \left[\alpha_{jnk} J_n(\mu_{nk} r) + \beta_{jnk} Y_n(\mu_{nk} r) \right] \left[\gamma_{jnk} \sinh(\mu_{nk} z) + \delta_{jnk} \cosh(\mu_{nk} z) \right] \right\} \cdot \left[\epsilon_{jn} \sin(n\phi) + \zeta_n \cos(n\phi) \right] +$$

$$+ \sum_{n=0}^{\infty} \left[\alpha_{jno} r^{n} + \beta_{jno} r^{-n}\right] \cdot \left[\gamma_{jno} + \delta_{jno} z\right] \cdot \left[\epsilon_{jn} \sin(n\phi) + \zeta_{jn} \cos(n\phi)\right] +$$

$$\left[\alpha_{joo} + \beta_{joo} \log r\right] \cdot \left[\gamma_{joo} + \delta_{joo} z\right] \qquad (5)$$

$$j = 1,2,3,0$$

Equation (5) represents three Papkovitch functions for each of the two materials with 36 constants in total. Introducing equation (5) into equation (3) and after transforming (3), we obtain for the displacements (see equations (A60) through (A76) in Appendix A):

in radial direction,

$$\xi_1 = P_1 - \frac{1}{4(1 - \nu)} \frac{\partial}{\partial r} \left[r P_1 + z P_3 + P_0\right]; \qquad (6)$$

in tangential direction,

$$\xi_2 = P_2 - \frac{1}{4(1 - \nu)} \frac{1}{r} \frac{\partial}{\partial \phi} \left[r P_1 + z P_3 + P_0\right]; \qquad (7)$$

in axial direction,

$$\xi_3 = P_3 - \frac{1}{4(1 - \nu)} \frac{\partial}{\partial z} \left[r P_1 + z P_3 + P_0\right]. \qquad (8)$$

The stress distribution from strain components is given by the physical components of the stress tensor.

$$\sigma_{ij} = \frac{E}{1 + \nu} \left\{ D_{ij} + \delta_{ij} \left(\frac{\nu}{1 - 2\nu} D_{kk} - \frac{1 + \nu}{1 - 2\nu} \left[\alpha T + \beta\right] \right) \right\} \qquad (9)$$

Here D_{ij} are the elements of the strain tensor in cylindrical coordinates and are restated as follows:

$$D_{11} = \frac{\partial \xi_1}{\partial r} \qquad (10)$$

$$D_{22} = \frac{1}{r}\left[\xi_1 + \frac{\partial \xi_2}{\partial \phi}\right] \tag{11}$$

$$D_{33} = \frac{\partial \xi_3}{\partial z} \tag{12}$$

$$D_{12} = \frac{1}{2}\left[\frac{1}{r}\frac{\partial \xi_1}{\partial \phi} + \frac{\partial \xi_2}{\partial r} - \frac{1}{r}\xi_2\right] \tag{13}$$

$$D_{23} = \frac{1}{2}\left[\frac{\partial \xi_2}{\partial z} + \frac{1}{r}\frac{\partial \xi_3}{\partial \phi}\right] \tag{14}$$

$$D_{31} = \frac{1}{2}\left[\frac{\partial \xi_3}{\partial r} + \frac{\partial \xi_1}{\partial z}\right]. \tag{15}$$

The stresses can be represented and calculated directly from the Papkovitch potentials through the following relation:

$$\sigma_{ij} = G\left(\frac{\partial}{\partial x_j} P_i + \frac{\partial}{\partial x_i} P_j\right) + \frac{G}{2(1-\nu)}\left[\left(\delta_{ij}\nu \nabla^2 - \frac{\partial^2}{\partial x_i \partial x_j}\right)\left(X_k P_k + P_o\right)\right] \tag{16}$$

$$i = 1,2,3 \quad j = 1,2,3 \quad k = 1,2,3.$$

Equations (5) through (16) are general, and they are valid in the reinforcement as well as in the matrix. After adaptation to the boundary conditions, the functions and constants will have superscripts I and II for fiber and resin respectively.

For the present purpose, equation (16) has to be transformed into cylindrical coordinates (Appendix A, equations (A1) through (A16)).

BOUNDARY CONDITIONS AT THE INTERFACE

A set of conditions results from the assumption that, at the fiber-matrix interface, two neighboring particles of the two materials remain

together during all displacements and that the total shrinkage of the matrix is greater than that of the fiber. Under chis condition, stresses will develop in both materials, depending on the definition of the displacement.

It was further assumed that the stress perpendicular to the interface and the shear stresses at the interface are continuous.

There are two possibilities for consideration of shrinkage. For explanation, one cylindrical fiber in a matrix cylinder shall be considered (Figure 1). As a first possibility, it is possible to describe the displacement with reference to the free shrunken position, where one material would shrink as if the other were not present; then the displacement of a point P at the interface would be in Figure 1 the vector $\overrightarrow{P_{II}\,P} = \xi^{II}$ and $\overrightarrow{P_I\,P} = \xi^I$ for material II and I respectively. In this case, the term β in equation (9) should be omitted. The second possibility is to define the vector $\overrightarrow{P_o\,P} = \xi^{II} = \xi^I$ as displacement at the interface. The second procedure is easier to use because in the first method the establishing of directional signs for forces and displacements and the two floating reference systems present major problems. In equations (A131) through (A135), it is shown that both methods yield the same results.

In total, the following boundary conditions have been assumed at the interface:

Displacements:

$$\xi_i^I(a,\phi,z) = \xi_i^{II}(a,\phi,z) \qquad i = 1,2,3 \tag{17}$$

Stresses:

$$\sigma_{1\,j}^I(a,\phi,z) = \sigma_{1\,j}^{II}(a,\phi,z) \qquad j = 1,2,3. \tag{18}$$

GEOMETRIC BOUNDARY CONDITIONS AT THE FIBER HEXAGON

Referring to Figure 2, it can be assumed for reasons of symmetry that the hexagonals will preserve their regular geometry during the shrinkage and axial loading process.

Therefore, the boundary condition will be

$$\xi_1^{II}\left(\frac{C_o}{\cos\phi}\,,\,\phi\,,\,z\right)\cos\phi - \xi_2^{II}\left(\frac{C_o}{\cos\phi}\,,\,\phi\,,\,z\right)\sin\phi = \epsilon \tag{19}$$

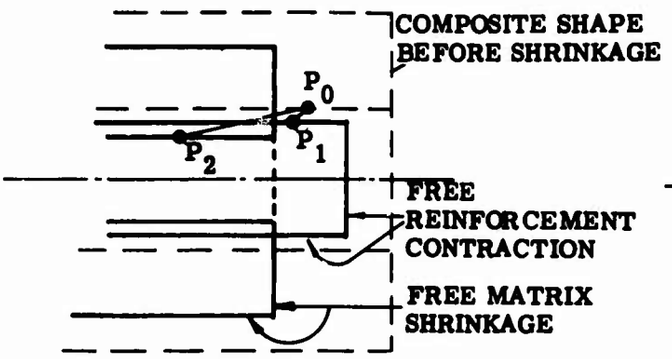

(a) Diagram Depicting Components Before and After Independent Shrinkage

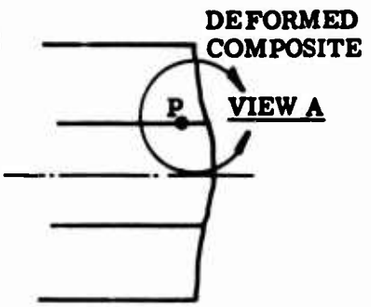

(b) Composite Shape Resulting from Combined Shrinkage

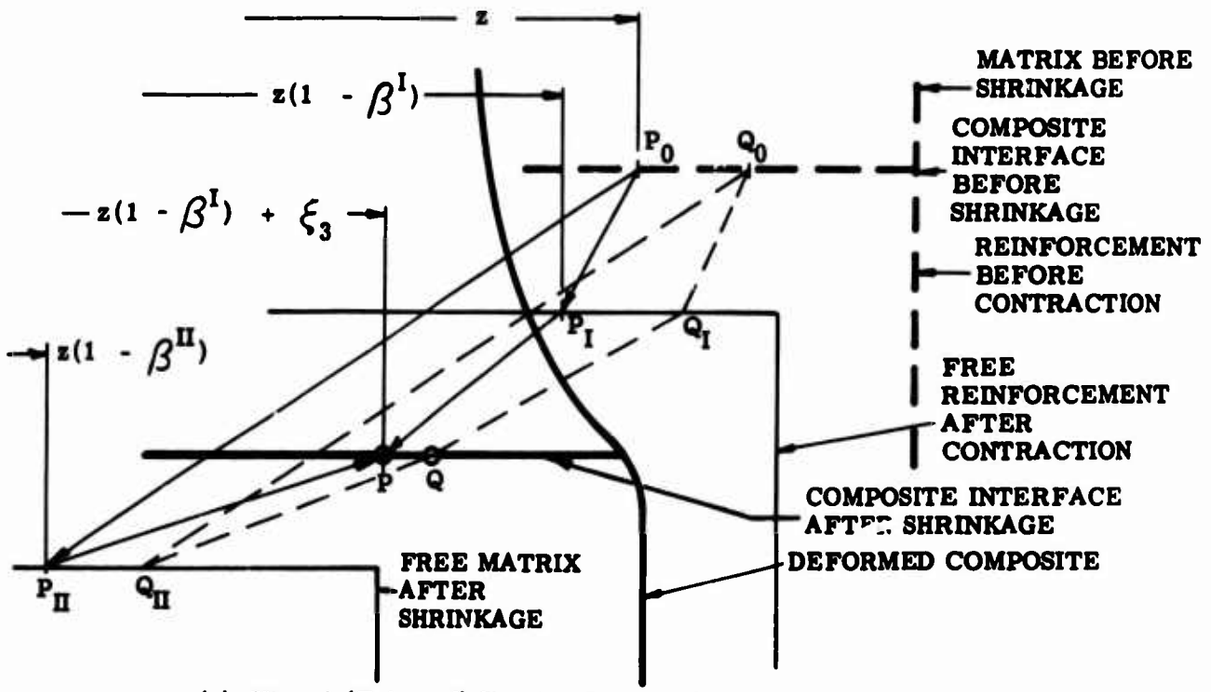

(c) View A (Enlarged) Showing Combined Shrinkage in Relation to Independent Shrinkage of Both Materials

Figure 1. Reinforcement Cylinder Embedded in Hollow Matrix Cylinder

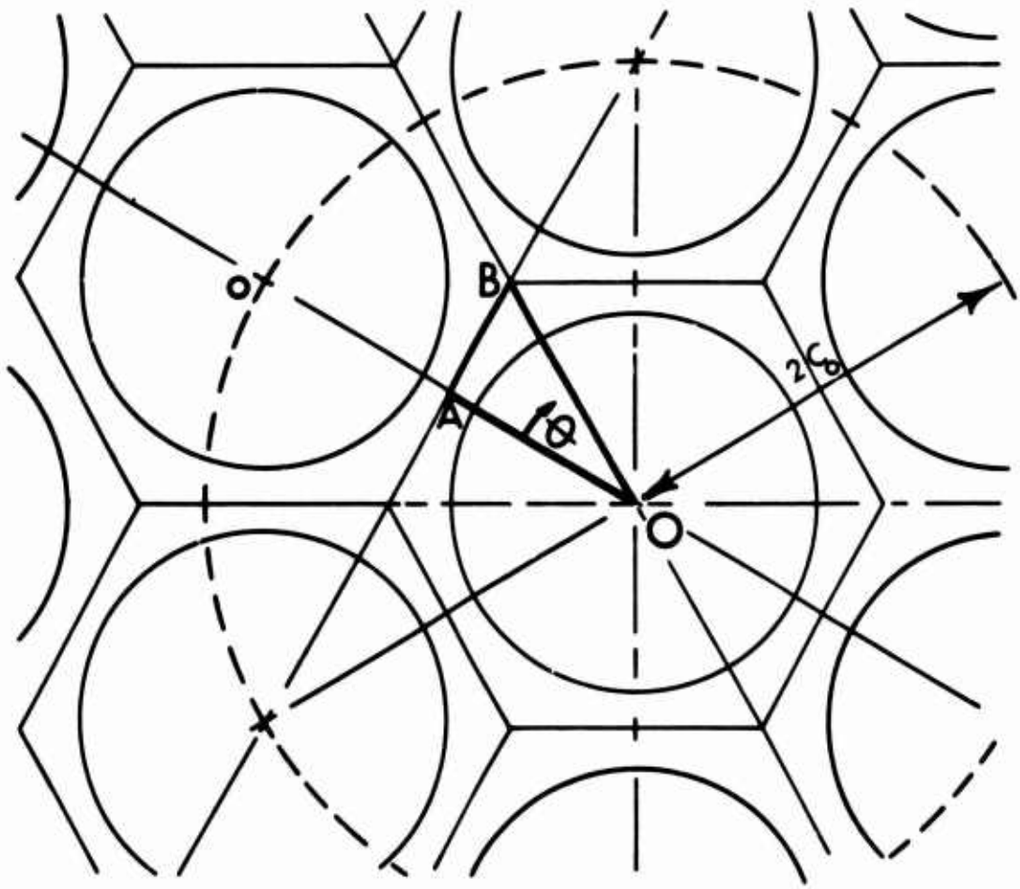

Figure 2. Multifiber Composite Model

where C_o is half the distance between two fibers before contraction and ϵ is the total shrinkage of the composite. For comparison with the left-hand side, the right-hand side in equation (19) has to be represented by a double Fourier series given in detail in equations (A77) through (A93).

In order that the fibers remain in the hexagonal arrangement, the tangential displacements at the lines OA and OB have to be zero, so that

$$\xi_2^{I,II}(r,0,z) = 0 \tag{20}$$

$$\xi_2^{I,II}\left(r,\frac{\pi}{6},z\right) = 0 . \tag{21}$$

Another geometric condition comes from the fact that the displacements (and stresses) are identical for every multiple of $\pi/3$ of the variable ϕ, so that in equation (5) the eigenvalue must be a multiple of 6:

$$n = 0, 6, 12, 18, \text{etc.} \tag{22}$$

To satisfy the boundary condition at the hexagon, which is a function of z and ϕ, it is necessary to have the solutions ξ represented in orthogonal functions of z and ϕ. Therefore, we let equation (5) become

$$\mu_k = \frac{ik\pi}{2\ell} \qquad k = 1, 3, 5, 7 \ldots \tag{23}$$

The general path of the function ξ_j is imposed by the geometry consideration of equations (A21) through (A23), which express the following:

$$\left.\begin{aligned} &\xi_1 \text{ is even in } \phi \text{ and even in } z ; \\ &\xi_2 \text{ is odd in } \phi \text{ and even in } z ; \\ &\xi_3 \text{ is even in } \phi \text{ and odd in } z . \end{aligned}\right\} \tag{24}$$

In order to repeat six times in 2π, the periodic characteristic implies that

$$\xi_i(r,\phi,z) = \xi_i\left(r,\phi+\frac{\pi}{3},z\right) . \tag{25}$$

Since the stresses are derived from the displacement vector by derivations (equations 9 through 15), they also repeat six times in 2π period (equations A24 through A27).

For computing the shrinkage alone (A40) without external loads, the boundary condition at the two ends is

$$\sigma_{33}^{I}(r,\phi,\pm\ell) = \sigma_{33}^{II}(r,\phi,\pm\ell) = 0 . \qquad (26)$$

The integration constants and the eigenvalues for μ_k are derived from equations (A44) through (A58).

The results of the multifiber case show that for the eigenvalue $n = 0$ the stresses are constant with ϕ, while for $n \neq 0$ the stresses repeat six times in 360 degrees.

SPECIAL CASE OF A SINGLE-FIBER MODEL

In the case of a cylindrical filament centrally embedded in a matrix cylinder, the potentials expressed in equation (5) degenerate into functions independent of ϕ (Reference 7, page 41-2).

The solutions of displacements and stresses due to differential contractions of the two constituents are given in Appendix B, equations (B8) through (B13).

For the axially loaded specimen, the displacement and stresses are given in Appendix B, equations (B48) through (B53). The total stress and the displacements in the composite are obtained by superposition of values from both cases.

The eigenvalues for the shrinkage case are determined by the boundary condition at the two ends, where, for the single-fiber specimen, equation (26) becomes

$$\sigma_{33}^{I}(r,\ell) = \sigma_{33}^{II}(r,\ell) = 0 . \qquad (27)$$

The only condition that makes the solution for the shrinkage case nontrivial is

$$\cos(k\ell) = 0 . \qquad (28)$$

This implies that

$$k\ell = \frac{n\pi}{2} \quad , \quad n = \pm 1 \, , \pm 3 \, , \pm 5 \, , \ldots \tag{29}$$

$$k = \frac{n\pi}{2\ell} \quad , \quad n = 1 \, , 3 \, , 5 \, , \ldots \tag{30}$$

The eigenvalues for the axially loaded single-fiber composite are determined from the boundary condition at the free cylindrical surface:

$$\sigma_{11}^{II}(b,z) = 0 \, . \tag{31}$$

The only condition that makes the solution of the loaded case nontrivial is

$$\mu_k b \, J_o\left(\mu_k b\right) - J_1\left(\mu_k b\right) = 0 \, . \tag{32}$$

The computed first six eigenvalues are

$$b\mu_k = 1.8411 \; ; \; 5.3314 \; ; \; 8.5363 \; ; \; 1.7060$$
$$14.8635 \; ; \; 18.0155 \; ; \; 21.1643 \; ; \; 24.3113 \, .$$

The boundary conditions at the interface of a single-fiber composite are the same as expressed by equations (17) and (18) but are not ϕ dependent.

NUMERICAL RESULTS

A single-fiber model loaded at the resin as shown in Figure 3 produces axial stresses in the fiber which are computed to be 25 times higher than the externally imposed stresses.

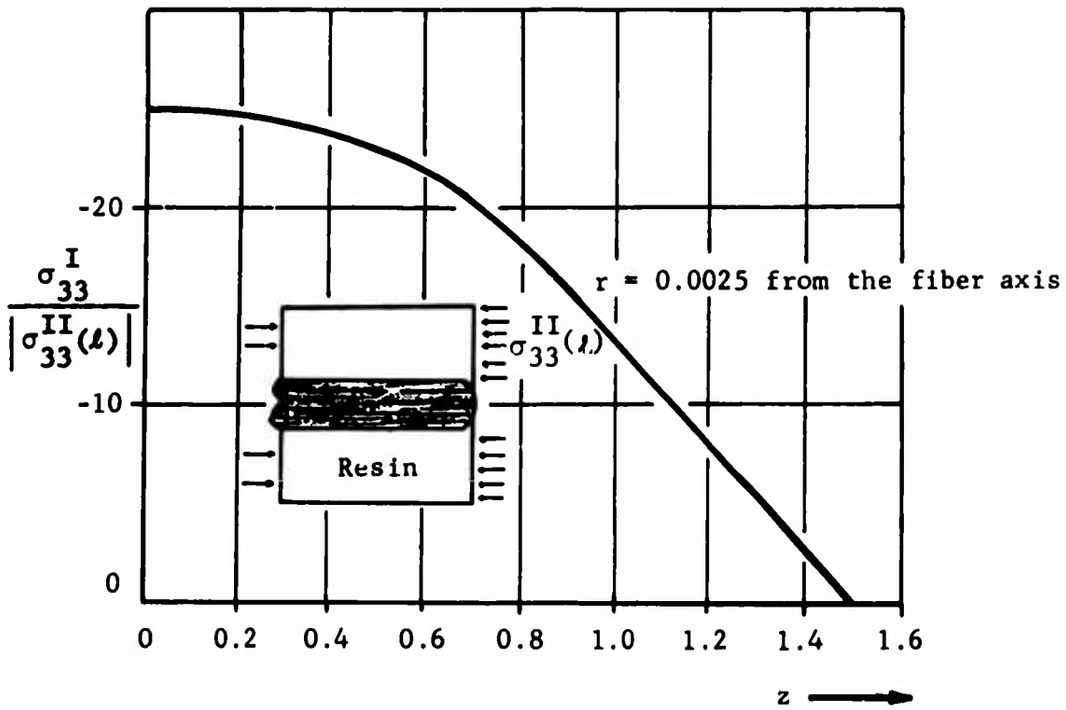

Figure 3. Axial Stress in the Fiber Produced by Load at the Resin End z = 1.5 inches (Single-fiber composite)

The following values were used in the equations of Appendix B:

E^{I} = 10×10^{6} psi (glass fiber)

E^{II} = 0.436×10^{6} psi (epoxy matrix)

ν^{I} = 0.20 (Poisson's ratio for glass)

ν^{II} = 0.35 (Poisson's ratio for resin)

a_o = 0.005 inch (fiber radius)

b_o = 0.6875 inch (resin cylinder radius)

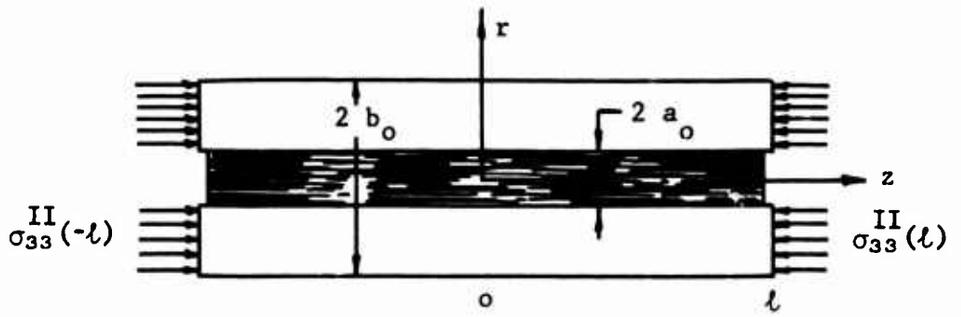

The shear stress σ_{13}^{I} decreases with distance from the load and becomes zero at the half length ($z = 0$, see Figure 4). The axial shear stress in the resin σ_{13}^{II} (see Figure 5) is a function similar to σ_{13}^{I}.

The radial stress in the resin σ_{11}^{II} is shown in Figure 6.

The tangential stress in the resin σ_{22}^{II} increases with z and decreases with r (see Figure 7). The tangential and radial stresses in the fiber σ_{22}^{I} and σ_{11}^{I} respectively are equal and constant for a certain cross section and increase with z (see Figure 8).

Shrinkage stresses due to differential shrinkage in the same specimen as above result in apparently undulated stress distribution (see Figure 9), which is more pronounced in a specimen with a very high resin content. A specimen with a thin resin coat of a thickness of 0.0025 inch was also computed. Here, the computer results indicated no undulation of stresses.

The multifiber problem equations given in Appendix A were programmed for an infinite fiber bundle. The numerical results show that the influence of the solution with the eigenvalue $n = 0$, Appendix A, equations (A96) through (A99), disappears at the interface at a certain total shrinkage ϵ of the composite and becomes a maximum at $\epsilon = 0$. It should be pointed out that ϵ is not identical with β^{II}, the resin shrinkage. If $\epsilon = 0$, it would mean that the total composite shrinkage is prevented for some external reasons (cross fibers, fiber contacts, etc.). This would produce very high tension stresses in the resin. In case the fibers touch each other, the total shrinkage ϵ would become almost zero and the shrinkage stress due to β^{II} would be higher.

The greater the total shrinkage ϵ becomes, the more effective will be the solutions for $n \neq 0$. The $n \neq 0$ solutions are ϕ-dependent and repeat themselves six times within 2π. The total solutions are, of course, the sum of both solutions. To indicate the influence of both solutions, Figure 10 shows at the left (a) the stress generated by the $n = 0$ solution as a function of the total shrinkage ϵ.

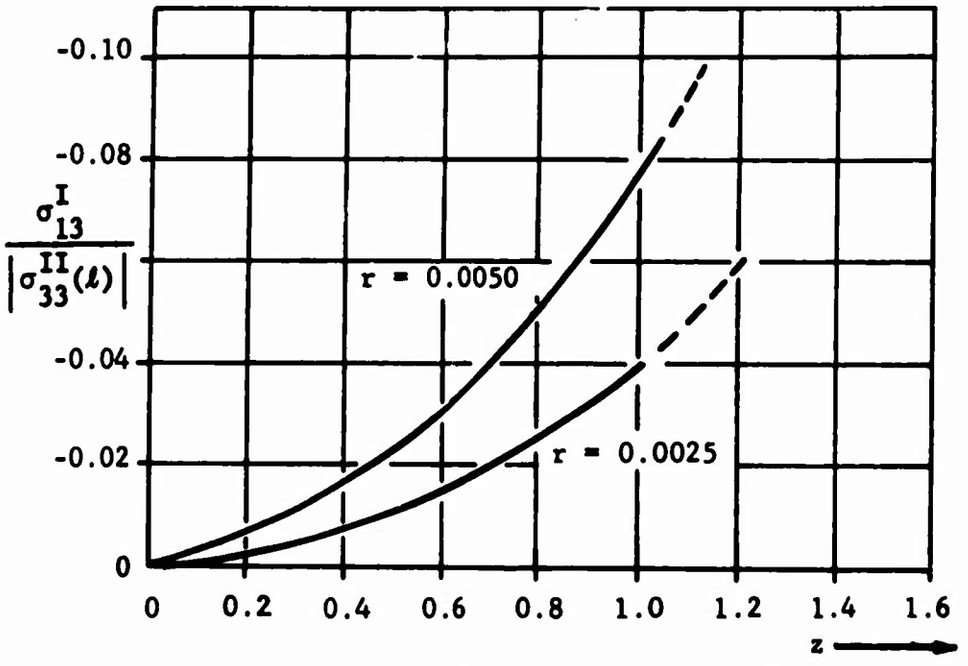

Figure 4. Axial Shear σ_{13} in the Fiber Produced by Load at the Resin End
z = 1.5 inches

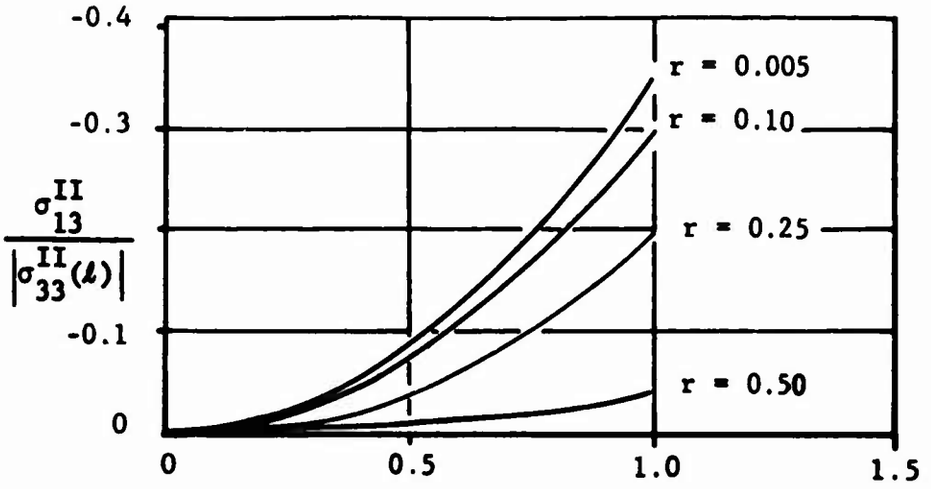

Figure 5. Axial Shear Stress in the Resin Produced by Axial Load at the Resin End z = 1.5 inches

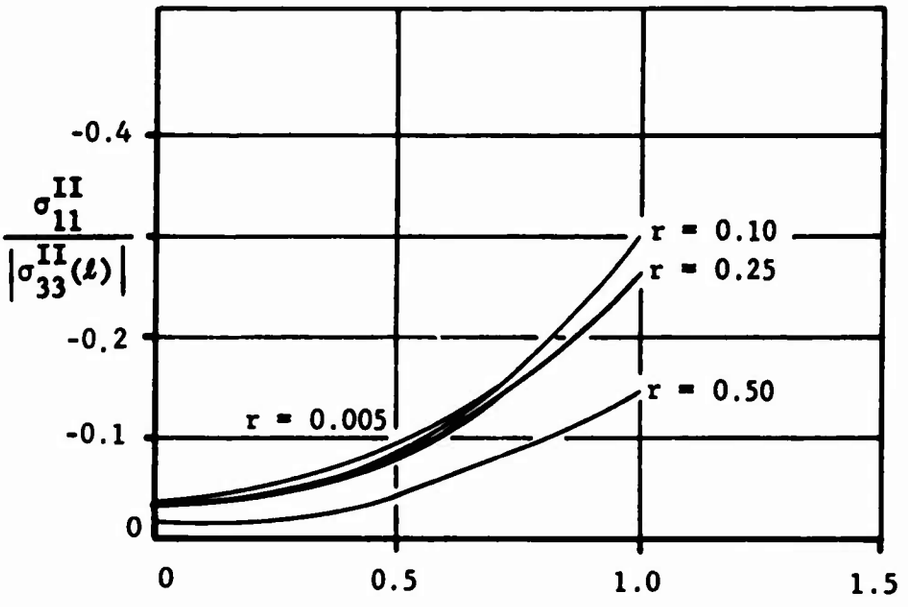

Figure 6. Radial Stress in the Resin Produced by Axial Load at the Resin End z = 1.5 inches

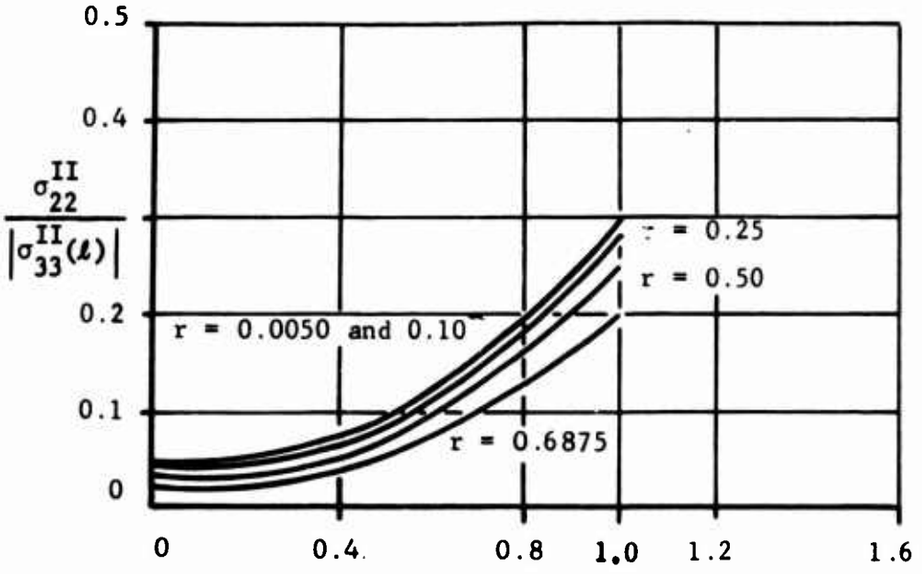

Figure 7. Tangential Stress in the Resin Produced by Load $\sigma_{33}^{II}(\ell)$ at the Resin End z = 1.5 inches
(single-fiber composite)

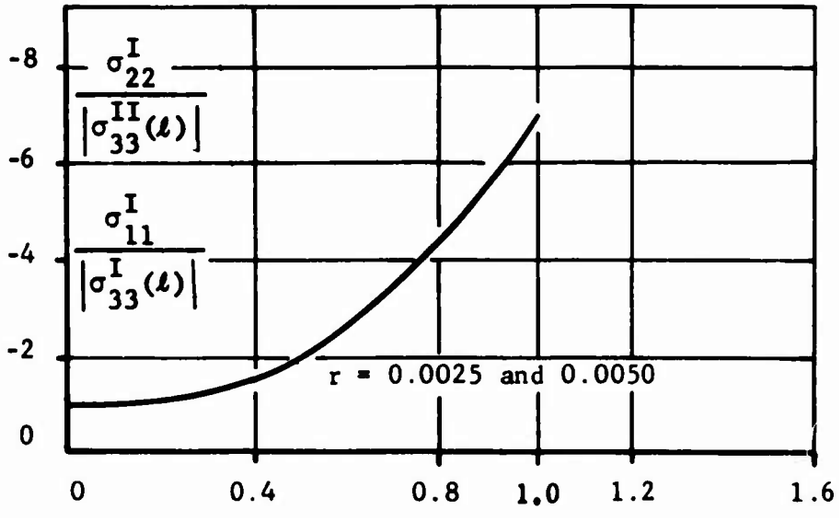

Figure 8. Tangential and Radial Stress in the Fiber Produced by Axial Load at the Resin End z = 1.5 inches
(single-fiber composite)

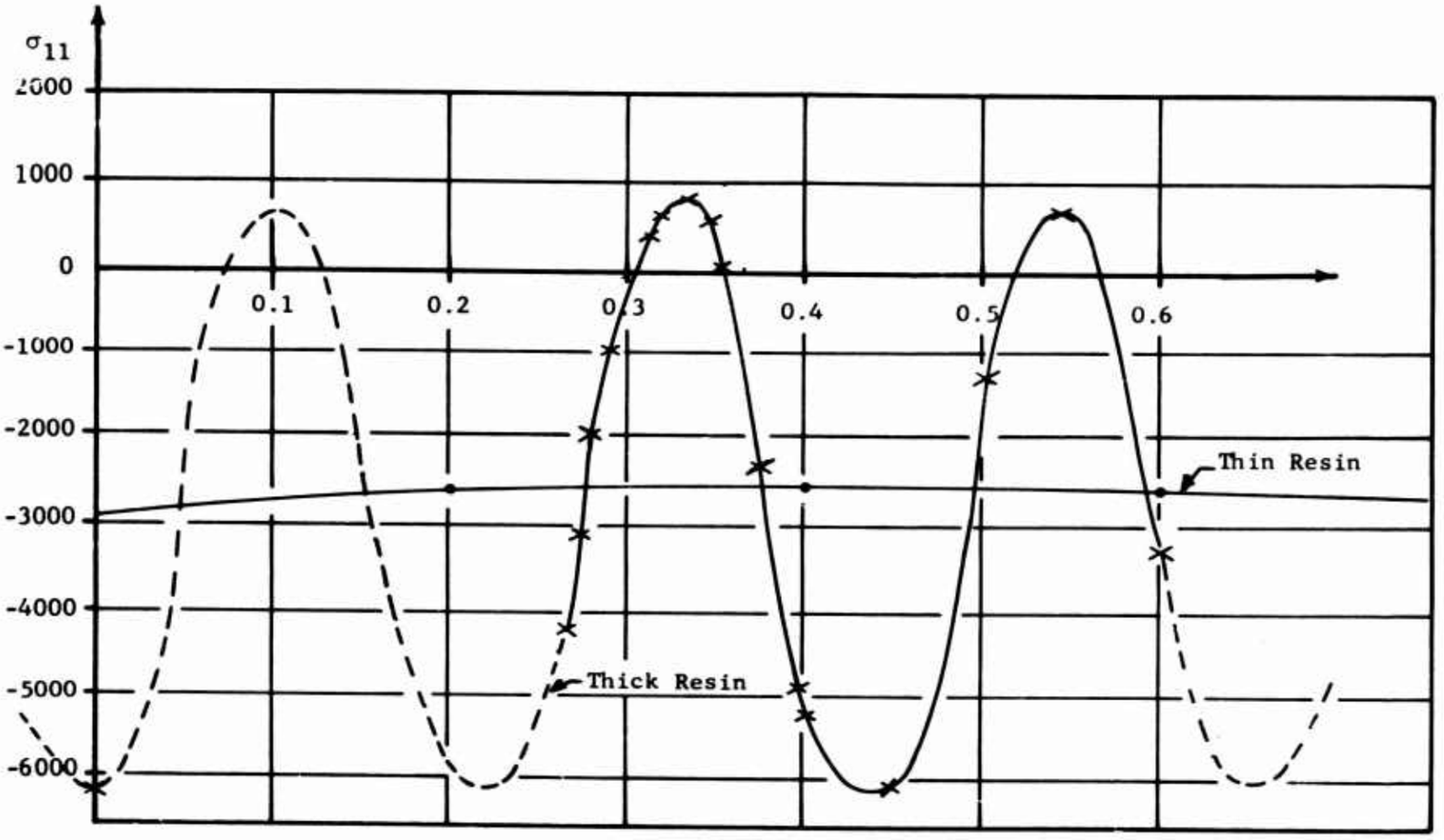

Figure 9. Shrinkage Stress in Radial Direction at the Interface r = 0.005 inch

Thin resin radius b_o = 0.0100
Thick resin radius b_o = 0.6875

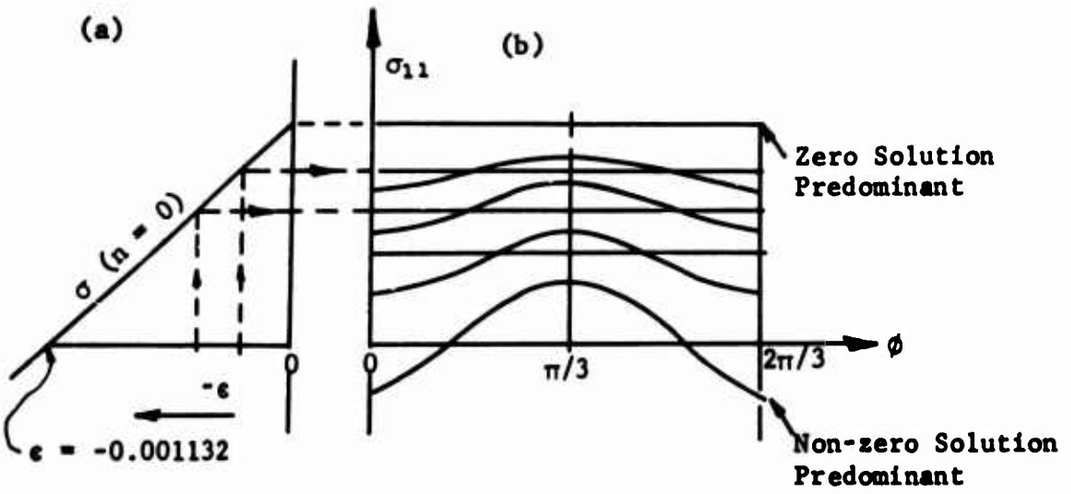

Figure 10. Shrinkage Stresses in Radial Direction as a Function of Total Shrinkage

At the right side (b) of Figure 10 is the sum of the $n = 0$ and $n \neq 0$ stresses as a function of ϕ. If the total shrinkage is not prevented and the total shrinkage ϵ assumes a certain value (in the case of epoxy and glass, -0.001132), then the non-zero solution is the only one which generates stresses at the interface. These stresses are recurring every 60°. The stress distributions around the fibers are very sensitive with respect to the total composite shrinkage ϵ. An additional equation or condition to circumvent or determine ϵ analytically would be very advantageous. In the search for an additional equation, we find that at the hexagonal boundary, the following conditions exist:

$$\int_0^{\pi/6} \left[\frac{1}{2} \left(\sigma_{11}^{II} + \sigma_{22}^{II} \right) + \frac{1}{2} \left(\sigma_{11}^{II} - \sigma_{22}^{II} \right) \cos 2\phi - \sigma_{12}^{II} \sin 2\phi \right] d\phi = 0$$

$$\sigma(r,\phi,z) = \sigma\left(\frac{C_o}{\cos\phi} , \phi , z \right) . \qquad (33)$$

If the correct ϵ is chosen, the conditions shown by equation (33) are automatically satisfied. The reason for this is given in the displacement boundary conditions of the hexagon (equation (19)).

One can visualize that the non-zero solution is additionally influenced by the distance $2\,C_o$ of the surrounding fibers and the relation of distance to the fiber diameter $2\,a_o$. The closer the fibers come, the more

pronounced are the circular six-times-repetitious stress distributions expressed by the non-zero solutions.

In Reference (9), page 4, a condition similar to those in equation (33) has been used to impose the hexagonal geometry during deformations. Using this condition for the present shrinkage case, similar to what was used in Reference (9) for a loading case, it would be possible to set up an inhomogeneous boundary condition at the hexagon which would not contain ϵ Such a boundary condition would contain only the shrinkage constants of both materials, β^{I} and β^{II} .

The numerical results (see Figure 11) show that the radial stress at the interface is in compression at points where the fibers are close and in tension where they are farther apart. The shear stress (Figure 12) at the interface is a maximum at $\phi = 22°$ and zero at $\phi = 0°$ and $30°$. The total shrinkage displacement between two fiber axes in the model was $2 \times (-0.001132)$. The dimensions of this particular multifiber specimen were $a_o = 0.14$ inch and $C_o = 0.20$ inch .

Appendix C describes the methods used and the results of a photoelastic determination of stresses of selected single-fiber and the multifiber models. They are represented as stress differences. It is now possible to present the theoretical analysis in the form of principal stresses, rather than in the form of stress differences, and to compare the theory with the experimental values.

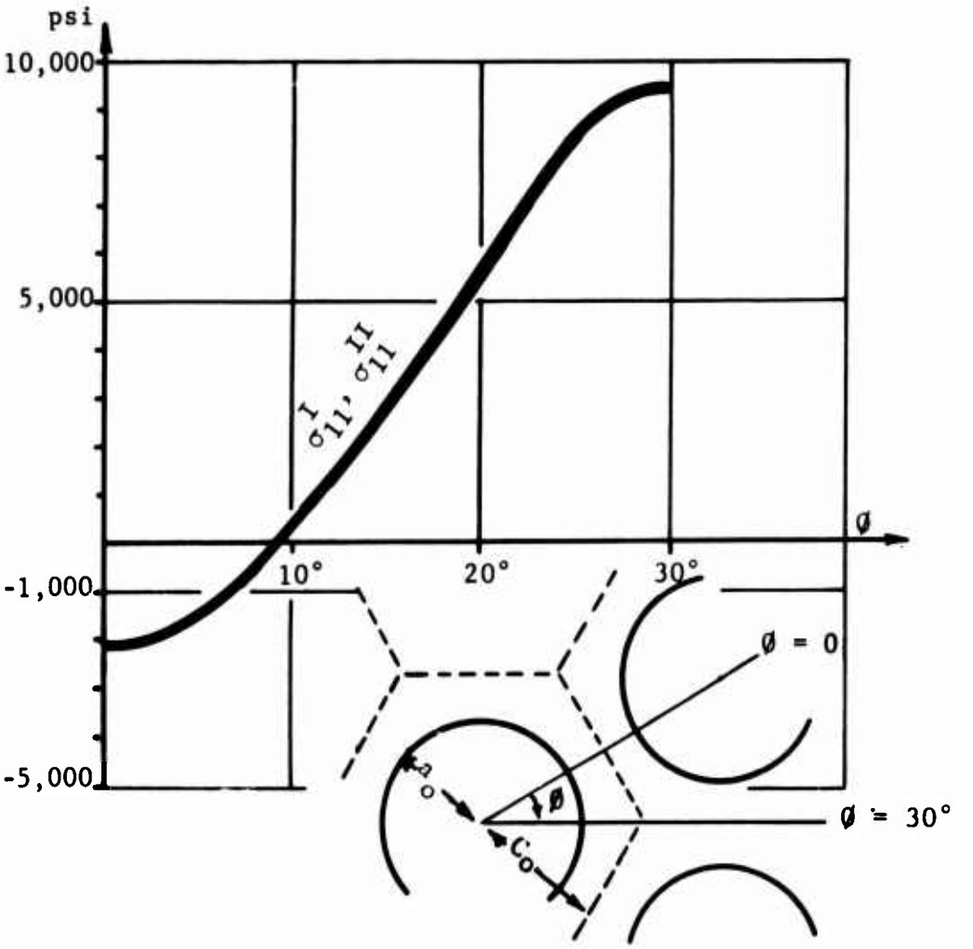

Figure 11. Radial Shrinkage Stresses at Interface in a Multifiber Composite Model a_o = 0.14 inch; C_o = 0.2 inch (Components: glass and epoxy)

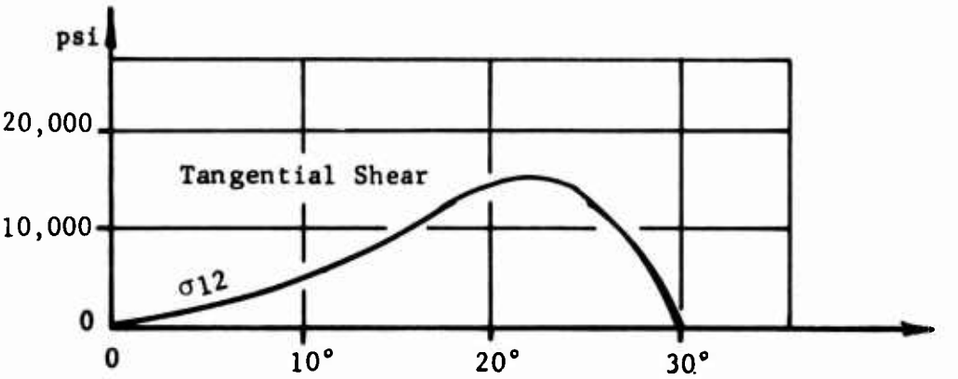

Figure 12. Shear Stress at Interface Due to Shrinkage a_o = 0.14 inch; C_o = 0.2 inch (Components: glass and epoxy)

REFERENCES

1. A. E. Green and W. Zerna, Theoretical Elasticity, Oxford University Press, New York, 1963

2. K. Marguerre, "Ansätze zur Lösung der Grundgeichungen der Elasticitätstheorie," Z. Angew. Math. Mech., 35 (1955), pp. 242-263

3. I. S. Sokolnikoff, Mathematical Theory of Elasticity, McGraw-Hill Book Company, Inc., New York, 1956

4. I. Szabó, Höhere Technische Mechanik, Springer, Berlin, 1958, pp. 331-332

5. B. A. Boley and J. H. Weiner, Theory of Thermal Stresses, J. Wiley and Sons, Inc., New York, London, 1960

6. R. D. Mindlin, "Force at a Point in the Interior of a Semi-Infinite Solid" (Proceedings of the Midwestern Conference on Solid Mechanics, Urbana, Illinois, 1953, pp. 56-59)

7. W. Flügge, Handbook of Engineering Mechanics, McGraw-Hill Book Company, Inc., New York, 1962, Chapter 41

8. R. A. Eubanks and E. Sternberg, "On the Completeness of Boussinesg-Papkovitch Stress Functions," J. Rat. Mech. Anal., 5 (1956), pp. 735-746

9. Henry R. Piehler, The Interior Elastic Stress Field in a Continuous, Close-Packed Filamentary Composite Material under Uniaxial Tension, AD 624 572, AFOSR 65-1426, ASRL TR 132-1

DISTRIBUTION

US Army Materiel Command	3
US Army Aviation Materiel Command	2
Chief of R&D, DA	2
US Army Aviation Materiel Laboratories	17
US Army R&D Group (Europe)	1
US Army Engineer R&D Laboratories	1
US Army Research Office-Durham	1
Plastics Technical Evaluation Center	1
Systems Engineering Group (RTD), Wright-Patterson AFB	2
Chief of Naval Research	1
Naval Air Systems Command	2
Director of Defense Research and Engineering	1
US Army Materials Research Agency	1
Defense Documentation Center	20

APPENDIX A

TRIDIMENSIONAL ANALYSIS OF THE UNIDIRECTIONAL MULTIFIBER COMPOSITE

LONG CYLINDER WITHOUT AXISYMMETRY

The displacement and stress components, in terms of Papkovitch functions, in rectangular coordinates, are quoted as follows:

$$\xi_i = P_i - \frac{1}{4(1-\nu)} \frac{\partial}{\partial x_i}(x_k P_k + P_0) \tag{A1}$$

$$\sigma_{ij} = G\left(\frac{\partial}{\partial x_j} P_i + \frac{\partial}{\partial x_i} P_j\right) + \frac{G}{2(1-\nu)}\left[\left(\delta_{ij}\nu \nabla_c^2 - \frac{\partial^2}{\partial x_i \partial x_j}\right)(x_k P_k + P_0)\right] \tag{A2}$$

To convert these expressions into a system of cylindrical coordinates, one can perform the following proper and admissible transformation.

One transforms from (x , y , z) to (r , θ , z)

$$(P_x, P_y, P_z) \text{ to } (P_1, P_2, P_3)$$

$$(u, v, w) \text{ to } (\xi_1, \xi_2, \xi_3)$$

$$\begin{pmatrix} \sigma_{xx}, \sigma_{yy}, \sigma_{zz} \\ \sigma_{xy}, \sigma_{yz}, \sigma_{zx} \end{pmatrix} \text{ to } \begin{pmatrix} \sigma_{11}, \sigma_{22}, \sigma_{33} \\ \sigma_{12}, \sigma_{23}, \sigma_{31} \end{pmatrix}.$$

The results are collected as follows:

for displacements,

$$\xi_1 = P_1 - \frac{1}{4(1-\nu)}\left[\frac{\partial}{\partial r}(rP_1 + zP_3 + P_0)\right] \quad \text{(A3)}$$

$$\xi_2 = P_2 - \frac{1}{4(1-\nu)}\left[\frac{1}{r}\frac{\partial}{\partial \phi}(rP_1 + zP_3 + P_0)\right] \quad \text{(A4)}$$

$$\xi_3 = P_3 - \frac{1}{4(1-\nu)}\left[\frac{\partial}{\partial z}(rP_1 + zP_3 + P_0)\right]; \quad \text{(A5)}$$

for stresses,

$$\sigma_{11} = 2G\left(\frac{1}{\cos\phi}\frac{\partial}{\partial r} - \frac{1}{r\sin\phi}\frac{\partial}{\partial \phi}\right)(P_1\cos\phi - P_2\sin\phi) + \frac{G}{2(1-\nu)}\left[\nu\nabla_c^2 - \left(\frac{1}{\cos\phi}\frac{\partial}{\partial r} - \frac{1}{r\sin\phi}\frac{\partial}{\partial \phi}\right)^2\right] \cdot (rP_1 + zP_3 + P_0) \quad \text{(A6)}$$

$$\sigma_{22} = 2G\left(\frac{1}{\sin\phi}\frac{\partial}{\partial r} + \frac{1}{r\cos\phi}\frac{\partial}{\partial \phi}\right)(P_1\sin\phi + P_2\cos\phi) + \frac{G}{2(1-\nu)}\left[\nu\nabla_c^2 - \left(\frac{1}{\sin\phi}\frac{\partial}{\partial r} + \frac{1}{r\cos\phi}\frac{\partial}{\partial \phi}\right)^2\right] \cdot (rP_1 + zP_3 + P_0) \quad \text{(A7)}$$

$$\sigma_{33} = 2G\frac{\partial}{\partial z}P_3 + \frac{G}{2(1-\nu)}(\nu\nabla_c^2 - \frac{\partial^2}{\partial z^2})(rP_1 + zP_3 + P_0); \quad \text{(A8)}$$

$$\sigma_{12} = G\left[\left(\frac{1}{\sin\phi}\frac{\partial}{\partial r} + \frac{1}{r\cos\phi}\frac{\partial}{\partial\phi}\right)(P_1\cos\phi - P_2\sin\phi)\right.$$
$$\left. + \left(\frac{1}{\cos\phi}\frac{\partial}{\partial r} - \frac{1}{r\sin\phi}\frac{\partial}{\partial\phi}\right)(P_1\sin\phi + P_2\cos\phi)\right]$$
$$- \frac{G}{2(1-\nu)}\left[\left(\frac{1}{\cos\phi}\frac{\partial}{\partial r} - \frac{1}{r\sin\phi}\frac{\partial}{\partial\phi}\right)\right.$$
$$\left.\cdot\left(\frac{1}{\sin\phi}\frac{\partial}{\partial r} + \frac{1}{r\cos\phi}\frac{\partial}{\partial\phi}\right)\right](rP_1 + zP_3 + P_0) \quad \text{(A9)}$$

$$\sigma_{23} = G\left[\left(\frac{\partial}{\partial z}\right)(P_1\sin\phi + P_2\cos\phi)\right.$$
$$\left. + \left(\frac{1}{\sin\phi}\frac{\partial}{\partial r} + \frac{1}{r\cos\phi}\frac{\partial}{\partial\phi}\right)P_3\right]$$
$$- \frac{G}{2(1-\nu)}\left[\left(\frac{1}{\sin\phi}\frac{\partial}{\partial r} + \frac{1}{r\cos\phi}\frac{\partial}{\partial\phi}\right)\cdot\frac{\partial}{\partial z}\right]$$
$$\cdot(rP_1 + zP_3 + P_0) \quad \text{(A10)}$$

$$\sigma_{31} = G\left[\left(\frac{1}{\cos\phi}\frac{\partial}{\partial r} - \frac{1}{r\sin\phi}\frac{\partial}{\partial\phi}\right)P_z\right.$$
$$\left. + \frac{\partial}{\partial z}(P_1\cos\phi - P_2\sin\phi)\right]$$
$$- \frac{G}{2(1-\nu)}\left[\frac{\partial}{\partial z}\left(\frac{1}{\cos\phi}\frac{\partial}{\partial r} - \frac{1}{r\sin\phi}\frac{\partial}{\partial\phi}\right)\right]$$
$$\cdot(rP_1 + zP_3 + P_0) \quad \text{(A11)}$$

for Laplace's equation of Papkovitch functions,

$$\nabla_c^2 (P_1 \cos\phi - P_2 \sin\phi) = 0 \tag{A12}$$

$$\nabla_c^2 (P_1 \sin\phi + P_2 \cos\phi) = 0 \tag{A13}$$

$$\nabla_c^2 P_3 = 0 \tag{A14}$$

$$\nabla_c^2 P_0 = 0. \tag{A15}$$

A solution of Laplace's equation in the finite cylinder in the domain ($0 < r \le a$, $0 \le \phi \le 2\pi$, $0 \le z \le \ell$) takes the following general form:

$$\begin{aligned}
&\sum_{n=0}^{\infty} \Bigg\{ \sum_{k=1}^{\infty} \Big[\alpha_{nk} J_n(\mu_{nk} r) + \beta_{nk} Y_n(\mu_{nk} r) \Big] \cdot \Big[\gamma_{nk} \sinh(\mu_{nk} z) \\
&\qquad + \delta_{nk} \cosh(\mu_{nk} z) \Big] \cdot \Big[\varepsilon_n \sin(n\phi) + \zeta_n \cos(n\phi) \Big] \\
&+ \sum_{n=1}^{\infty} \Big[\alpha_{no} r^n + \beta_{no} r^{-n} \Big] \cdot \Big[\gamma_{no} + \delta_{no} z \Big] \cdot \Big[\varepsilon_n \sin(n\phi) \\
&\qquad + \zeta_n \cos(n\phi) \Big] \\
&+ (\alpha_{oo} + \beta_{oo} \log r)(\gamma_{oo} + \delta_{oo} z).
\end{aligned} \tag{A16}$$

Combination of equations (A12) to (A16) gives the following results of Papkovitch functions:

$$
\begin{aligned}
P_1 = & \sum_{n=1}^{\infty} \left[A_{n0} r^n + B_{n0} r^{-n} \right] \cdot \left[C_{n0} + D_{n0} z \right] \\
& \cdot \left[E_{n1} \sin(n\phi) + F_{n1} \cos(n\phi) \right] \cos\phi \\
& + \sum_{m=1}^{\infty} \left[G_{m0} r^m + H_{m0} r^{-m} \right] \cdot \left[L_{m0} + M_{m0} z \right] \\
& \cdot \left[N_m \sin(m\phi) + P_m \cos(m\phi) \right] \sin\phi \\
& + (C_{00} + D_{00} z)(A_{00} + B_{00} \log r) \cos\phi \\
& + (L_{00} + M_{00} z)(G_{00} + H_{00} \log r) \sin\phi \\
& + \sum_{n=0}^{\infty} \left\{ \sum_{k=1}^{\infty} \left[A_{nk1} J_n(\mu_{nk1} r) + B_{nk1} Y_n(\mu_{nk1} r) \right] \right. \\
& \cdot \left[C_{nk1} \sinh(\mu_{nk1} z) + D_{nk1} \cosh(\mu_{nk1} z) \right] \\
& \cdot \frac{1}{2} \left[E_n (\sin(n+1)\phi + \sin(n-1)\phi) \right. \\
& \left. \left. + F_n (\cos(n+1)\phi + \cos(n-1)\phi) \right] \right]
\end{aligned}
$$

$$+\sum_{m=0}^{\infty}\left\{\sum_{l=1}^{\infty}\left[G_{ml}J_m(\lambda_{ml}r)+H_{ml}Y_m(\lambda_{ml}r)\right]\right.$$
$$\cdot\left[L_{ml}\sinh(\lambda_{ml}z)+M_{ml}\cosh(\lambda_{ml}z)\right]$$
$$\left.\cdot\frac{1}{2}\left[N_m(\cos(m-1)\phi-\cos(m+1)\phi)\right.\right.$$
$$\left.\left.+P_m(\sin(m+1)\phi-\sin(m-1)\phi)\right]\right\}$$

(A17)

$$P_2=\sum_{n=0}^{\infty}\left\{\sum_{k=1}^{\infty}\left[A_{nk}J_n(\mu_{nk}r)+B_{nk}Y_n(\mu_{nk}r)\right]\right.$$
$$\cdot\left[C_{nk}\sinh(\mu_{nk}z)+D_{nk}\cosh(\mu_{nk}z)\right]$$
$$\left.\cdot\frac{1}{2}\left[E_n(\cos(n+1)\phi-\cos(n-1)\phi)\right.\right.$$
$$\left.\left.+F_n(\sin(n-1)\phi-\sin(n+1)\phi)\right]\right\}$$
$$+\sum_{m=0}^{\infty}\left\{\sum_{l=1}^{\infty}\left[G_{ml}J_m(\lambda_{ml}r)+H_{ml}Y_m(\lambda_{ml}r)\right]\right.$$
$$\cdot\left[L_{ml}\sinh(\lambda_{ml}z)+M_{ml}\cosh(\lambda_{ml}z)\right]$$
$$\left.\cdot\frac{1}{2}\left[N_m(\sin(m+1)\phi+\sin(m-1)\phi)\right.\right.$$
$$\left.\left.+P_m(\cos(m+1)\phi+\cos(m-1)\phi\right]\right\}$$

$$+\sum_{m=1}^{\infty}\left[G_{mo}r^{m}+H_{mo}r^{-m}\right]\cdot\left[L_{mo}+M_{mo}z\right]$$
$$\cdot\left[N_{m}\sin(m\phi)+P_{m}\cos(m\phi)\right]\cos\phi$$
$$-\sum_{n=1}^{\infty}\left[A_{no}r^{n}+B_{no}r^{-n}\right]\cdot\left[C_{no}+D_{no}z\right]$$
$$\cdot\left[E_{n}\sin(n\phi)+F_{n}\cos(n\phi)\right]\sin\phi$$
$$+(L_{oo}+M_{oo}z)(G_{oo}+H_{oo}\log r)\cos\phi$$
$$-(C_{oo}+D_{oo}z)(A_{oo}+B_{oo}\log r)\sin\phi \qquad \text{(A18)}$$

and

$$P_{3}=\sum_{q=0}^{\infty}\left\{\sum_{p=1}^{\infty}\left[Q_{qp}J_{q}(\delta_{qp}r)+R_{qp}Y_{q}(\delta_{qp}r)\right]\right.$$
$$\cdot\left[S_{qp}\sinh(\delta_{qp}z)+T_{qp}\cosh(\delta_{qp}z)\right]$$
$$\left.\cdot\left[W_{q}\sin(q\phi)+X_{q}\cos(q\phi)\right]\right.$$
$$+\sum_{q=1}^{\infty}\left[Q_{qo}r^{q}+R_{qo}r^{-q}\right]\cdot\left[S_{qo}+T_{qo}z\right]$$
$$\cdot\left[W_{q}\sin(q\phi)+X_{q}\cos(q\phi)\right]$$
$$+(S_{oo}+T_{oo}z)(Q_{oo}+R_{oo}\log r). \qquad \text{(A19)}$$

Domain and Boundary Conditi.ns

Domain:

$$\begin{cases} 0 \leq r \leq a \\ a \leq r \leq c_0/\cos\phi \\ 0 \leq \phi \leq \pi/6 \\ 0 \leq z \leq l \end{cases} \quad \begin{matrix} \text{for fiber} \\ \text{for resin} \end{matrix} \qquad \text{(A20)}$$

Geometry consideration:

For ξ_1:

$$\begin{cases} \xi_1(r,\phi,z) = \xi_1(r,-\phi,z) \\ \xi_1(r,\phi,z) = \xi_1(r,\phi,-z) \end{cases} \qquad \text{(A21)}$$

For ξ_2:

$$\begin{cases} \xi_2(r,\phi,z) = -\xi_2(r,-\phi,z) \\ \xi_2(r,\phi,z) = \xi_2(r,\phi,-z) \end{cases} \qquad \text{(A22)}$$

For ξ_3:

$$\begin{cases} \xi_3(0,\phi,z) = \text{finite} \\ \xi_3(r,\phi,z) = \xi_3(r,-\phi,z) \\ \xi_3(r,\phi,z) = -\xi_3(r,\phi,-z) \end{cases} \qquad \text{(A23)}$$

Periodic characteristic of $\pi/3$ period implies that

$$\xi_i(r,\phi,z) = \xi_i(r,\phi+\tfrac{\pi}{3},z), \quad \text{(A24)}$$

$$\frac{\partial \xi_i}{\partial \phi}(r,\phi,z) = \frac{\partial \xi_i}{\partial \phi}(r,\phi+\tfrac{\pi}{3},z); \quad \text{(A25)}$$

and

$$\sigma_{ij}(r,\phi,z) = \sigma_{ij}(r,\phi+\tfrac{\pi}{3},z), \quad \text{(A26)}$$

$$\frac{\partial \sigma_{ij}}{\partial \phi}(r,\phi,z) = \frac{\partial \sigma_{ij}}{\partial \phi}(r,\phi+\tfrac{\pi}{3},z). \quad \text{(A27)}$$

Displacements

Substitution of equations (A21) to (A23) into equations (A3) to (A6), (A9), and (A11) and taking into account the consideration of the previous section yields:

Radial displacement for fiber,

$$\xi_1^I = \sum_{n=0,6,\cdots}^{\infty} \left\{ \sum_{k=1,2,\cdots}^{\infty} (A_{11}^I)_{nk} (n+2-4\nu^I) J_{n-1}(\mu_{(n-1)k} r) \cosh(\mu_{(n-1)k} z) \right\} \cdot \cos(n\phi)$$

$$+ \sum_{n=6,\cdots}^{\infty} \left\{ \sum_{k=1,2,\cdots}^{\infty} (A_{11}^I)_{nk} (-\mu_{(n-1)k} r) J_{n-2}(\mu_{(n-1)k} r) \cosh(\mu_{(n-1)k} z) \right\} \cdot \cos(n\phi)$$

$$+ \sum_{n=0,6,\cdots}^{\infty} \left\{ \sum_{k=1,2,\cdots}^{\infty} (A_{21}^I)_{nk} (n+4(1-\nu^I)) J_{n+1}(\mu_{(n+1)k} r) \cosh(\mu_{(n+1)k} z) \right\} \cdot \cos(n\phi)$$

$$+\sum_{n=0,1,\cdots}^{\infty}\left\{\sum_{k=1,2,\cdots}^{\infty}\left(A_{21}^{I}\right)_{nk}\left(-\mu_{(n+1)k}r\right)J_n\left(\mu_{(n+1)k}r\right)\cosh\left(\mu_{(n+1)k}z\right)\right\}\cdot\cos(n\phi)$$

$$+\sum_{n=0,1,\cdots}^{\infty}\left\{\sum_{k=1,2,\cdots}^{\infty}\left(Q_{11}^{I}\right)_{nk}\left(-\mu_{nk}\right)J_{n-1}\left(\mu_{nk}r\right)z\sinh\left(\mu_{nk}z\right)\right\}\cdot\cos(n\phi)$$

$$+\sum_{n=0,1,\cdots}^{\infty}\left\{\sum_{k=1,2,\cdots}^{\infty}\left(Q_{11}^{I}\right)_{nk}\,n\,\frac{J_n\left(\mu_{nk}r\right)}{r}\,z\sinh\left(\mu_{nk}z\right)\right\}\cdot\cos(n\phi)$$

$$+\sum_{n=0}^{\infty}\left[\left(A_{11}^{I}\right)_{n0}\left(4-4\nu^{I}-n\right)r^{n-1}+\left(A_{21}^{I}\right)_{n0}\left(2-4\nu^{I}-n\right)r^{n+1}\right.$$

$$\left.-\left(Q_{11}^{I}\right)_{n0}nr^{n-1}z^{2}\right]\cos(n\phi)$$

$$+\left(A_{21}^{I}\right)_{00}\left(2-4\nu^{I}\right)r\ ; \qquad \text{(A28)}$$

Radial displacement for resin,

$$\xi_1^{II}=\sum_{n=0,1,\cdots}^{\infty}\left\{\sum_{k=1,2,\cdots}^{\infty}\left(A_{11}^{II}\right)_{nk}\left(n+2-4\nu^{II}\right)J_{n-1}\left(\mu_{(n-1)k}r\right)\cosh\left(\mu_{(n-1)k}z\right)\right\}\cdot\cos(n\phi)$$

$$+\sum_{n=0,1,\cdots}^{\infty}\left\{\sum_{k=1,2,\cdots}^{\infty}\left(A_{11}^{II}\right)_{nk}\left(-\mu_{(n-1)k}r\right)J_{n-2}\left(\mu_{(n-1)k}r\right)\cosh\left(\mu_{(n-1)k}z\right)\right\}\cdot\cos(n\phi)$$

$$+\sum_{n=0,1,\cdots}^{\infty}\left\{\sum_{k=1,2,\cdots}^{\infty}\left(B_{11}^{II}\right)_{nk}\left(n+2-4\nu^{II}\right)Y_{n-1}\left(\mu_{(n-1)k}r\right)\cosh\left(\mu_{(n-1)k}z\right)\right\}\cdot\cos(n\phi)$$

$$+\sum_{n=0,1,\cdots}^{\infty}\left\{\sum_{k=1,2,\cdots}^{\infty}\left(B_{11}^{II}\right)_{nki}\left(-\mu_{(n-2)ki}r\right)Y_{n-2}\left(\mu_{(n-2)ki}r\right)\cosh\left(\mu_{(n-2)ki}z\right)\right\}\cdot\cos(n\phi)$$

$$+\sum_{n=0,1,\cdots}^{\infty}\left\{\sum_{k=1,2,\cdots}^{\infty}\left(A_{21}^{II}\right)_{nki}\left(n+4(1-\nu^{II})\right)J_{n+1}\left(\mu_{(n+1)ki}r\right)\cosh\left(\mu_{(n+1)ki}z\right)\right\}\cdot\cos(n\phi)$$

$$+\sum_{n=0,1,\cdots}^{\infty}\left\{\sum_{k=1,2,\cdots}^{\infty}\left(A_{21}^{II}\right)_{nki}\left(-\mu_{(n+1)ki}r\right)J_{n}\left(\mu_{(n+1)ki}r\right)\cosh\left(\mu_{(n+1)ki}z\right)\right\}\cdot\cos(n\phi)$$

$$+\sum_{n=0,1,\cdots}^{\infty}\left\{\sum_{k=1,2,\cdots}^{\infty}\left(B_{21}^{II}\right)_{nki}\left(n+4(1-\nu^{II})\right)Y_{n+1}\left(\mu_{(n+1)ki}r\right)\cosh\left(\mu_{(n+1)ki}z\right)\right\}\cdot\cos(n\phi)$$

$$+\sum_{n=0,1,\cdots}^{\infty}\left\{\sum_{k=1,2,\cdots}^{\infty}\left(B_{21}^{II}\right)_{nki}\left(-\mu_{(n+1)ki}r\right)Y_{n}\left(\mu_{(n+1)ki}r\right)\cosh\left(\mu_{(n+1)ki}z\right)\right\}\cdot\cos(n\phi)$$

$$+\sum_{n=0,1,\cdots}^{\infty}\left\{\sum_{k=1,2,\cdots}^{\infty}\left(Q_{11}^{II}\right)_{nki}\left(-\mu_{nki}\right)J_{n-1}\left(\mu_{nki}r\right)z\sinh\left(\mu_{nki}z\right)\right\}\cdot\cos(n\phi)$$

$$+\sum_{n=0,1,\cdots}^{\infty}\left\{\sum_{k=1,2,\cdots}^{\infty}\left(Q_{11}^{II}\right)_{nki}n\frac{J_{n}\left(\mu_{nki}r\right)}{r}z\sinh\left(\mu_{nki}z\right)\right\}\cdot\cos(n\phi)$$

$$+\sum_{n=0,1,\cdots}^{\infty}\left\{\sum_{k=1,2,\cdots}^{\infty}\left(R_{11}^{II}\right)_{nki}\left(-\mu_{nki}\right)Y_{n-1}\left(\mu_{nki}r\right)z\sinh\left(\mu_{nki}z\right)\right\}\cdot\cos(n\phi)$$

$$+\sum_{n=0,1,\cdots}^{\infty}\left\{\sum_{k=1,2,\cdots}^{\infty}\left(R_{11}^{II}\right)_{nki}n\frac{Y_{n}\left(\mu_{nki}r\right)}{r}z\sinh\left(\mu_{nki}z\right)\right\}\cdot\cos(n\phi)$$

$$+\sum_{n=6}^{\infty}\Big[\big(A_{11}^{II}\big)_{n0}(4-4\nu^{II}-n)r^{n-1}+\big(A_{21}^{II}\big)_{n0}(2-4\nu^{II}-n)r^{n+1}$$
$$+\big(B_{11}^{II}\big)_{n0}(2-4\nu^{II}+n)r^{-n+1}+\big(B_{21}^{II}\big)_{n0}(4-4\nu^{II}+n)r^{-n-1}\Big]$$
$$\cdot\cos(n\phi)$$
$$+\sum_{n=6}^{\infty}\Big[-\big(Q_{11}^{II}\big)_{n0}\,n\,r^{n-1}+\big(R_{11}^{II}\big)_{n0}\,n\,r^{-n-1}\Big]z^2\cos(n\phi)$$
$$-\big(R_{11}^{II}\big)_{00}z^2r^{-1}+\big(A_{21}^{II}\big)_{00}(2-4\nu^{II})r+\big(B_{21}^{II}\big)_{00}r^{-1};$$

(A29)

Tangential displacement for fiber,

$$\xi_2^{I}=\sum_{n=6,12,\cdots}^{\infty}\Big\{\sum_{k=1,3,\cdots}^{\infty}\big(A_{11}^{I}\big)_{nk}(n-4(1-\nu^{I}))J_{n-1}\big(\mu_{(n-1)k}r\big)\cosh\big(\mu_{(n-1)k}z\big)\Big\}\sin(n\phi)$$
$$+\sum_{n=6,12,\cdots}^{\infty}\Big\{\sum_{k=1,3,\cdots}^{\infty}\big(A_{21}^{I}\big)_{nk}(n+4(1-\nu^{I}))J_{n+1}\big(\mu_{(n+1)k}r\big)\cosh\big(\mu_{(n+1)k}z\big)\Big\}\sin(n\phi)$$
$$+\sum_{n=6,12,\cdots}^{\infty}\Big\{\sum_{k=1,3,\cdots}^{\infty}\big(Q_{11}^{I}\big)_{nk}\,n\,\frac{J_n(\mu_{nk}r)}{r}z\sinh\big(\mu_{nk}z\big)\Big\}\sin(n\phi)$$
$$+\sum_{n=6}^{\infty}\Big[\big(A_{11}^{I}\big)_{n0}(n-4(1-\nu^{I}))r^{n-1}+\big(A_{21}^{I}\big)_{n0}(n+4(1-\nu^{I}))\cdot$$
$$\cdot r^{n+1}+\big(Q_{11}^{I}\big)_{n0}\,n\,r^{n-1}z^2\Big]\sin(n\phi);$$

(A30)

Tangential displacement for resin,

$$
\begin{aligned}
\xi_2^{II} = &\sum_{n=6,12,\cdots}^{\infty}\left\{\sum_{k=1,2,\cdots}^{\infty}(A_{11}^{II})_{nk}\left(n-4(1-\nu^{II})\right)J_{n-1}(\mu_{(n-1)k}r)\cosh(\mu_{nk}z)\right\}\sin(n\phi)\\
&+\sum_{n=6,12,\cdots}^{\infty}\left\{\sum_{k=1,2,\cdots}^{\infty}(B_{11}^{II})_{nk}\left(n-4(1-\nu^{II})\right)Y_{n-1}(\mu_{(n-1)k}r)\cosh(\mu_{nk}z)\right\}\sin(n\phi)\\
&+\sum_{n=6,12,\cdots}^{\infty}\left\{\sum_{k=1,2,\cdots}^{\infty}(A_{21}^{II})_{nk}\left(n+4(1-\nu^{II})\right)J_{n+1}(\mu_{(n+1)k}r)\cosh(\mu_{(n+1)k}z)\right\}\sin(n\phi)\\
&+\sum_{n=6,12,\cdots}^{\infty}\left\{\sum_{k=1,2,\cdots}^{\infty}(B_{21}^{II})_{nk}\left(n+4(1-\nu^{II})\right)Y_{n+1}(\mu_{(n+1)k}r)\cosh(\mu_{(n+1)k}z)\right\}\sin(n\phi)\\
&+\sum_{n=6,12,\cdots}^{\infty}\left\{\sum_{k=1,2,\cdots}^{\infty}(Q_{11}^{II})_{nk}\,n\,\frac{J_n(\mu_{nk}r)}{r}z\sinh(\mu_{nk}z)\right\}\sin(n\phi)\\
&+\sum_{n=6,12,\cdots}^{\infty}\left\{\sum_{k=1,2,\cdots}^{\infty}(R_{11}^{II})_{nk}\,n\,\frac{Y_n(\mu_{nk}r)}{r}z\sinh(\mu_{nk}z)\right\}\sin(n\phi)\\
&+\sum_{n=6}^{\infty}\Big[(A_{11}^{I})_{n0}\left(n-4(1-\nu^{II})\right)r^{n-1}+(B_{11}^{II})_{n0}\left(n-4(1-\nu^{II})\right)r^{-n+1}\\
&\quad+(A_{21}^{II})_{n0}\left(n+4(1-\nu^{II})\right)r^{n+1}+(B_{21}^{II})_{n0}\left(n+4(1-\nu^{II})\right)r^{-n-1}\\
&\quad+(Q_{11}^{II})_{n0}\,n\,r^{n-1}z^2+(R_{11}^{II})_{n0}\,n\,r^{-n-1}z^2\Big]\sin(n\phi)\,;
\end{aligned}
\tag{A31}
$$

Axial displacement for fiber,

$$\xi_3^{I} = \sum_{n=0,1,\cdots}^{\infty} \left\{ \sum_{k=1,2,\cdots}^{\infty} (A_{11}^{I})_{nk} (-\mu_{(n-1)k} r) J_{n-1}(\mu_{(n-1)k} r) \sinh(\mu_{(n-1)k} z) \right\} \cdot \cos(n\phi)$$

$$+ \sum_{n=0,1,\cdots}^{\infty} \left\{ \sum_{k=1,2,\cdots}^{\infty} (A_{21}^{I})_{nk} (-\mu_{(n+1)k} r) J_{n+1}(\mu_{(n+1)k} r) \sinh(\mu_{(n+1)k} z) \right\} \cdot \cos(n\phi)$$

$$+ \sum_{n=0,1,\cdots}^{\infty} \left\{ \sum_{k=1,2,\cdots}^{\infty} (Q_{11}^{I})_{nk} (3-4\nu^{I}) J_n(\mu_{nk} r) \sinh(\mu_{nk} z) \right\} \cdot \cos(n\phi)$$

$$+ \sum_{n=0,1,\cdots}^{\infty} \left\{ \sum_{k=1,2,\cdots}^{\infty} (Q_{11}^{I})_{nk} (-\mu_{nk}) J_n(\mu_{nk} r) z \cosh(\mu_{nk} z) \right\} \cdot \cos(n\phi)$$

$$+ \sum_{n=0}^{\infty} \left[(Q_{11}^{I})_{n0} (2-4\nu^{I}) r^{n} z \right] \cos(n\phi)$$

$$+ \left[(Q_{11}^{I})_{00} + (R_{11}^{I})_{00} \log r \right] (2-4\nu^{I}) z \; ; \qquad \text{(A32)}$$

Axial displacement for resin,

$$\xi_3^{II} = \sum_{n=0,1,\cdots}^{\infty} \left\{ \sum_{k=1,2,\cdots}^{\infty} (A_{11}^{II})_{nk} (-\mu_{(n-1)k} r) J_{n-1}(\mu_{(n-1)k} r) \sinh(\mu_{(n-1)k} z) \right\} \cdot \cos(n\phi)$$

$$+ \sum_{n=0,1,\cdots}^{\infty} \left\{ \sum_{k=1,2,\cdots}^{\infty} (B_{11}^{II})_{nk} (-\mu_{(n-1)k} r) Y_{n-1}(\mu_{(n-1)k} r) \sinh(\mu_{(n-1)k} z) \right\} \cdot \cos(n\phi)$$

$$+\sum_{n=0,1,\dots}^{\infty}\left\{\sum_{k=1,2,\dots}^{\infty}\left(A_{21}^{II}\right)_{nk}\left(-\mu_{(n+1)k}r\right)J_{n+1}\left(\mu_{(n+1)k}r\right)\sinh\left(\mu_{(n+1)k}z\right)\right\}\cdot\cos(n\phi)$$

$$+\sum_{n=0,1,\dots}^{\infty}\left\{\sum_{k=1,2,\dots}^{\infty}\left(B_{21}^{II}\right)_{nk}\left(-\mu_{(n+1)k}r\right)Y_{n+1}\left(\mu_{(n+1)k}r\right)\sinh\left(\mu_{(n+1)k}z\right)\right\}\cdot\cos(n\phi)$$

$$+\sum_{n=0,1,\dots}^{\infty}\left\{\sum_{k=1,2,\dots}^{\infty}\left(Q_{11}^{II}\right)_{nk}\left(3-4\nu^{I}\right)J_n\left(\mu_{nk}r\right)\sinh\left(\mu_{nk}z\right)\right\}\cdot\cos(n\phi)$$

$$+\sum_{n=0,1,\dots}^{\infty}\left\{\sum_{k=1,2,\dots}^{\infty}\left(R_{11}^{II}\right)_{nk}\left(3-4\nu^{II}\right)Y_n\left(\mu_{nk}r\right)\sinh\left(\mu_{nk}z\right)\right\}\cdot\cos(n\phi)$$

$$+\sum_{n=0,1,\dots}^{\infty}\left\{\sum_{k=1,2,\dots}^{\infty}\left(Q_{11}^{II}\right)_{nk}\left(-\mu_{nk}\right)J_n\left(\mu_{nk}r\right)z\cosh\left(\mu_{nk}z\right)\right\}\cdot\cos(n\phi)$$

$$+\sum_{n=0,1,\dots}^{\infty}\left\{\sum_{k=1,2,\dots}^{\infty}\left(R_{11}^{II}\right)_{nk}\left(-\mu_{nk}\right)Y_n\left(\mu_{nk}r\right)z\cosh\left(\mu_{nk}z\right)\right\}\cdot\cos(n\phi)$$

$$+\sum_{n=0}^{\infty}\left[\left(Q_{11}^{I}\right)_{no}\left(2-4\nu^{II}\right)r^{n}+\left(R_{11}^{I}\right)_{no}\left(2-4\nu^{II}\right)r^{-n}\right]$$

$$\cdot(z)\cdot\cos(n\phi)$$

$$+\left[\left(Q_{11}^{II}\right)_{oo}+\left(R_{11}^{II}\right)_{oo}\log r\right]\left(2-4\nu^{III}\right)z\,.$$

(A33)

Stresses

Radial stress for fiber,

$$\sigma_{11}^{I} = \frac{E^{I}}{1+\nu^{I}}\Bigg[\sum_{n=0,1,\ldots}^{\infty}\Bigg\{\sum_{k=1,2,\ldots}^{\infty}(A_{11}^{I})_{nk}\Bigg[-(n-1)(n-4(1-\nu^{I}))\frac{J_{n-1}(\mu_{(n-1)k}r)}{r}$$

$$+\mu_{(n-1)k}^{2}\, r\, J_{n-1}(\mu_{(n-1)k}r)$$

$$+\frac{\nu^{I}\mu_{(n-1)k}-(1-\nu^{I})(3-4\nu^{I})}{1-2\nu^{I}}J_{n}(\mu_{(n-1)k}r)\Bigg]$$

$$\cdot\cosh(\mu_{(n-1)k}z)\Bigg\}\cdot\cos(n\phi)$$

$$+\sum_{n=0,1,\ldots}^{\infty}\Bigg\{\sum_{k=1,2,\ldots}^{\infty}(A_{21}^{I})_{nk}\Bigg[(3-2\nu^{I})\mu_{(n+1)k}J_{n}(\mu_{(n+1)k}r)$$

$$+(\mu_{(n+1)k}^{2}r)J_{n+1}(\mu_{(n+1)k}r)$$

$$+\frac{(n+1+(1-\nu^{I}))(\nu^{I}(n+3)-(n+1))}{1-2\nu^{I}}\frac{J_{n+1}(\mu_{(n+1)k}r)}{r}\Bigg]$$

$$\cdot\cosh(\mu_{(n+1)k}z)\Bigg\}\cdot\cos(n\phi)$$

$$+\sum_{n=0,1,\ldots}^{\infty}\Bigg\{\sum_{k=1,2,\ldots}^{\infty}(Q_{11}^{I})_{nk}\Bigg[\Bigg[\mu_{nk}\frac{J_{(n-1)}(\mu_{nk}r)}{r}$$

$$+\mu_{nk}^{2}J_{n}(\mu_{nk}r)$$

$$-n(n+1)\frac{J_{n}(\mu_{nk}r)}{r^{2}}\Bigg]$$

$$\cdot z \sinh(\mu_{nk} z)$$

$$+ 2\nu^{I} \mu_{nk} J_n(\mu_{nk} r)\Big] \cdot \cosh(\mu_{nk} z)\Big\} \cdot$$

$$\cdot \cos(n\phi)$$

$$+ \sum_{n=1,2,\ldots}^{\infty} (A_{11}^{I})_{n0} (4(1-\nu^{I}) - n)(n-1) r^{n-2} \cos(n\phi)$$

$$+ (A_{21}^{I})_{00} 2 + (Q_{11}^{I})_{00} 2\nu^{I} + \frac{1+\nu^{I}}{1-2\nu^{I}} \beta^{I} \Big]\Big] . \quad \text{(A34)}$$

Radial stress for resin has all terms defined in the same form as equation (A34) except for replacing all superscripts I by II, plus the terms involving Bessel functions of the second kind and

$$\sum_{n=6}^{\infty} (B_{21}^{II})_{n0} \frac{E^{II}}{1+\nu^{II}} (n+4(1-\nu^{II}))(n+1) r^{-n-2} \cos(n\phi) - 2(B_{21}^{II})_{00} \frac{E}{1+\nu^{II}} .$$

Shear stresses,

$$\sigma_{12}^{I} = \frac{E^{I}}{1+\nu^{I}} \Bigg[\Bigg[\sum_{n=1,2,\ldots}^{\infty} \Bigg\{ \sum_{k=1,2,\ldots}^{\infty} (A_{11}^{I})_{nk} \Big[(n-1)(n-4(1-\nu^{I})) \frac{J_{n-1}(\mu_{(n-1)k} r)}{r}$$

$$- \mu_{(n-1)k} (n-2(1-\nu^{I})) J_n(\mu_{(n-1)k} r) \Big]$$

$$\cdot \cosh(\mu_{(n-1)k} z) \Bigg\} \cdot \sin(n\phi)$$

$$+ \sum_{n=1,2,\ldots}^{\infty} \Bigg\{ \sum_{k=1,2,\ldots}^{\infty} (A_{21}^{I})_{nk} \Big[-(n+1) \frac{J_{n+1}(\mu_{(n+1)k} r)}{r}$$

$$+\mu_{(n+1)k}\,(n+2(1-\nu^{I}))J_n(\mu_{(n+1)k}r)\Big]$$

$$\cdot\cosh(\mu_{(n+1)k}z)\Big\}\cdot\sin(n\phi)$$

$$+\sum_{n=6,\dots}^{\infty}\Bigg\{\sum_{k=1,2,\dots}^{\infty}(Q_{11}^{I})_{nk}\Big[n(n-1)\frac{J_n(\mu_{nk}r)}{r^2}-n\mu_{nk}\frac{J_{(n+1)}(\mu_{nk}r)}{r}\Big]$$

$$\cdot z\sinh(\mu_{nk}z)\Big\}\cdot\sin(n\phi)$$

$$+\sum_{n=6}^{\infty}\Big[(A_{11}^{I})_{n0}\,n(n-4(1-\nu^{I}))r^{n-2}\Big]\cdot\sin(n\phi)\Bigg].$$

(A35)

σ_{12}^{II} has all terms defined in the same form as equation (A35) except for replacing all superscripts I by II, plus the terms involving Bessel functions of the second kind and $\sum_{n=6,\dots}^{\infty}(B_{21}^{II})_{n0}\left(\frac{E^{II}}{1+\nu^{II}}\right)n(n+4+(1-\nu^{II}))r^{-n-2}\sin(n\phi)$.

$$\sigma_{13}^{I}=\frac{E^{I}}{1+\nu^{I}}\Bigg[\sum_{n=0,\dots}^{\infty}\Bigg\{\sum_{k=1,2,\dots}^{\infty}(A_{11}^{I})_{nk}\Big[\mu_{(n-1)k}^{2}\,r\,J_n(\mu_{(n-1)k}r)$$

$$+\mu_{(n-1)k}(2(1-\nu^{I})-n)J_{n-1}(\mu_{(n-1)k}r)\Big]$$

$$\cdot\sinh(\mu_{(n-1)k}z)\Big\}\cdot\cos(n\phi)$$

$$+\sum_{n=0,\dots}^{\infty}\Bigg\{\sum_{k=1,2,\dots}^{\infty}(A_{21}^{I})_{nk}\Big[\mu_{(n+1)k}(n+2(1-\nu^{I}))J_{n+1}(\mu_{(n+1)k}r)$$

$$-\mu_{(n+1)k}^{2}J_n(\mu_{(n+1)k}r)\Big]$$

$$\cdot \sinh(\mu_{(n+1)k} z)\Big\} \cdot \cos(n\phi)$$

$$+\sum_{n=0,1,\ldots}^{\infty}\left\{\sum_{k=1,2,\ldots}^{\infty}(Q_{11}^{I})_{nk}\left[\left[(1-2\nu^{I})J_{n-1}(\mu_{nk} r) - n(1-2\nu^{I})\frac{J_n(\mu_{nk} r)}{r}\right]\cdot\sinh(\mu_{nk} z)\right.\right.$$

$$+\left[-\mu_{nk}^{2} J_{n-1}(\mu_{nk} r) + n\mu_{nk}\frac{J_n(\mu_{nk} r)}{r}\right] z\cosh(\mu_{nk} z)\Big]$$

$$\left.\left.\cdot\cos(n\phi)\right]\right] . \qquad \text{(A36)}$$

σ_{13}^{II} has all terms defined in the same form as equation (A36) except for replacing all superscripts I by II, plus the terms involving Bessel functions of the second kind.

Axial stress for fiber,

$$\sigma_{33}^{I} = \frac{E^{I}}{1+\nu^{I}}\left[\left[\sum_{n=0,1,\ldots}^{\infty}\left\{\sum_{k=1,2,\ldots}^{\infty}(A_{11}^{I})_{nk}\left[-\mu_{(n-1)k}^{2} r J_{n-1}(\mu_{(n-1)k} r) + \nu^{I}(\mu_{(n-1)k} - (3-4\nu^{I}))J_n(\mu_{(n-1)k} r)\right]\right.\right.\right.$$

$$\left.\left.\cdot\cosh(\mu_{(n-1)k} z)\right\}\cdot\cos(n\phi)\right.$$

$$+\sum_{n=0,1,\ldots}^{\infty}\left\{\sum_{k=1,2,\ldots}^{\infty}(A_{21}^{I})_{nk}\left[-\mu_{(n-1)k}^{2} r J_{n+1}(\mu_{(n+1)k} r)\right.\right.$$

$$+2\mu_{n+1,k}\nu^{I} J_n(\mu_{n+1,k} r)\Big]$$

$$\cdot \cosh(\mu_{n+1,k} z)\Big\} \cdot \cos(n\phi)$$

$$+\sum_{n=0,1,\ldots}^{\infty}\Bigg\{\sum_{k=1,2,\ldots}^{\infty}(Q_{11}^{I})_{nk}\Bigg[\Big[2(1-\nu^{I})J_n(\mu_{nk} r)\cosh(\mu_{nk} z)$$

$$-\Big[(+\mu_{nk}^{2})J_n(\mu_{nk} r)$$

$$+\mu_{nk}\nu^{I}\frac{J_{n-1}(\mu_{nk} r)}{r}\Big]\cdot z\sinh(\mu_{nk} z)\Big]\Bigg\}$$

$$\cdot \cos(n\phi)$$

$$+\sum_{n=0,1,2,\ldots}^{\infty}(A_{21}^{I})_{n0}\,4\nu^{I}(n+1)\,r^{n}\cos(n\phi)$$

$$+\sum_{n=0,1,2,\ldots}^{\infty}(Q_{11}^{I})_{n0}\,2(1-\nu^{I})\,r^{n}\cos(n\phi)$$

$$+4\nu^{I}(A_{21}^{I})_{00}+2(1-\nu^{I})\big((Q_{11}^{I})_{00}+(R_{11}^{I})_{00}\log r\big)$$

$$+\frac{1+\nu^{I}}{1-2\nu^{I}}\beta^{I}\Bigg] \qquad \text{(A37)}$$

Axial stress for resin, σ_{33}^{II}, has all

terms defined in the same manner as equation (A38) except for replacing all superscripts I by II, plus the terms involving Bessel functions of one second kind and

$$\frac{E^{II}}{1+\nu^{II}}\left[\sum_{n=1,2,4}^{\infty}(B_{21}^{II})_{no}\,4\nu^{II}(n+1)\,r^{-n}\cos(n\phi)\right.$$
$$\left.+\sum_{n=1,2,4}^{\infty}(R_{21}^{II})_{no}\,2(1-\nu^{II})\,r^{-n}\cos(n\phi)\right].$$

Boundary Conditions at the Interface

The continuity of displacements implies

$$\xi_1^I(a,\phi,z)=\xi_1^{II}(a,\phi,z)$$
$$\xi_2^I(a,\phi,z)=\xi_2^{II}(a,\phi,z)$$
$$\xi_3^I(a,\phi,z)=\xi_3^{II}(a,\phi,z) \qquad \text{(A38)}$$

The continuity of stresses implies

$$\sigma_{11}^I(a,\phi,z)=\sigma_{11}^{II}(a,\phi,z)$$
$$\sigma_{12}^I(a,\phi,z)=\sigma_{12}^{II}(a,\phi,z)$$
$$\sigma_{13}^I(a,\phi,z)=\sigma_{13}^{II}(a,\phi,z). \qquad \text{(A39)}$$

Axial stresses at the ends should vanish; i.e.,

$$\sigma_{33}^{I}(r, \phi, \pm l) = \sigma_{33}^{II}(r, \phi, \pm l) = 0. \tag{A40}$$

The sides of the hexagon should remain fixed; i.e., .

$$\xi_1^{I}\left(\frac{c_0}{\cos\phi}, \phi, z\right)\cos\phi - \xi_2^{I}\left(\frac{c}{\cos\phi}, \phi, z\right)\sin\phi = \varepsilon. \tag{A41}$$

Since $\xi_2^{I}\sin\phi$ is approximately 5% of $\xi_1^{I}\cos\phi$, we then get

$$\xi_1^{II}\left(\frac{c_0}{\cos\phi}, \phi, z\right)\cos\phi = \varepsilon \tag{A42}$$

or

$$\xi_1^{II}\left(\frac{c_0}{\cos\phi}, \phi, z\right) = \varepsilon \sec\phi. \tag{A43}$$

Equations to Determine Coefficients

The constants to be determined are listed as follows:

$$(A^{I}_{11})_{nk}, (A^{I}_{21})_{nk}, (Q^{I}_{11})_{nk}, \quad - \quad , \quad - \quad , \quad - \quad ,$$

$$(A^{II}_{11})_{nk}, (A^{II}_{21})_{nk}, (Q^{II}_{11})_{nk}, (B^{II}_{11})_{nk}, (B^{II}_{21})_{nk}, (R^{II}_{11})_{nk}$$

$$\begin{cases} n = 0, 6, 12, \cdots \\ k = 1, 3, 5, \cdots \end{cases}$$

$$(A^{I}_{11})_{n0}, \quad - \quad ,$$
$$(A^{II}_{11})_{n0}, (B^{I}_{21})_{n0}, \qquad (n = 6, 12, 18, \cdots)$$

$$(A^{I}_{21})_{00} \quad - \quad , (Q^{I}_{11})_{00}$$
$$(A^{II}_{21})_{00}, (B^{II}_{21})_{00}, (Q^{I}_{11})_{00}.$$

These constants will be determined by the following equations.

Combination of equations (A30), (A31), and (A38) yields

$$
\begin{aligned}
&(A_{11}^{\mathrm{I}})_{nk_i}\left[n-4(1-\nu^{\mathrm{I}})\right]J_{n-1}(\mu_{(n-1)k_i}a)\\
&+(A_{21}^{\mathrm{I}})_{nk_i}\left[n+4(1-\nu^{\mathrm{I}})\right]J_{n+1}(\mu_{(n+1)k_i}a)\\
&-(A_{11}^{\mathrm{II}})_{nk_i}\left[-n+4(1-\nu^{\mathrm{II}})\right]J_{n-1}(\mu_{(n-1)k_i}a)\\
&-(A_{21}^{\mathrm{II}})_{nk_i}\left[-(n+4(1-\nu^{\mathrm{II}})\right]J_{n+1}(\mu_{(n+1)k_i}a)\\
&-(B_{11}^{\mathrm{II}})_{nk_i}\left[-n+4(1-\nu^{\mathrm{I}})\right]Y_{n-1}(\mu_{(n-1)k_i}a)\\
&-(B_{21}^{\mathrm{II}})_{nk_i}\left[-n-4(1-\nu^{\mathrm{I}})\right]Y_{n+1}(\mu_{(n+1)k_i}a)=0. \qquad \text{(A44)}
\end{aligned}
$$

Combination of equations (A32), (A33), and (A38) gives

$$
\begin{aligned}
&(A_{11}^{\mathrm{I}})_{nk_i}(-\mu_{(n-1)k_i}a)J_{n-1}(\mu_{(n-1)k_i}a)\\
&+(A_{21}^{\mathrm{I}})_{nk_i}(-\mu_{(n+1)k_i}a)J_{n+1}(\mu_{(n+1)k_i}a)\\
&+(A_{11}^{\mathrm{II}})_{nk_i}(-\mu_{(n-1)k_i}a)J_{n-1}(\mu_{(n-1)k_i}a)\\
&+(A_{21}^{\mathrm{II}})_{nk_i}(-\mu_{(n+1)k_i}a)J_{n+1}(\mu_{(n+1)k_i}a)\\
&+(B_{11}^{\mathrm{II}})_{nk_i}(-\mu_{(n-1)k_i}a)Y_{n-1}(\mu_{(n-1)k_i}a)\\
&+(B_{21}^{\mathrm{II}})_{nk_i}(-\mu_{(n+1)k_i}a)Y_{n+1}(\mu_{(n+1)k_i}a)=0. \qquad \text{(A45)}
\end{aligned}
$$

Equations (A34) and (A39) yield

$$(A_{11}^{I})_{nk_i}\left(\frac{E^{I}}{1+\nu^{I}}\right)\Bigg[-(n-1)\left(n-4(1-\nu^{I})\right)\frac{J_{n-1}(\mu_{(n-1)k_i}a)}{a}$$

$$+\mu_{(n-1)k_i}^{2}\,a\,J_{n-1}(\mu_{(n-1)k_i}a)$$

$$-\frac{(1-\nu^{I})(3-4\nu^{I})-\nu^{I}\mu_{(n-1)k_i}}{1-2\nu^{I}}J_{n}(\mu_{(n-1)k_i}a)\Bigg]$$

$$+(A_{21}^{I})_{nk_i}\left(\frac{E^{I}}{1+\nu^{I}}\right)\Bigg[(3-2\nu^{I})\mu_{(n+1)k_i}J_{n}(\mu_{(n+1)k_i}a)$$

$$+\mu_{(n+1)k_i}^{2}\,a\,J_{n+1}(\mu_{(n+1)k_i}a)$$

$$+\frac{\nu^{I}(n+3)-(n+1)\left(n+4(1-\nu^{I})\right)}{1-2\nu^{I}}\frac{J_{n+1}(\mu_{(n+1)k_i}a)}{a}\Bigg]$$

$$+(A_{11}^{II})_{nk_i}\left(\frac{E^{II}}{1+\nu^{II}}\right)\Bigg[-(n-1)\left(n-4(1-\nu^{II})\right)\frac{J_{n-1}(\mu_{(n-1)k_i}a)}{a}$$

$$-\mu_{(n-1)k_i}^{2}\,a\,J_{n-1}(\mu_{(n-1)k_i}a)$$

$$+\frac{(1-\nu^{II})(3-4\nu^{II})-\nu^{II}\mu_{(n-1)k_i}}{1-2\nu^{II}}J_{n}(\mu_{(n-1)k_i}a)\Bigg]$$

$$+(A_{21}^{II})_{nk_i}\left(\frac{E^{II}}{1+\nu^{II}}\right)\Bigg[-(3-2\nu^{II})\mu_{(n+1)k_i}J_{n}(\mu_{(n+1)k_i}a)$$

$$-\mu_{(n+1)k_i}^{2}\,a\,J_{n+1}(\mu_{(n+1)k_i}a)$$

$$-\frac{\nu^{II}(n+3)-(n+1)\left(n+4(1-\nu^{II})\right)}{1-2\nu^{II}}\frac{J_{n+1}(\mu_{(n+1)k_i}a)}{a}\Bigg]$$

$$
\begin{aligned}
&- \left(B_{11}^{I}\right)_{mk}\left(\frac{E^{II}}{1+\nu^{II}}\right)\Big[-(n-1)(n+4(1-\nu^{II}))\,\frac{Y_{n-1}(\mu_{(n-1)k}a)}{a} \\
&\qquad + \mu_{(n-1)k}^{2}\, a\, Y_{n-1}(\mu_{(n-1)k}a) \\
&\qquad - \frac{(1-\nu^{II})(3-4\nu^{II}) - \nu^{II}\mu_{(n-1)k}}{1-2\nu^{II}}\, Y_n(\mu_{(n-1)k}a)\Big] \\
&- \left(B_{21}^{II}\right)_{mk}\left(\frac{E^{II}}{1+\nu^{II}}\right)\Big[(3-2\nu^{II})\,\mu_{(n+1)k}\, Y_n(\mu_{(n+1)k}a) \\
&\qquad + \mu_{(n+1)k}^{2}\, a\, Y_{n+1}(\mu_{(n+1)k}a) \\
&\qquad + \frac{\nu^{II}(n+3) - (n+1)(n+4(1-\nu^{II}))}{1-2\nu^{II}}\, \frac{Y_{n+1}(\mu_{(n+1)k}a)}{a}\Big]
\end{aligned}
$$

$$= 0. \qquad \text{(A46)}$$

Equations (A35) and (A39) yield

$$
\begin{aligned}
&\left(A_{11}^{I}\right)_{mk}\left(\frac{E^{I}}{1+\nu^{I}}\right)\Big[(n-1)(n-4(1-\nu^{I}))\,\frac{J_{n-1}(\mu_{(n-1)k}a)}{a} \\
&\qquad - \mu_{(n-1)k}(n-2(1-\nu^{I}))\, J_n(\mu_{(n-1)k}a)\Big] \\
&+ \left(A_{21}^{I}\right)_{mk}\left(\frac{E^{I}}{1+\nu^{I}}\right)\Big[\mu_{(n+1)k}(n+2(1-\nu^{I}))\, J_{n+1}(\mu_{(n+1)k}a) \\
&\qquad - \mu_{(n+1)k}^{2}\, J_n(\mu_{(n+1)k}a)\Big]
\end{aligned}
$$

$$-\left(A_{11}^{II}\right)_{nk}\left(\frac{E^{II}}{1+\nu^{II}}\right)\left[(n-1)(n-4(1-\nu^{II}))\,\frac{J_{n-1}(\mu_{(n-1)k}a)}{a}\right.$$

$$\left.-\mu_{(n-1)k}(n-2(1-\nu^{II}))\,J_n(\mu_{(n-1)k}a)\right]$$

$$-\left(A_{21}^{II}\right)_{nk}\left(\frac{E^{II}}{1+\nu^{II}}\right)\left[-(n+1)\,\frac{J_{n+1}(\mu_{(n+1)k}a)}{a}+\mu_{(n+1)k}(n+2(1-\nu^{II}))\cdot\right.$$

$$\left.\cdot J_n(\mu_{(n+1)k}a)\right]$$

$$-\left(B_{11}^{II}\right)_{nk}\left(\frac{E^{II}}{1+\nu^{II}}\right)\left[(n-1)(n-4(1-\nu^{II})\,Y_{n-1}(\mu_{(n-1)k}a)/a\right.$$

$$\left.-\mu_{(n-1)k}(n-2(1-\nu^{II}))\,Y_n(\mu_{(n-1)k}a)\right]$$

$$-\left(B_{21}^{II}\right)_{nk}\left(\frac{E^{II}}{1+\nu^{II}}\right)\left[-(n+1)\,\frac{Y_{n+1}(\mu_{(n+1)k}a)}{a}\right.$$

$$\left.+\mu_{(n+1)k}(n+2(1-\nu^{II}))\,J_n(\mu_{(n+1)k}a)\right]$$

$$=0. \qquad \text{(A47)}$$

Equations (A36) and (A39) yield

$$\left(A_{11}^{I}\right)_{nk}\left(\frac{E^{I}}{1+\nu^{I}}\right)\left[\mu_{(n-1)k}^{2}\,a\,J_n(\mu_{(n-1)k}a)\right.$$

$$\left.+\mu_{(n-1)k}(2(1-\nu^{I})-n)J_{n-1}(\mu_{(n-1)k}a)\right]$$

$$+\left(A_{21}^{I}\right)_{nk}\left(\frac{E^{I}}{1+\nu^{I}}\right)\left[\mu_{(n+1)k}(n+2(1-\nu^{I}))J_{n+1}(\mu_{(n+1)k}a)\right.$$

$$\left.-\mu_{(n+1)k}^{2}J_n(\mu_{(n+1)k}a)\right]$$

$$+(A_{11}^{II})_{n\alpha}\left(\frac{-E^{I}}{1+\nu^{II}}\right)\Big[\mu_{(n-\alpha)}^{2}\,a\,J_n(\mu_{(n-\alpha)}a)$$
$$+\mu_{(n-\alpha)}(2(1-\nu^{II})-n)J_{n-1}(\mu_{(n-\alpha)}a)\Big]$$
$$+(A_{21}^{II})_{n\alpha}\left(\frac{-E^{I}}{1+\nu^{II}}\right)\Big[\mu_{(n+\alpha)}(n+2(1-\nu^{II}))J_{n+1}(\mu_{(n+\alpha)}a)$$
$$-\mu_{(n+\alpha)}^{2}J_n(\mu_{(n+\alpha)}a)\Big]$$
$$+(B_{11}^{II})_{n\alpha}\left(\frac{-E^{I}}{1+\nu^{II}}\right)\Big[\mu_{(n-\alpha)}^{2}\,a\,Y_n(\mu_{(n-\alpha)}a)$$
$$+\mu_{(n-\alpha)}(2(1-\nu^{II})-n)\,Y_{n-1}(\mu_{(n-\alpha)}a)\Big]$$
$$+(B_{21}^{II})_{n\alpha}\left(\frac{-E^{I}}{1+\nu^{II}}\right)\Big[\mu_{(n+\alpha)}(n+2(1-\nu^{II}))\,Y_{n+1}(\mu_{(n+\alpha)}a)$$
$$-\mu_{(n+\alpha)}^{2}\,Y_n(\mu_{(n+\alpha)}a)\Big]$$

$$=0. \qquad \text{(A48)}$$

Equations (A29) and (A41) yield

$$(A_{11}^{II})_{n\alpha}\Big[(n+2-4\nu^{II})\,J_{n-1}\left(\mu_{(n-\alpha)}\frac{c_0}{\cos\phi}\right)$$
$$+\mu_{(n-\alpha)}\frac{c_0}{\cos\phi}J_{n-2}\left(\mu_{(n-\alpha)}\frac{c_0}{\cos\phi}\right)\Big]$$
$$+(A_{21}^{II})_{n\alpha}\Big[(n+4(1-\nu^{II}))\,J_{n+1}\left(\mu_{(n+\alpha)}\frac{c_0}{\cos\phi}\right)$$
$$+\mu_{(n+\alpha)}\frac{c_0}{\cos\phi}J_n\left(\mu_{(n+\alpha)}\frac{c_0}{\cos\phi}\right)$$

$$+\left(B_{11}^{II}\right)_{nk}\left[(n+2-4\nu^{II})\,Y_{n-1}\left(\mu_{(n-1)k}\frac{c_0}{\cos\phi}\right)\right.$$
$$\left.+\mu_{(n-1)k}\frac{c_0}{\cos\phi}\,Y_{n-2}\left(\mu_{(n-1)k}\frac{c_0}{\cos\phi}\right)\right]$$
$$+\left(B_{21}^{II}\right)_{nk}\left[(n+4(1-\nu^{II}))\,Y_{n+1}\left(\mu_{(n+1)k}\frac{c_0}{\cos\phi}\right)\right.$$
$$\left.+\mu_{(n+1)k}\frac{c_0}{\cos\phi}\,Y_n\left(\mu_{(n+1)k}\frac{c_0}{\cos\phi}\right)\right]$$

$$= \begin{cases} \dfrac{6\varepsilon(-1)^{(k-1)/2}}{k\pi^2}\log 3 \\ \dfrac{24\varepsilon}{k\pi^2}(-1)^{\frac{k-1}{2}}\displaystyle\sum_{i=1}^{m}\frac{(-1)^{i+1}\,8}{(6i-1)(6i-3)(6i-5)}+(-1)^m\frac{1}{2}\log 3 \end{cases} \tag{A49}$$

$$\begin{cases} \dfrac{24\varepsilon}{k\pi^2}(-1)^{\frac{k-1}{2}}\displaystyle\sum_{i=1}^{m}\frac{(-1)^{i}\,8}{(6i-1)(6i-3)(6i-5)}+(-1)^m\frac{1}{2}\log 3 \end{cases} \tag{A50}$$

$$\left(Q_{11}^{I}\right)_{nk}=\left(Q_{11}^{III}\right)_{nk}=\left(R_{11}^{III}\right)_{nk}=0.$$

From equations (A37) and (A40), we get

$$\mu_k=\frac{ik\pi}{2l}, \qquad k=1,3,5,\cdots. \tag{A51}$$

Equations (A34) and (A39) give

$$\left(A_{11}^{I}\right)_{no}\left(4(1-\nu^{I})-n\right)(n-1)\,a^{n-2}\frac{E^{I}}{1+\nu^{I}}$$

$$+\left(A_{11}^{II}\right)_{no}\left(4(1-\nu^{II})-n\right)(n-1)\,a^{n-2}\left(-\frac{E^{II}}{1+\nu^{II}}\right)$$

$$+\left(B_{21}^{II}\right)_{no}\left(4(1-\nu^{II})-n\right)(n+1)\,a^{-n-2}\left(-\frac{E^{II}}{1+\nu^{II}}\right)=0 \qquad \text{(A52)}$$

and

$$\left(A_{21}^{I}\right)_{00}2\frac{E^{I}}{1+\nu^{I}}+\left(Q_{11}^{I}\right)_{00}2\frac{E^{I}\nu^{I}}{1+\nu^{I}}$$

$$-\left(A_{21}^{II}\right)_{00}2\frac{E^{II}}{1+\nu^{II}}+\left(B_{21}^{II}\right)_{00}2\frac{E^{II}}{1+\nu^{II}}-\left(Q_{11}^{II}\right)_{00}\frac{2E^{II}\nu^{II}}{1+\nu^{II}}$$

$$=\frac{E^{II}}{1-2\nu^{II}}\beta^{I}-\frac{E^{I}}{1-2\nu^{I}}\beta^{I}. \qquad \text{(A53)}$$

Equations (A35) and (A39) yield

$$\left(A_{11}^{I}\right)_{no}\left(\frac{E^{I}}{1+\nu^{I}}\right)n\left(n-4(1-\nu^{I})\right)a^{n-2}$$

$$-\left(A_{11}^{II}\right)_{no}\left(\frac{E^{II}}{1+\nu^{II}}\right)n\left(n-4(1-\nu^{II})\right)a^{n-2}$$

$$+\left(B_{21}^{II}\right)_{no}\left(\frac{E^{II}}{1+\nu^{II}}\right)n\left(n+4(1-\nu^{II})\right)a^{-n-2}$$

$$=0. \qquad \text{(A54)}$$

Equations (A37) and (A39) give

$$\left(A_{21}^{I}\right)_{00} 4\nu^{I}(1-2\nu^{I}) + \left(Q_{11}^{I}\right)_{00} 2(1-2\nu^{I}) = -(1+\nu^{I})\beta^{I} \tag{A55}$$

and

$$\left(A_{21}^{I}\right)_{00} 4\nu^{I}(1-2\nu^{II}) + \left(Q_{11}^{II}\right)_{00} 2(1-2\nu^{I}) = -(1+\nu^{II})\beta^{II}. \tag{A56}$$

Equations (A30), (A31), (A39), and (A40) give

$$\left(A_{11}^{I}\right)_{no} (n-4(1-\nu^{I}))\, a^{n-1}$$

$$-\left(A_{11}^{I}\right)_{no} (n-4(1-\nu^{II}))\, a^{n-1} - \left(B_{21}^{II}\right)_{no} (n+4(1-\nu^{II}))\, a^{-n-1}$$

$$= 0. \tag{A57}$$

Equations (A29) and (A42) yield

$$\left(A_{11}^{II}\right)_{no} (4(1-\nu^{I})-n)\left(\frac{c_0}{\cos\phi}\right)^{n-1}$$

$$+\left(B_{21}^{II}\right)_{no} (4(1-\nu^{II})+n)\left(\frac{c_0}{\cos\phi}\right)^{-n-1}$$

$$= \begin{cases} \dfrac{6\epsilon}{\pi}\displaystyle\sum_{i=1}^{m} \dfrac{(-1)^{i} 8}{(6i-1)(6i-3)(6i-5)} + (-1)^{m}\dfrac{1}{2}\log 3\left(\dfrac{6\epsilon}{\pi}\right) \\ \qquad\qquad m = \text{odd} \\ \dfrac{6\epsilon}{\pi}\displaystyle\sum_{i=1}^{m} \dfrac{(-1)^{i} 8}{(6i-1)(6i-3)(6i-5)} + (-1)^{m}\dfrac{1}{2}\log 3\left(\dfrac{6\epsilon}{\pi}\right) \\ \qquad\qquad m = \text{even} \end{cases} \tag{A58}$$

and

$$(A^{II}_{21})_{00}\, 2(1-2\nu^{II})\left(\frac{c_0}{\cos\phi}\right) + (B^{II}_{21})_{00}\left(\frac{c_0}{\cos\phi}\right) \qquad \text{(A59)}$$

$$= \frac{3\epsilon}{\Gamma}\log 3 .$$

Transformation of Coordinate Systems

One has the following transformation:

$$
\begin{aligned}
(x, y, z) &\longrightarrow (r, \phi, \bar{z}) \\
(p_x, p_y, p_z) &\longrightarrow (p_1, p_2, p_3) \qquad \text{(A60)} \\
(u, v, w) &\longrightarrow (\xi_1, \xi_2, \xi_3)
\end{aligned}
$$

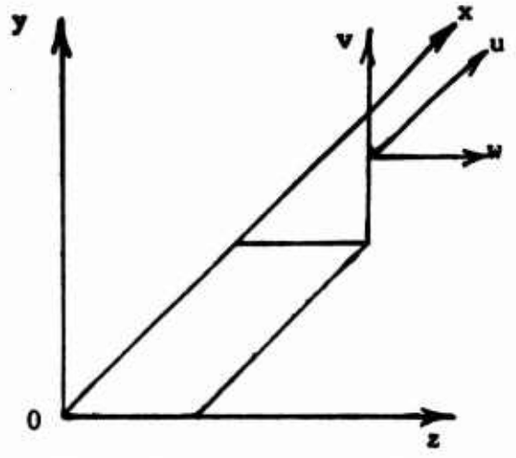

Cartesian Coordinate System

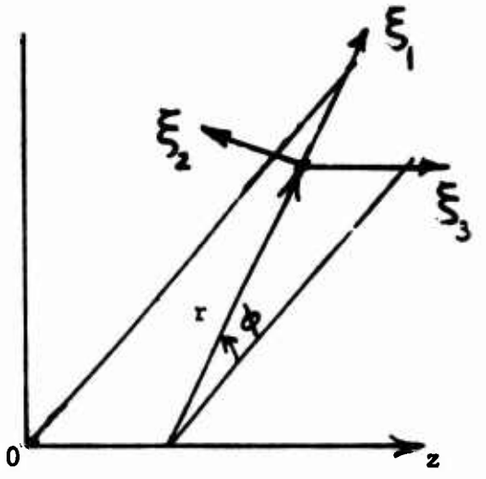

Cylindrical Coordinate System

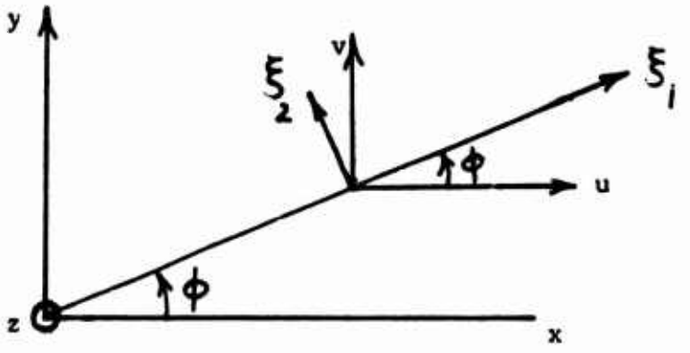

The transformation relationships are as follows:

$$\begin{cases} x = r\cos\phi \\ y = r\sin\phi \\ z = \bar{z} \end{cases} \tag{A61}$$

$$\begin{cases} r = \sqrt{x^2+y^2} \\ \phi = \tan^{-1}\left(\frac{y}{x}\right) \end{cases} \tag{A62}$$

$$\frac{\partial r}{\partial x} = \frac{1}{2}\frac{2x}{\sqrt{x^2+y^2}} = \frac{x}{r} = \cos\phi \tag{A63}$$

$$\frac{\partial r}{\partial y} = \frac{1}{2}\frac{2y}{\sqrt{x^2+y^2}} = \frac{y}{r} = \sin\phi \tag{A64}$$

$$\frac{\partial \phi}{\partial x} = \frac{-y/x^2}{1+y^2/x^2} = -\frac{y}{x^2+y^2} = -\frac{\sin\phi}{r} \tag{A65}$$

$$\frac{\partial \phi}{\partial y} = \frac{1/x}{1+y^2/x^2} = \frac{x}{x^2+y^2} = \frac{\cos\phi}{r}. \tag{A66}$$

From equations (A63) to (A66), we get

$$\frac{\partial}{\partial x} = \frac{\partial r}{\partial x}\frac{\partial}{\partial r} + \frac{\partial \phi}{\partial x}\frac{\partial}{\partial \phi} + \frac{\partial \bar{z}}{\partial x}\frac{\partial}{\partial \bar{z}}$$

$$= \cos\phi \frac{\partial}{\partial r} - \frac{\sin\phi}{r}\frac{\partial}{\partial \phi} \qquad \text{(A67)}$$

$$\frac{\partial}{\partial y} = \frac{\partial r}{\partial y}\frac{\partial}{\partial r} + \frac{\partial \phi}{\partial y}\frac{\partial}{\partial \phi} + \frac{\partial \bar{z}}{\partial y}\frac{\partial}{\partial \bar{z}}$$

$$= \sin\phi \frac{\partial}{\partial r} + \frac{\cos\phi}{r}\frac{\partial}{\partial \phi} \qquad \text{(A68)}$$

$$\frac{\partial}{\partial z} = \frac{\partial r}{\partial z}\frac{\partial}{\partial r} + \frac{\partial \phi}{\partial z}\frac{\partial}{\partial \phi} + \frac{\partial \bar{z}}{\partial z}\frac{\partial}{\partial \bar{z}}$$

$$= \frac{\partial}{\partial \bar{z}}. \qquad \text{(A69)}$$

The relationships between two coordinate systems for displacements and Papkovitch functions are

$$\begin{aligned} u &= \xi_1 \cos\phi - \xi_2 \sin\phi \\ v &= \xi_1 \sin\phi + \xi_2 \cos\phi \\ w &= \xi_3 \end{aligned} \qquad \text{(A70)}$$

$$\begin{aligned} P_x &= P_1 \cos\phi - P_2 \sin\phi \\ P_y &= P_1 \sin\phi + P_2 \cos\phi \\ P_z &= P_3 . \end{aligned} \qquad \text{(A71)}$$

Combination of equations (A3), (A70), and (A71), and dropping the P_o term yields

$$
\begin{aligned}
u &= \xi_1 \cos\phi - \xi_2 \sin\phi \\
&= P_1 \cos\phi - P_2 \sin\phi \\
&\quad - \frac{1}{4(1-\nu)} \left\{ \cos\phi \frac{\partial}{\partial r} \left[r\cos\phi (P_1 \cos\phi - P_2 \sin\phi) \right.\right. \\
&\qquad \left. + r \sin\phi (P_1 \sin\phi + P_2 \cos\phi) + \bar{z} P_3 \right] \\
&\quad - \frac{\sin\phi}{r} \frac{\partial}{\partial\phi} \left[r\cos\phi (P_1 \cos\phi - P_2 \sin\phi) \right. \\
&\qquad \left.\left. + r \sin\phi (P_1 \sin\phi + P_2 \cos\phi) + \bar{z} P_3 \right] \right\} \\
&= P_1 \cos\phi - P_2 \sin\phi \\
&\quad - \frac{1}{4(1-\nu)} \left\{ \cos\phi \frac{\partial}{\partial r} \left[r P_1 + \bar{z} P_3 \right] \right. \\
&\qquad \left. - \frac{\sin\phi}{r} \frac{\partial}{\partial\phi} \left[r P_1 + \bar{z} P_3 \right] \right\} . \qquad \text{(A72)}
\end{aligned}
$$

Similarly, combination of equations (A4), (A70), and (A71), and dropping the P_o term yields

$$V = \xi_1 \sin\phi + \xi_2 \cos\phi$$

$$= P_1 \sin\phi + P_2 \cos\phi$$

$$- \frac{1}{4(1-\nu)} \left\{ \sin\phi \frac{\partial}{\partial r}\left[r P_1 + z P_3 \right] + \frac{\cos\phi}{r} \frac{\partial}{\partial \phi}\left[r P_1 + z P_3 \right] \right\} . \qquad \text{(A73)}$$

Multiplying (A72) by $\cos\phi$ and (A73) by $\sin\phi$, adding together, and then making use of the trigonometric identity $\sin^2\phi + \cos^2\phi = 1$, one gets

$$\xi_1 = P_1 - \frac{1}{4(1-\nu)} \left\{ \frac{\partial}{\partial r}\left[r P_1 + z P_3 \right] \right\} . \qquad \text{(A74)}$$

Similarly,

$$\xi_2 = P_2 - \frac{1}{4(1-\nu)} \left\{ \frac{1}{r} \frac{\partial}{\partial \phi}\left[r P_1 + z P_3 \right] \right\} \qquad \text{(A75)}$$

$$\xi_3 = P_3 - \frac{1}{4(1-\nu)} \left\{ \frac{\partial}{\partial z}\left[r P_1 + z P_3 \right] \right\} \qquad \text{(A76)}$$

Fourier Representation of Boundary Condition Equation at the Outer Surface of the Hexagon

At the outer surface of the hexagon, one has

$$\xi_1^{II}\left(\frac{c_0}{\cos\phi}, \phi, z\right)\cos\phi - \xi_2^{II}\left(\frac{c_0}{\cos\phi}, \phi, z\right)\sin\phi = \varepsilon \qquad \text{(A77)}$$

or

$$\xi_1^{II}\left(\frac{c_0}{\cos\phi}, \phi, z\right) \doteq \varepsilon \sec\phi. \qquad \text{(A78)}$$

We want to represent

$$\begin{aligned}\varepsilon \sec\phi &= \sum_{m=0}^{\infty}\left\{\sum_{k=0}^{\infty}\alpha_{mk}\cos\left(\frac{k\pi z}{2l}\right)\right\}\cos(6m\phi) \\ &= \alpha_{00} + \sum_{\substack{m=1\\(k=0)}}^{\infty}\alpha_{m0}\cos(6m\phi) \\ &\quad + \sum_{\substack{k=1\\(m=0)}}^{\infty}\alpha_{0k}\cos\left(\frac{k\pi z}{2l}\right) \\ &\quad + \sum_{m=1}^{\infty}\sum_{k=1}^{\infty}\alpha_{mk}\cos\left(\frac{k\pi z}{2l}\right)\cos(6m\phi).\end{aligned} \qquad \text{(A79)}$$

Now define a function

$$f(z,\phi) = \begin{cases} \varepsilon\sec\phi, & \left\{\begin{matrix} 0 < z < l \\ 0 < \phi < \pi/6 \end{matrix}\right\} \\ 0, & \left\{\begin{matrix} l < z < 2l \\ 0 < \phi < \pi/6 \end{matrix}\right\} \end{cases} \qquad \text{(A80)}$$

The coefficients of the Fourier representation are as follows:

1) α_{oc}

$$\int_0^{\pi/6}\int_0^{l} \Sigma \sec\phi \, dz \, d\phi = \int_0^{\pi/6}\int_0^{2l} \alpha_{oo} \, dz \, d\phi \qquad \text{(A81)}$$

$$\alpha_{oo} = \frac{3\varepsilon}{\pi}\int_0^{\pi/6} \sec\phi \, d\phi = \frac{3\varepsilon}{\pi}\left[\frac{1}{2}\log\frac{1+\sin\phi}{1-\sin\phi}\right]_0^{\pi/6}$$

$$= \frac{1.5\log 3}{\pi}\varepsilon \qquad \text{(A82)}$$

2) α_{mo}

$$\int_0^{\pi/6}\int_0^{l} \varepsilon \sec\phi \cos(6m\phi) dz \, d\phi \qquad \text{(A83)}$$

$$= \int_0^{\pi/6}\int_0^{2l} \alpha_{mo} \frac{1-\cos(12m\phi)}{2} dz d\phi$$

$$\alpha_{mo} = \frac{6\varepsilon}{\pi}\int_0^{\pi/6} \frac{\cos(6m\phi)}{\cos\phi} d\phi$$

$$= \frac{6\varepsilon}{\pi}\left[\int_0^{\pi/6} 2\cos(6m-1)\phi d\phi - \int_0^{\pi/6} \frac{\cos(6m-2)\phi}{\cos\phi} d\phi\right]$$

$$= \left[\frac{2\sin[(6m-1)\pi/6]}{6m-1} - \int_0^{\pi/6} 2\cos(6m-3)\phi d\phi \right.$$

$$\left. + \int_0^{\pi/6} \frac{\cos(6m-4)\phi}{\cos\phi} d\phi\right]\frac{6\varepsilon}{\pi} \qquad \text{(A84)}$$

$$\alpha_{m0} = \left[\frac{2\sin[(6m-1)\pi/6]}{6m-1} - \frac{2\sin[(6m-3)\pi/6]}{6m-3} + \frac{2\sin[(6m-5)\pi/6]}{6m-5} - \int_0^{\pi/6} \frac{\cos[(6m-6)\phi]}{\cos\phi}\, d\phi\right]\frac{6\varepsilon}{\pi}$$

$$= \left[\frac{1}{6m-1} - \frac{2}{6m-3} + \frac{1}{6m-5} - \int_0^{\pi/6} \frac{\cos(6m-6)\phi}{\cos\phi}\, d\phi\right]\frac{6\varepsilon}{\pi}$$

$$= \frac{6\varepsilon}{\pi}\left[\frac{8}{(6m-1)(6m-3)(6m-5)} - \int_0^{\pi/6} \frac{\cos(6m-6)\phi}{\cos\phi}\, d\phi\right].$$

(A85)

When $m = 1$,

$$\frac{6\varepsilon}{\pi}\int_0^{\pi/6} \frac{\cos(6\phi)}{\cos\phi}\, d\phi = \frac{6\varepsilon}{\pi}\left[\frac{8}{5\cdot 3\cdot 1} - \frac{1}{2}\log 3\right]. \qquad \text{(A86)}$$

When $m = 2$,

$$\frac{6\varepsilon}{\pi}\int_0^{\pi/6} \frac{\cos(12\phi)}{\cos\phi}\, d\phi = \left[\frac{8}{11\cdot 9\cdot 7} - \int_0^{\pi/6} \frac{\cos(6\phi)}{\cos\phi}\, d\phi\right]\frac{6\varepsilon}{\pi}$$

$$= \frac{6\varepsilon}{\pi}\left[\frac{8}{11\cdot 9\cdot 7} - \frac{8}{5\cdot 3\cdot 1} + \frac{1}{2}\log 3\right].$$

(A87)

Continuing to assume numbers, one gets

$$\alpha_{m0} = \frac{6\varepsilon}{\pi}\left[\frac{8}{(6m-1)(6m-3)(6m-5)} - \frac{8}{(6m-7)(6m-9)(6m-11)}\right.$$

$$+ \frac{8}{(6m-13)(6m-15)(6m-17)} - \cdots$$

$$\left. + (-1)^m \frac{1}{2}\log 3\right]$$

$$= \begin{cases} \frac{6\varepsilon}{\pi}\left[\sum_{i=1}^{m} \frac{(-1)^{i+1} 8}{(6i-1)(6i-3)(6i-5)} + (-1)^m \frac{1}{2}\log 3\right] \\ \qquad \text{when } m = \text{odd} \\ \frac{6\varepsilon}{\pi}\left[\sum_{i=1}^{m} \frac{(-1)^{i} 8}{(6i-1)(6i-3)(6i-5)} + (-1)^m \frac{1}{2}\log 3\right] \\ \qquad \text{when } m = \text{even} \end{cases} \tag{A88}$$

3) α_{0N}

$$\int_0^{\pi/b}\int_0^{l} \varepsilon \sec\phi \cos\frac{b\pi z}{2l}\, dz\, d\phi = \alpha_{0N}\int_0^{\pi/b}\int_0^{l} \frac{1+\cos\frac{b\pi z}{l}}{2}\, dz\, d\phi \tag{A89}$$

$$\alpha_{0N} = \frac{6\varepsilon}{b\pi^2}\log 3 \sin\frac{b\pi}{2} \tag{A90}$$

$$\alpha_{0k} = \begin{cases} \dfrac{6\epsilon(-1)^{\frac{k-1}{2}}}{k\pi^2}\log 3 & \text{when } k = \text{odd} \\ 0 & \text{when } k = \text{even} \end{cases} \qquad \text{(A91)}$$

4) α_{mk}

$$\int_0^{\pi/6}\int_0^{l} \epsilon \sec\phi \cos\left(\frac{k\pi z}{2l}\right)\cos(6m\phi)\, dz\, d\phi$$

$$= \alpha_{mk}\int_0^{\pi/6}\int_0^{2l} \frac{1}{4}\, dz\, d\phi \qquad \text{(A92)}$$

$$\alpha_{mk} = \frac{24\epsilon}{2l\pi}\int_0^{\pi/6} \frac{\cos(6m\phi)}{\cos\phi}\, d\phi \int_0^{l} \cos\frac{k\pi z}{2l}\, dz$$

$$= \begin{cases} \dfrac{24\epsilon}{k\pi^2}(-1)^{\frac{k-1}{2}}\displaystyle\int_0^{\pi/6} \frac{\cos(6m\phi)}{\cos\phi}\, d\phi & \text{when } k = \text{odd} \\ 0 & \text{when } k = \text{even} \end{cases}$$

$$= \begin{cases} \left[\dfrac{24\epsilon}{k\pi^2}(-1)^{\frac{k-1}{2}}\right]\left[\displaystyle\sum_{i=1}^{m} \frac{(-1)^{i+1}8}{(6i-1)(6i-3)(6i-5)} + (-1)^m\frac{1}{2}\log 3\right] & \text{when } m = \text{odd} \\ \left[\dfrac{24\epsilon}{k\pi^2}(-1)^{\frac{k-1}{2}}\right]\left[\displaystyle\sum_{i=1}^{m} \frac{(-1)^{i}8}{(6i-1)(6i-3)(6i-5)} + (-1)^m\frac{1}{2}\log 3\right] & \text{when } m = \text{even}. \end{cases} \qquad \text{(A93)}$$

PLANE STRESS FIELDS WITHOUT POLAR SYMMETRY

The solution to the biharmonic function in cylindrical coordinates, for the stress fields without polar symmetry, is

$$L = \sum_{n=6,12,\cdots}^{\infty} \left(A_{1n} r^{n} + A_{2n} r^{n+2} + A_{3n} r^{-n} + A_{4n} r^{-n+2}\right)\cos(n\phi) + A_5 \log r + A_6 r^2 + A_7 \phi \cdot \tag{A94}$$

Then, the stresses and displacements are as follows:

$$\sigma_{11} = \sum_{n=6,12,\cdots}^{\infty} \left[A_{1n} F_{1n}(r) + A_{2n} F_{2n}(r) + A_{3n} F_{3n}(r) + A_{4n} F_{4n}(r)\right]\cos(n\phi) + A_5 r^{-2} + 2A_6 + \frac{E^{II}\beta^{II}}{1-2\nu^{II}} \tag{A95}$$

$$\sigma_{22} = \sum_{n=6,12,\cdots}^{\infty} \left[A_{1n} F_{5n}(r) + A_{2n} F_{6n}(r) + A_{3n} F_{7n}(r) + A_{4n} F_{8n}(r)\right]\cos(n\phi) - A_5 r^{-2} + 2A_6 + \frac{E^{II}\beta^{II}}{1-2\nu^{II}} \tag{A96}$$

$$\sigma_{12} = \sum_{n=6,12,\cdots}^{\infty} \left[A_{1n} F_{9n}(r) + A_{2n} F_{10n}(r) + A_{3n} F_{11n}(r) + A_{4n} F_{12n}(r)\right]\sin(n\phi) + A_7 r^{-2} \tag{A97}$$

$$\xi_1 = \sum_{n=6,12,\cdots}^{\infty} \left[A_{1n} F_{13n}(r) + A_{2n} F_{14n}(r) + A_{3n} F_{15n}(r) + A_{4n} F_{16n}(r)\right]\cos(n\phi) - A_5(1+\nu) r^{-1}/E + 2(1-\nu)A_6 r/E \tag{A98}$$

$$\xi_2 = \sum_{n=0,2,n1}^{\infty} \left[A_{1n} F_{1n}(r) + A_{2n} F_{2n}(r) + A_{3n} F_{3n}(r) + A_{4n} F_{4n}(r) \right] \sin(n\phi) + (1+\nu) A_7 r^{-1} \qquad \text{(A99)}$$

where F(r)'s are functions of r only and are defined in the next section.

Definitions of F(r)

$$F_{1n}(r) = -(n-1) n r^{n-2} \qquad \text{(A100)}$$

$$F_{2n}(r) = -(n-2)(n+1) r^{n} \qquad \text{(A101)}$$

$$F_{3n}(r) = -n(n+1) r^{-n-2} \qquad \text{(A102)}$$

$$F_{4n}(r) = -(n-1)(n+2) r^{-n} \qquad \text{(A103)}$$

$$F_{5n}(r) = (n-1) n r^{n-2} \qquad \text{(A104)}$$

$$F_{6n}(r) = (n+1)(n+2) r^{n} \qquad \text{(A105)}$$

$$F_{7n}(r) = n(n+1) r^{-n-2} \qquad \text{(A106)}$$

$$F_{8n}(r) = (n-2)(n-1) r^{-n} \qquad \text{(A107)}$$

$$F_{9n}(r) = (n-1)-n\,r^{n-2} \tag{A108}$$

$$F_{10n}(r) = n(n+1)\,r^{n} \tag{A109}$$

$$F_{11n}(r) = -n(n+1)\,r^{-n-2} \tag{A110}$$

$$F_{12n}(r) = -(n-1)n\,r^{-n} \tag{A111}$$

$$F_{13n}(r) = -\frac{n(1+\nu)}{E}\,r^{n-1} \tag{A112}$$

$$F_{14n}(r) = -\frac{n(1+\nu)-2(1-\nu)}{E}\,r^{n+1} \tag{A113}$$

$$F_{15n}(r) = -\frac{n(1+\nu)}{E}\,r^{-n-1} \tag{A114}$$

$$F_{16n}(r) = \frac{n(1+\nu)+2(1-\nu)}{E}\,r^{-n+1} \tag{A115}$$

$$F_{17n}(r) = \frac{n(1+\nu)}{E}\,r^{n-1} \tag{A116}$$

$$F_{18n}(r) = \frac{n(1+\nu)+4}{E}\,r^{n+1} \tag{A117}$$

$$F_{19n}(r) = \frac{n(1+\nu)}{E}\,r^{-n-1} \tag{A118}$$

$$F_{20n}(r) = \frac{n(1+\nu)-4}{E}\,r^{-n+1} \tag{A119}$$

Boundary Conditions for n = 6, 12, 18, . . .

1. At the interface, the stresses and displacements should be continuous; i.e.,

a. $$\sigma_{11}^{I}(a,\phi) = \sigma_{11}^{II}(a,\phi)$$

$$A_{1n}^{I}F_{1n}^{I}(a) + A_{2n}^{I}F_{2n}^{I}(a) - A_{1n}^{II}F_{1n}^{II}(a) - A_{2n}^{II}F_{2n}^{II}(a)$$
$$- A_{3n}^{II}F_{3n}^{II}(a) - A_{4n}^{II}F_{4n}^{II}(a) = 0 \qquad \text{(A120)}$$

b. $$\sigma_{12}^{I}(a,\phi) = \sigma_{12}^{II}(a,\phi)$$

$$A_{1n}^{I}F_{9n}^{I}(a) + A_{2n}^{I}F_{10n}^{I}(a) - A_{1n}^{II}F_{9n}^{II}(a) - A_{2n}^{II}F_{10n}^{II}(a)$$
$$- A_{3n}^{II}F_{11n}^{II}(a) - A_{4n}^{II}F_{12n}^{II}(a) = 0 \qquad \text{(A121)}$$

c. $$\xi_{1}^{I}(a,\phi) = \xi_{1}^{II}(a,\phi)$$

$$A_{1n}^{I}F_{13n}^{I}(a) + A_{2n}^{I}F_{14n}^{I}(a) - A_{1n}^{II}F_{13n}^{II}(a) - A_{2n}^{II}F_{14n}^{II}(a)$$
$$- A_{3n}^{II}F_{15n}^{II}(a) - A_{4n}^{II}F_{16n}^{II}(a) = 0 \qquad \text{(A122)}$$

d.

$$\xi_2^{I}(a,\phi) = \xi_2^{II}(a,\phi)$$

$$A_{1n}^{I} F_{17n}^{I}(a) + A_{2n}^{I} F_{18n}^{I}(a) - A_{1n}^{II} F_{17n}^{II}(a) - A_{2n}^{II} F_{18n}^{II}(a)$$
$$- A_{3n}^{II} F_{19n}^{II}(a) - A_{4n}^{II} F_{20n}^{II}(a) = 0. \qquad \text{(A123)}$$

2. At the outer surface of resin, it should remain a regular hexagon after deformation; i.e.,

$$\xi_1^{II}\left(\frac{c_0}{\cos\phi}, \phi\right)\cos\phi = \varepsilon$$

$$A_{1n}^{II} F_{13n}^{II}\left(\frac{c_0}{\cos\phi}\right) + A_{2n}^{II} F_{14n}^{II}\left(\frac{c_0}{\cos\phi}\right) + A_{3n}^{II} F_{15n}^{II}\left(\frac{c_0}{\cos\phi}\right)$$
$$+ A_{4n}^{II} F_{16n}^{II}\left(\frac{c_0}{\cos\phi}\right) = \begin{cases} \dfrac{6\varepsilon}{\pi}\left[\displaystyle\sum_{i=1}^{m} \frac{(-1)^{i+1} 8}{(6i-1)(6i-3)(6i-5)} + (-1)^m \frac{1}{2}\log 3\right] \\ \qquad \text{when } m = \text{odd} \\ \dfrac{6\varepsilon}{\pi}\left[\displaystyle\sum_{i=1}^{m} \frac{(-1)^{i} 8}{(6i-1)(6i-3)(6i-5)} + (-1)^m \frac{1}{2}\log 3\right] \\ \qquad \text{when } m = \text{even} \end{cases} \qquad \text{(A124)}$$

$$n = 6m, \quad m = 1, 2, 3, \cdots$$

and $\xi_1^{II}(0, c_0) = \xi_1^{II}(\pi/6,\ c_0/\cos\pi/6)\cos\pi/6$

$$A_{1n}^{II} F_{13n}^{II}(c_0) + A_{2n}^{II} F_{14n}^{II}(c_0) + A_{3n}^{II} F_{15n}^{II}(c_0) + A_{4n}^{II} F_{16n}^{II}(c_0)$$

$$- \frac{\sqrt{3}}{2}\left[A_{1n}^{II} F_{13n}^{II}\left(\frac{c_0}{\cos\pi/6}\right) + A_{2n}^{II} F_{14n}^{II}\left(\frac{c_0}{\cos\pi/6}\right) + A_{3n}^{II} F_{15n}^{II}\left(\frac{c_0}{\cos\pi/6}\right) \right.$$

$$\left. + A_{4n}^{II} F_{16n}^{II}\left(\frac{c_0}{\cos\pi/6}\right)\right] \cos\left(\frac{n\pi}{6}\right) = 0$$

$n = 6, 12, 18, \cdots$ (A125)

Boundary Conditions for n = 0

1. At the interface, the stresses and displacements should continue.

a. $$\sigma_{11}^{I}(a,0) = \sigma_{11}^{II}(a,0) .$$

It implies

$$A_5^{I} = 0 \tag{A126}$$

and

$$2A_6^{I} - 2A_6^{II} - A_5^{II} a^{-2} = \frac{E^{I}\beta^{I}}{1-2\nu^{I}} . \tag{A127}$$

b. $$\sigma_{12}^{I}(a,\phi) = \sigma_{12}^{II}(a,\phi) .$$

It implies

$$A_7^{I} = A_7^{II} = 0 . \tag{A128}$$

c. $$\xi_1^{I}(a,\phi) - \xi_1^{II}(a,\phi) = 0 .$$

This yields

$$A_6^{I}\frac{2(1-\nu^{I})a}{E^{I}} - A_6^{II}\frac{2(1-\nu^{II})a}{E^{II}} + A_5^{II}\frac{(1+\nu^{II})a^{-1}}{E^{II}} = 0 . \tag{A129}$$

2. At the outer surface, the hexagon remains regular after deformation.

$$A_5^{II}\left[-\frac{1+\nu^{II}}{E^{II}}\left(\frac{c_0}{\cos\phi}\right)^{-1}\right]+A_6^{II}\left[\frac{2(1-\nu^{II})}{E^{II}}\left(\frac{c_0}{\cos\phi}\right)\right]$$

$$=\frac{3\epsilon}{\pi}\log 3. \qquad \text{(A130)}$$

3. Comparison of Two Reference Systems

With reference to the original position of a particle before shrinkage, the shrinkage stress in the shrunken, equilibrium position is, from equation (9),

$$\sigma_{\parallel}^{II}(r) = \frac{E^{II}}{1+\nu^{II}}\left(\frac{\partial \xi_1^{II}}{\partial r} - \beta^{II}\right) \qquad \text{(A131)}$$

$r = a_o$ = composite interface before shrinkage

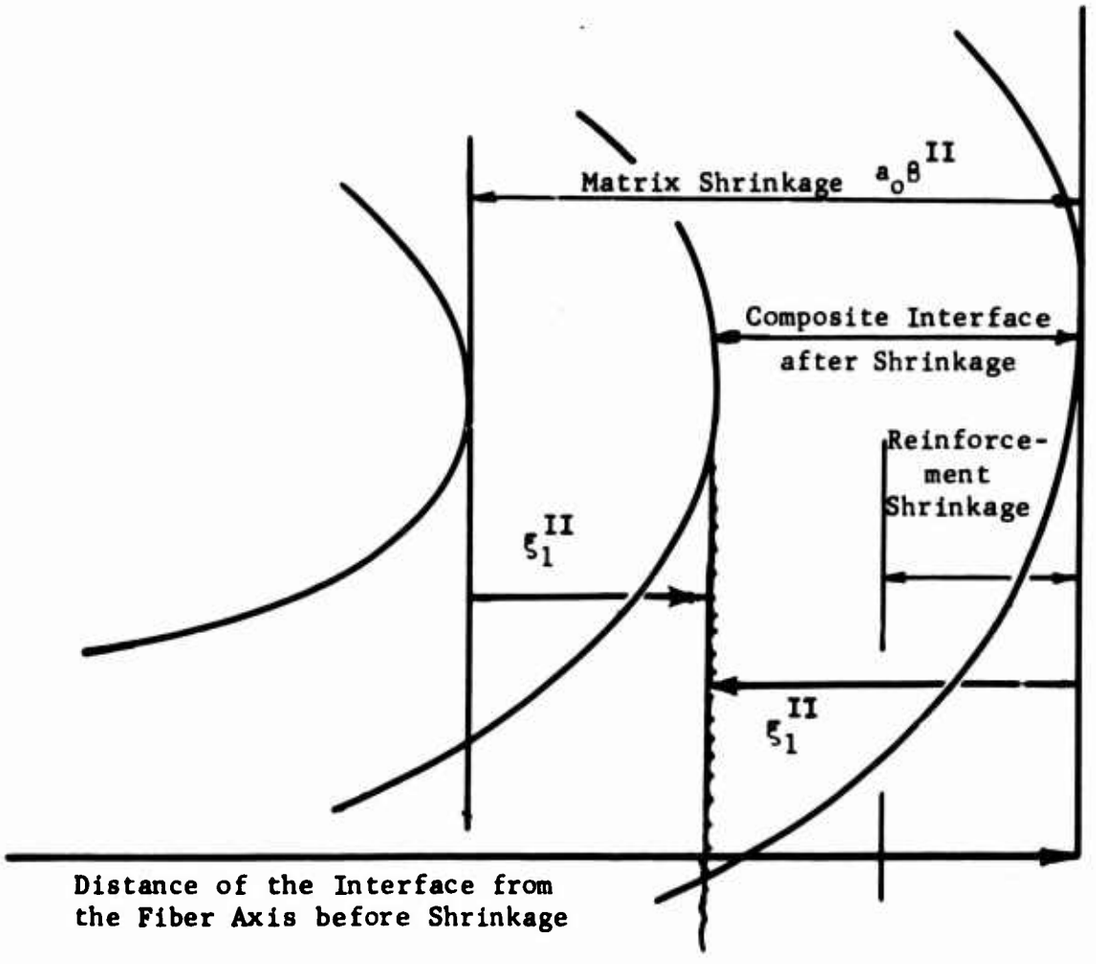

Figure 13. Graphs Showing the Comparison of Two Reference Systems

With reference to the location where the material particles would shrink if the other material would not be present, the tensor equation (9) for stresses in the matrix in one dimension becomes

$$\overline{\sigma}_{11}^{II}(r) = \frac{E^{II}}{1+\nu^{II}} \frac{\partial \overline{\xi}_1^{II}}{\partial r} . \tag{A132}$$

In Figure 13, the relationship between the displacements is

$$\begin{aligned} -\overline{\xi}_1^{I} + \xi_1^{I} &= +r\beta^{I} \\ \overline{\xi}_1^{II} &= \xi_1^{II} - r\beta^{II} \\ \frac{\partial \overline{\xi}_1^{II}}{\partial r} &= \frac{\partial \xi_1^{II}}{\partial r} - \beta^{II} . \end{aligned} \tag{A133}$$

Substituting equation (A3) into equation (A2),

$$\overline{\sigma}_{11}^{II} = \frac{E^{II}}{1+\nu^{II}} \left(\frac{\partial \xi_1^{II}}{\partial r} - \beta^{II} \right) . \tag{A134}$$

shows that both reference systems yield the same shrinkage stresses σ_{11} , equations (A1) and (A11). The comparison could be made in three dimensions and would show that, in general,

$$\overline{\sigma}_{ij}(r, \phi, z) = \sigma_{ij}(r, \phi, z) . \tag{A135}$$

APPENDIX B

TRIDIMENSIONAL ANALYSIS OF THE SINGLE-FIBER COMPOSITE

SHRINKAGE CASE

The solutions for a biharmonic equation in a system of cylindrical coordinates with axisymmetry are as follows:

$$L = \sum_k (\sin \mu_k z)\left[A_{1k} I_0(\mu_k r) + A_{3k} \mu_k r I_1(\mu_k r) + A_{2k} K_0(\mu_k r) + A_{4k} \mu_k r K_1(\mu_k r)\right] \tag{B1}$$

where $I_0(\mu_k r)$ and $I_1(\mu_k r)$ are modified Bessel functions of the first kind and of the zeroth and first order respectively; and $K_0(\mu_k r)$ and $K_1(\mu_k r)$ are those of the second kind in their corresponding zeroth and first order.

Displacements and Stresses

The displacements and stresses in terms of strain function are:

$$\xi_1 = -\frac{1+\nu}{E}\frac{\partial^2 L}{\partial r \partial z} \tag{B2}$$

$$\xi_3 = \left(\frac{1+\nu}{E}\right)\left[2(1-\nu)\nabla^2 L - \frac{\partial^2 L}{\partial z^2}\right] \tag{B3}$$

$$\sigma_{11} = \frac{\partial}{\partial z}\left(\nu \nabla^2 L - \frac{\partial^2 L}{\partial r^2}\right) \tag{B4}$$

$$\sigma_{22} = \frac{\partial}{\partial z}\left(\nu \nabla^2 L - \frac{1}{r}\frac{\partial L}{\partial r}\right) \tag{B5}$$

$$\sigma_{33} = \frac{\partial}{\partial z}\left[(2-\nu)\nabla^2 L - \frac{\partial^2 L}{\partial z^2}\right] \tag{B6}$$

$$\sigma_{13} = \frac{\partial}{\partial r}\left[(1-\nu)\nabla^2 L - \frac{\partial^2 L}{\partial z^2}\right] \tag{B7}$$

Combination of equations (B1) to (B7) yields

$$\xi_1 = \sum_k \cos(\mu_k z)\left[A_{1k} F_{1k}(r) + A_{2k} F_{2k}(r) + A_{3k} G_{1k}(r) + A_{4k} G_{2k}(r)\right] \tag{B8}$$

$$\xi_3 = \sum_k \sin(\mu_k z)\left[A_{1k} F_{3k}(r) + A_{3k} F_{4k}(r) + A_{2k} G_{3k}(r) + A_{4k} G_{4k}(r)\right] \tag{B9}$$

$$\sigma_{11} = \sum_k \cos(\mu_k z)\left[A_{1k} F_{5k}(r) + A_{3k} F_{6k}(r) + A_{2k} G_{5k}(r) + A_{4k} G_{6k}(r)\right] \tag{B10}$$

$$\sigma_{22} = \sum_k \cos(\mu_k z)\left[A_{1k} F_{7k}(r) + A_{3k} F_{8k}(r) + A_{2k} G_{7k}(r) + A_{4k} G_{8k}(r)\right] \tag{B11}$$

$$\sigma_{33} = \sum_k \cos(\mu_k z)\left[A_{1k} F_{9k}(r) + A_{3k} F_{10k}(r) + A_{2k} G_{9k}(r) + A_{4k} G_{10k}(r)\right] \tag{B12}$$

$$\sigma_{13} = \sum_k \sin(\mu_k z)\left[A_{1k} F_{11k}(r) + A_{3k} F_{12k}(r) + A_{2k} G_{11k}(r) + A_{4k} G_{12k}(r)\right] \tag{B13}$$

where $F_1(r)$, . . . , $F_{12}(r)$ are functions of r involving $I_o(\mu_k r)$ and $I_1(\mu_k r)$, and $G_1(r)$, . . . , $G_1\mu(r)$ are functions involving $K_o(\mu_k r)$ and $K_1(\mu_k r)$.

Definitions of F(r) and G(r) :

$$F_{1kj}(r) = -\left(\frac{1+\nu}{E}\right) k_j^2 I_1(\mu_{kj} r) \tag{B14}$$

$$F_{2kj}(r) = -\left(\frac{1+\nu}{E}\right) k_j^3 r\, I_0(\mu_{kj} r) \tag{B15}$$

$$F_{3kj}(r) = \left(\frac{1+\nu}{E}\right) \mu_{kj}^2 I_0(\mu_{kj} r) \tag{B16}$$

$$F_{4kj}(r) = \frac{(1+\nu)\mu_{kj}^2}{E}\left[4(1-\nu) I_0(\mu_{kj} r) + k_j r I_1(\mu_{kj} r)\right] \tag{B17}$$

$$F_{5kj}(r) = \mu_{kj}^2\left[-\mu_{kj} I_0(\mu_{kj} r) + \frac{I_1(\mu_{kj} r)}{r}\right] \tag{B18}$$

$$F_{6kj}(r) = \mu_{kj}^3\left[(2\nu-1) I_0(\mu_{kj} r) - \mu_{kj} r I_1(\mu_{kj} r)\right] \tag{B19}$$

$$F_{7kj}(r) = -\mu_{kj}^2 \frac{I_1(\mu_{kj} r)}{r} \tag{B20}$$

$$F_{8kj}(r) = \mu_{kj}^3 (2\nu-1) I_0(\mu_{kj} r) \tag{B21}$$

$$F_{9kj}(r) = \mu_{kj}^3 I_0(\mu_{kj} r) \tag{B22}$$

$$F_{10kj}(r) = \mu_{kj}^3\left[2(2-\nu) I_0(\mu_{kj} r) + \mu_{kj} r I_1(\mu_{kj} r)\right] \tag{B23}$$

$$F_{11kj}(r) = \mu_{kj}^3 I_1(\mu_{kj} r) \tag{B24}$$

$$F_{12kj}(r) = \mu_{kj}^3\left[\mu_{kj} r I_0(\mu_{kj} r) + 2(1-\nu) I_1(\mu_{kj} r)\right] \tag{B25}$$

$$G_{1kj}(r) = \frac{(1+\nu)\mu_{kj}^2}{E} K_1(\mu_{kj} r) \tag{B26}$$

$$G_{2k}(r) = \left(\frac{1+\nu}{E}\right)\mu_{ki}^3 r\, K_0(\mu_{ki} r) \tag{B27}$$

$$G_{3k}(r) = \left(\frac{1+\nu}{E}\right)\mu_{ki}^2 K_0(\mu_{ki} r) \tag{B28}$$

$$G_{4k}(r) = \left(\frac{1+\nu}{E}\right)\mu_{ki}^2\left[-4(1-\nu)K_0(\mu_{ki} r) + \mu_{ki} r K_1(\mu_{ki} r)\right] \tag{B29}$$

$$G_{5k}(r) = \mu_{ki}^2\left[-\mu_{ki} K_0(\mu_{ki} r) - \frac{K_1(\mu_{ki} r)}{r}\right] \tag{B30}$$

$$G_{6k}(r) = \mu_{ki}^3\left[(1-2\nu)K_0(\mu_{ki} r) - \mu_{ki} r K_1(\mu_{ki} r)\right] \tag{B31}$$

$$G_{7k}(r) = \mu_{ki}^2\left[\frac{K_1(\mu_{ki} r)}{r}\right] \tag{B32}$$

$$G_{8k}(r) = \mu_{ki}^3 (1-2\nu) K_0(\mu_{ki} r) \tag{B33}$$

$$G_{9k}(r) = \mu_{ki}^3 K_0(\mu_{ki} r) \tag{B34}$$

$$G_{10k}(r) = \mu_{ki}^3\left[-2(2-\nu)K_0(\mu_{ki} r) + \mu_{ki} r K_1(\mu_{ki} r)\right] \tag{B35}$$

$$G_{11k}(r) = -\mu_{ki}^3 K_1(\mu_{ki} r) \tag{B36}$$

$$G_{12k}(r) = \mu_{ki}^3\left[-\mu_{ki} r K_0(\mu_{ki} r) + 2(1-\nu) K_1(\mu_{ki} r)\right] \tag{B37}$$

Superscripts I, II were omitted in equations (B1) to (B37).

Imposing Boundary Conditions

1. At the interface, the continuities of stresses and displacements are assured.

a) $\xi_1^{I}(a,z) + \xi_1^{II}(a,z) = a(\beta^{II} - \beta^{I})$

This implies

$$A_{1k}^{I} F_{1k}^{I}(a) + A_{3k}^{I} F_{2k}^{I}(a) + A_{1k}^{II} F_{1k}^{II}(a) + A_{3k}^{II} F_{2k}^{II}(a)$$

$$+ A_{2k}^{I} G_{1k}^{II}(a) + A_{4k}^{II} G_{2k}^{II}(a) = a(\beta^{II} - \beta^{I}) \frac{4}{k\pi} \sin\left(\frac{k\pi}{2}\right) \quad \text{(B38)}$$

$k = 1, 3, 5, \ldots$

b) $\xi_3^{I}(a,z) + \xi_3^{II}(a,z) = z(\beta^{II} - \beta^{I})$

$$A_{1k}^{I} F_{3k}^{I}(a) + A_{3k}^{I} F_{4k}^{I}(a) + A_{1k}^{II} F_{3k}^{II}(a) + A_{3k}^{II} F_{4k}^{II}(a)$$

$$+ A_{2k}^{I} G_{3k}^{I}(a) + A_{4k}^{I} G_{4k}^{I}(a) = (\beta^{II} - \beta^{I}) \frac{8l}{(k\pi)^2} \sin\left(\frac{k\pi}{2}\right) \quad \text{(B39)}$$

$k = 1, 3, 5, \ldots$

c) $\sigma_{11}^{I}(a,z) = \sigma_{11}^{II}(a,z)$

$$A_{1k}^{I} F_{5k}^{I}(a) + A_{3k}^{I} F_{6k}^{I}(a) - A_{1k}^{II} F_{5k}^{II}(a) - A_{3k}^{II} F_{6k}^{II}(a)$$

$$- A_{2k}^{II} G_{5k}^{II}(a) - A_{4k}^{II} G_{6k}^{I}(a) = 0 \quad \text{(B40)}$$

d) $\sigma_{13}^{I}(a,z) = \sigma_{13}^{II}(a,z)$

$$A_{1k}^{I} F_{11k}^{I}(a) + A_{3k}^{I} F_{12k}^{I}(a) - A_{1k}^{II} F_{11k}^{I}(a) - A_{3k}^{II} F_{12k}^{II}(a) - A_{2k}^{II} G_{11k}^{I}(a) - A_{4k}^{II} G_{12k}^{II}(a) = 0 \quad \text{(B41)}$$

2. At the outer surface of the matrix, the resin should be free from normal and shear stresses.

a) $\sigma_{11}^{II}(b,z) = 0$

$$A_{1k}^{II} F_{5k}^{I}(b) + A_{3k}^{II} F_{6k}^{II}(b) + A_{2k}^{II} G_{5k}^{II}(b) + A_{4k}^{II} G_{6k}^{II}(b) = 0 \quad \text{(B42)}$$

b) $\sigma_{13}^{I}(b,z) = 0$

$$A_{1k}^{I} F_{11k}^{II}(b) + A_{3k}^{I} F_{12k}^{II}(b) + A_{2k}^{II} G_{11k}^{II}(b) + A_{4k}^{II} G_{12k}^{I}(b) = 0 \quad \text{(B43)}$$

3. At the ends, axial stresses for both fiber and resin should vanish.

$$\sigma_{33}^{I}(r,l) = \sigma_{33}^{II}(r,l) = 0$$

The only condition that makes the solution nontrivial is

$$\cos(\mu_k l) = 0. \tag{B44}$$

This implies that

$$\mu_k l = \frac{k\pi}{2}, \quad k = \pm 1, \pm 3, \pm 5, \cdots \tag{B45}$$

$$\mu_k = \frac{k\pi}{2l}, \quad k = 1, 3, 5, \cdots \tag{B46}$$

Remarks

1. In deriving equations (B38) and (B39), we have used Fourier expansion for a constant and a function z.

2. It is interesting to notice that the eigenvalues determined by equation (B46) are consistent with the argument of the orthonormal function used in the Fourier representations in equations (B38) and (B39). The coincidence is not accidental; rather, it is intentional.

3. The constants to be determined for each k are A_1^I, A_3^I, A_1^{II}, A_2^{II}, A_3^{II}, and A_4^{II}. These six constants can be found by solving the simultaneous equations (B38) to (B43).

AXIAL LOADING CASE

The superposition-product solutions of the biharmonic equation in cylindrical coordinates with axisymmetry has the following general form:

$$L = \sum_k \sinh(\mu_k z)\left[A_{1k} J_0(\mu_k r) + A_{3k} \mu_k r J_1(\mu_k r) + A_{2k} Y_0(\mu_k r) + A_{4k} \mu_k r Y_1(\mu_k r)\right] \tag{B47}$$

where $J_0(\mu_k r)$ and $J_1(\mu_k r)$ are cylindrical harmonics of the first kind and of the zeroth and first order respectively, and $Y_0(\mu_k r)$ and $Y_1(\mu_k r)$ are that of the second kind.

Stresses and Displacements

$$\xi_1 = \sum_k \cosh(\mu_k z)\left[A_{1k} F_{1k}(r) + A_{3k} F_{2k}(r) + A_{2k} G_{1k}(r) + A_{4k} G_{2k}(r)\right] \tag{B48}$$

$$\xi_3 = \sum_k \sinh(\mu_k z)\left[A_{1k} F_{3k}(r) + A_{3k} F_{4k}(r) + A_{2k} G_{3k}(r) + A_{4k} G_{4k}(r)\right] \tag{B49}$$

$$\sigma_{11} = \sum_k \cosh(\mu_k z)\left[A_{1k} F_{5k}(r) + A_{3k} F_{6k}(r) + A_{2k} G_{5k}(r) + A_{4k} G_{6k}(r)\right] \tag{B50}$$

$$\sigma_{22} = \sum_k \cosh(\mu_k z)\left[A_{1k} F_{7k}(r) + A_{3k} F_{8k}(r) + A_{2k} G_{7k}(r) + A_{4k} G_{8k}(r)\right] \tag{B51}$$

$$\sigma_{33} = \sum_k \cosh(\mu_k z)\left[A_{1k} F_{9k}(r) + A_{3k} F_{10k}(r) + A_{2k} G_{9k}(r) + A_{4k} G_{10k}(r)\right] \tag{B52}$$

$$\sigma_{13} = \sum_{k} \sinh(\mu_k z)\left[A_{1k} F_{11k}(r) + A_{3k} F_{12k}(r) + A_{2k} G_{11k}(r) + A_{4k} G_{12k}(r)\right] \tag{B53}$$

where $F_1(r)$, . . . , $F_{12}(r)$ are functions of r involving $J_0(\mu_k r)$ and $J_1(\mu_k r)$, and $G_1(r)$, . . . , $G_{12}(r)$ are functions of r involving $Y_0(\mu_k r)$ and $Y_1(\mu_k r)$.

Definitions of F(r) and G(r) :

$$F_{1k}(r) = \left(\frac{1+\nu}{E}\right)\mu_k^2 J_1(\mu_k r) \tag{B54}$$

$$F_{2k}(r) = -\left(\frac{1+\nu}{E}\right)\mu_k^3 J_0(\mu_k r) \tag{B55}$$

$$F_{3k}(r) = -\left(\frac{1+\nu}{E}\right)\mu_k^2 J_0(\mu_k r) \tag{B56}$$

$$F_{4k}(r) = \left(\frac{1+\nu}{E}\right)\mu_k^2 \left[4(1-\nu) J_0(\mu_k r) - \mu_k r J_1(\mu_k r)\right] \tag{B57}$$

$$F_{5k}(r) = \mu_k^2 \left[\mu_k J_0(\mu_k r) - \frac{J_1(\mu_k r)}{r}\right] \tag{B58}$$

$$F_{6k}(r) = \mu_k^3 \left[(1-2\nu) J_0(\mu_k r) + \mu_k r J_1(\mu_k r)\right] \tag{B59}$$

$$F_{7k}(r) = \mu_k^2 \frac{J_1(\mu_k r)}{r} \tag{B60}$$

$$F_{8k}(k) = -(1-2\nu)\mu_k^3 J_0(\mu_k k) \quad \text{(B61)}$$

$$F_{9k}(k) = -\mu_k^3 J_0(\mu_k k) \quad \text{(B62)}$$

$$F_{10k}(k) = \mu_k^3 \left[2(2-\nu)J_0(\mu_k k) - \mu_k k J_1(\mu_k k)\right] \quad \text{(B63)}$$

$$F_{11k}(k) = \mu_k^3 J_1(\mu_k k) \quad \text{(B64)}$$

$$F_{12k}(k) = -\mu_k^3 \left[\mu_k k J_0(\mu_k k) + 2(1-\nu) J_1(\mu_k k)\right] \quad \text{(B65)}$$

$G_1(r)$, . . . , $G_{12}(r)$ are defined exactly in the same manner as equations (B54) to (B65) except replacing $J_0(\mu_k r)$ and $J_1(\mu_k r)$ by $K_0(\mu_k r)$ and $K_1(\mu_k r)$ respectively. Superscripts I and II were omitted in equations (B47) to (B65).

Imposing Boundary Conditions

1. At the interface, the continuities of displacements exist. This implies

$$a)\ \xi_1^{I}(a,z) = \xi_1^{II}(a,z)$$

$$A_{1k}^{I} F_{1k}^{I}(a) + A_{3k}^{I} F_{2k}^{I}(a) - A_{1k}^{II} F_{1k}^{II}(a) - A_{3k}^{II} F_{2k}^{II}(a) = 0 \quad \text{(B66)}$$

b) $\xi_3^{I}(a,z) = \xi_3^{II}(a,z)$

$$A_{1k}^{I} F_{3k}^{I}(a) + A_{3k}^{I} F_{4k}^{I}(a) - A_{1k}^{II} F_{3k}^{II}(a) - A_{3k}^{II} F_{4k}^{II}(a) = 0 \qquad \text{(B67)}$$

2. At the outer surface, radial stress of resin should vanish; i.e.,

$$\sigma_{11}^{II}(b,z) = 0 .$$

It implies

$$A_{1k}^{II} F_{5k}^{II}(b) + A_{3k}^{II} F_{6k}^{II}(b) = 0 . \qquad \text{(B68)}$$

3. At the ends, resin is subjected to axial loading; i.e.,

$$\sigma_{33}^{I}(r,l) = F(r) = \text{load per unit area} .$$

This yields

$$-\mu_k^3 \cosh(\mu_k l)\left[A_{1k}^{I} - A_{3k}^{II} 2(2-D^{II})\right] = C_k \qquad \text{(B69)}$$

and

$$A_{3k}^{I} \mu_k^4 = 0 . \qquad \text{(B70)}$$

Equation (B70) implies

$$A_{3k}^{II} = 0 . \tag{B71}$$

Then combination of equation (B69) and (B71) gives

$$A_{1k}^{II} = - \frac{C_k}{\mu_k^3 \cosh(\mu_k l)} . \tag{B72}$$

Determination of Eigenvalues and the Dini-Bessel Representation of Loading at Ends

1. Eigenvalues are determined from equation (B68); i.e.,

$$A_{1k}^{II} \mu_k^2 \left[\mu_k J_0(\mu_k b) - \frac{J_1(\mu_k b)}{b} \right] = 0 ; \tag{B73}$$

then

$$\mu_k b J_0(\mu_k b) = J_1(\mu_k b) . \tag{B74}$$

2. The loading at ends can be represented as Dini-Bessel expansion; namely,

$$F(r) = \sum_{\mu_k} C_k J_0(\mu_k r) \tag{B75}$$

where

$$C_k = \frac{2}{b^2 \left[\{J_0(\mu_k b)\}^2 + \{J_1(\mu_k b)\}^2 \right]} \int_0^b r F(r) J_0(\mu_k r) dr . \tag{B76}$$

For the case $F(r) = 1$,

$$C_k = \frac{2J_1(\mu_k b)}{\mu_k b\left[\{J_0(\mu_k b)\}^2 + \{J_1(\mu_k b)\}^2\right]} . \qquad \text{(B77)}$$

Remarks

1. Eigenvalues μ_k (> 0) are determined by equation (B74).

2. Coefficients of Dini-Bessel expansion for loading at ends can be found from equation (B76) or (B77).

3. Constants to be determined are A^{I}_{1k} , A^{I}_{3k} , and A^{II}_{1k} . These values can be found by solving equations (B66), (B67), and (B72) simultaneously.

4. The condition that a/b is much smaller than unity is assumed.

APPENDIX C

PHOTOELASTIC EXPERIMENTS

SINGLE-FIBER SPECIMEN PREPARATION

To perform an experimental evaluation of the shrinkage stresses for a single fiber and epoxy resin matrix via photoelasticity, four cylindrical specimens were fabricated. Typical dimensions of the cylinders are shown in Figure 14. Specimen one contained no fiber; specimen two contained a 4-mil-diameter boron fiber; specimen three contained a 5-mil glass fiber; and specimen four contained a 10-mil glass fiber.

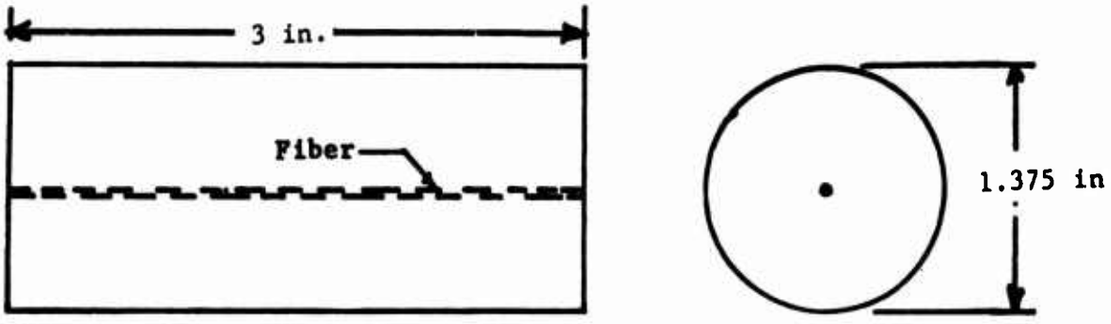

Figure 14. Typical Dimensions of Cylindrical Specimens

The method of fabrication for the cylinders and fibers was to locate a fiber in the center of a metal tube (the fiber was supported to allow axial freedom of movement as the resin cured) and to pour Shell Epon 815 resin with dyethynolamine 15 PHR (parts per hundred weight ratio) slowly in to fill up the tube, allowing air bubbles to be forced to the surface. A rubber stopper was used to plug the bottom tube end (the fiber end simply "rested" on this stopper).

The resin cure temperature cycle was 200°F for 12 hours, with post-cure at 250°F for 4 hours. A parting agent applied to the inner surface of the tube allowed the resin to shrink during the curing process and during the cooling period.

Figures 15 through 18 show the specimens photographed under direct polarized light (quarter wave plates are in the system to allow only stress magnitudes to be seen). White light was used for the photoelastic analysis because the various colors indicate very clearly the stress magnitudes present in the specimens.

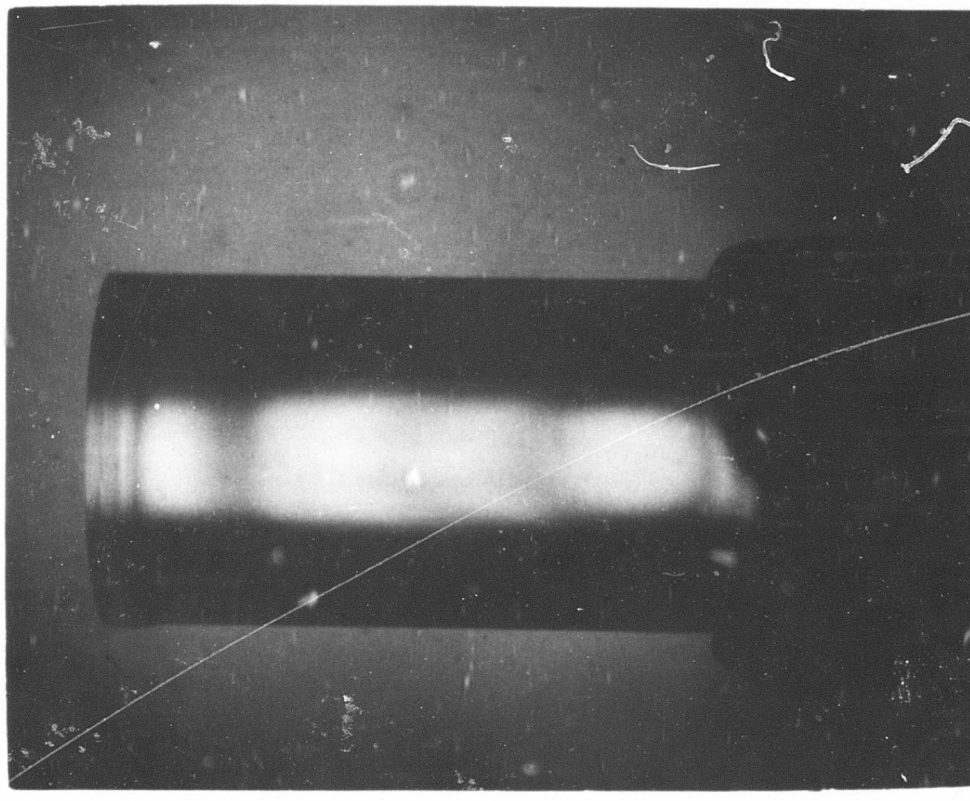

Figure 15. Epoxy Resin Cylinder without Fiber Viewed under Polarized Light (Quarter wave plates are in the optic system)

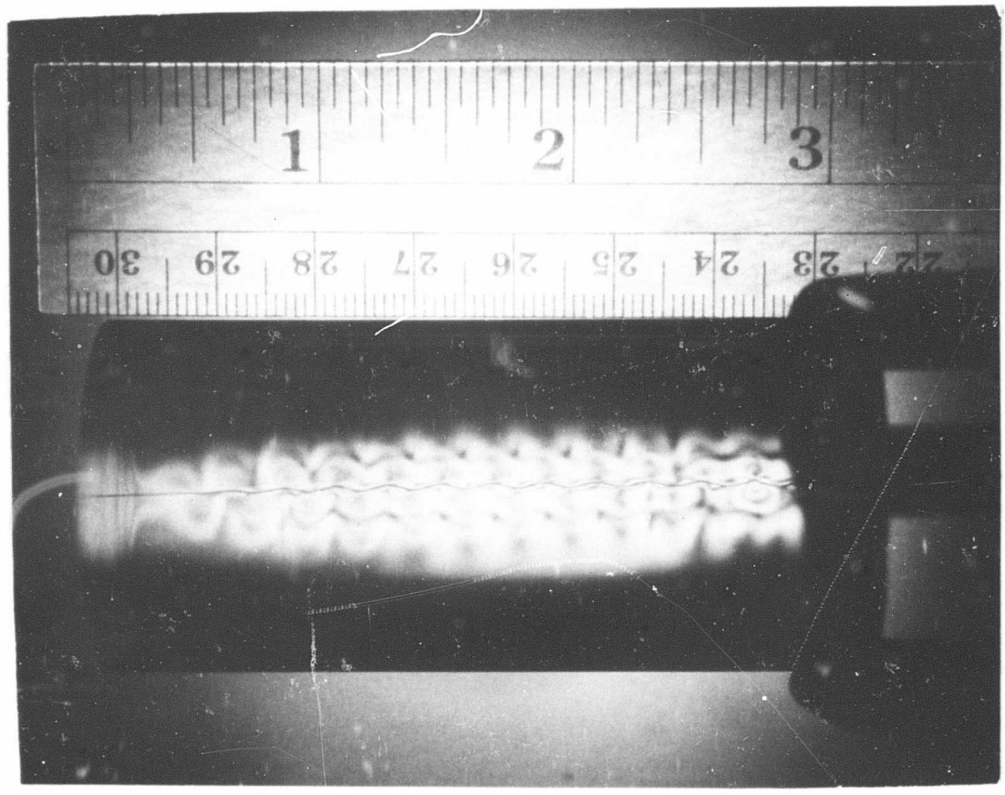

Figure 16. Boron Fiber (0.004-inch Diameter) in an Epoxy Resin Cylinder Viewed under Polarized Light (Quarter wave plates are in the optic system)

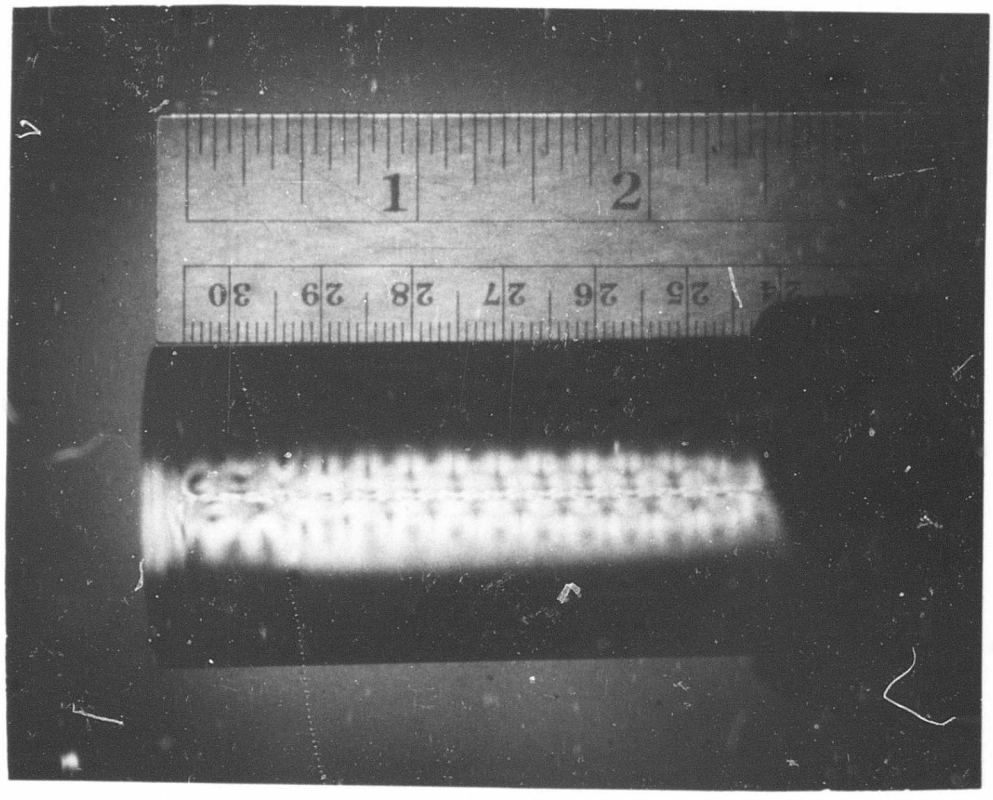

Figure 17. Glass Fiber (0.005-inch Diameter) in an Epoxy Resin Cylinder Viewed under Polarized Light (Quarter wave plates are in the optic system)

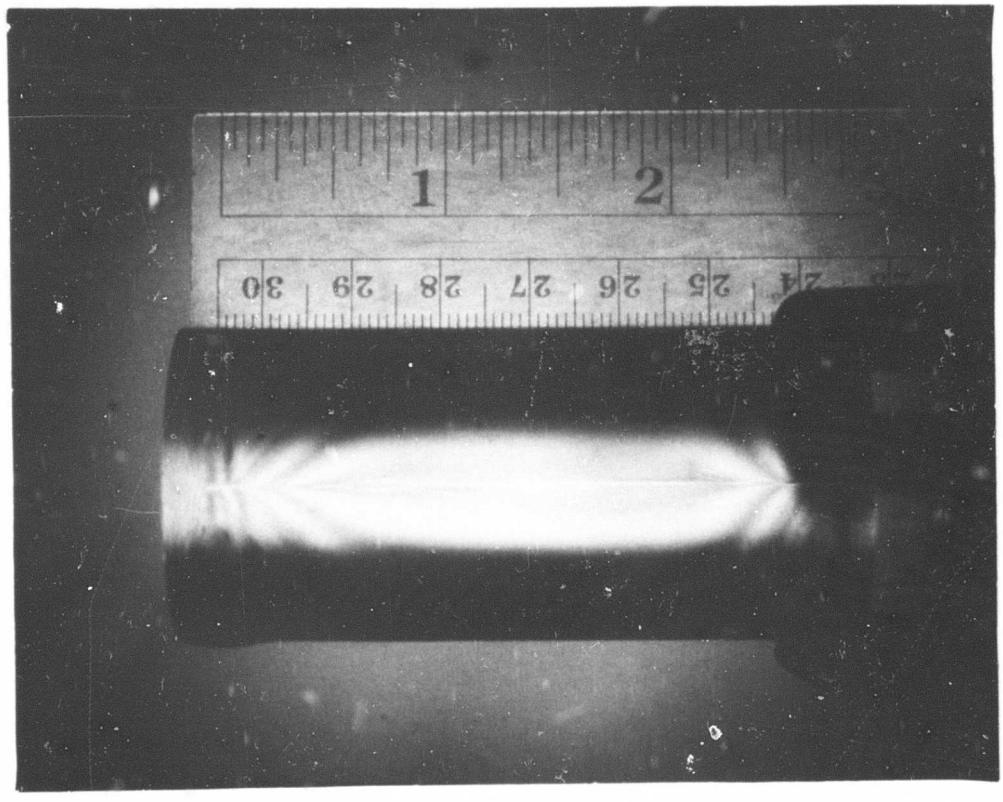

Figure 18. Glass Fiber (0.010-inch Diameter) in an Epoxy Resin Cylinder Viewed under Polarized Light (Quarter wave plates are in the optic system)

As can be seen from Figures 15 through 18, the boron and 5-mil glass fiber buckled due to the compressive load applied to the fiber by resin shrinkage. As nearly as can be seen, the 10-mil glass fiber specimen did not buckle, but remained straight.

From the photographs of the boron fiber and 5-mil glass fiber specimens, the following information was obtained:

Boron Fiber (4-mil diameter)

Buckle wavelength = 0.238 inch/cycle

Double amplitude = 0.0125 inch

5-mil Glass Fiber

Buckle wavelength = 0.212 inch/cycle

Double amplitude = 0.015 inch

Since the theoretical analysis is predicated upon the fiber's not buckling, the specimen chosen for quantitative stress evaluation was the 10-mil glass fiber specimen.

In order to photoelastically analyze the stresses in the resin around the fiber, a thin slice along the fiber axis from a cylindrical specimen must be used. This is to allow the polarized light to incident perpendicular to the specimen surface and also to make the stress field appear two-dimensional, by having the thickness of the specimen small enough that the thickness stress component can be neglected. To cut slices for analysis from a specimen at points and in directions of desired stresses is a standard technique for photoelastic measurements. A problem is encountered with slicing when thermal stresses are the quantities to be measured, since during cutting, heat is produced and this perhaps distorts the original stress values. In addition, the remainder of the resin material might result in stress releasing of the fiber.

It was therefore decided to slice the 10-mil fiber cylinder in three steps in order to observe this effect. The cutting was also done under a high-pressure water jet to minimize the effects on the original thermal stresses present in the specimen.

It was decided to cut the specimen first to 1 inch across the flats, then to 1/2 inch thickness, and finally to 1/8 inch as a goal for analysis evaluation. A diagram of the cuts is shown in Figure 19.

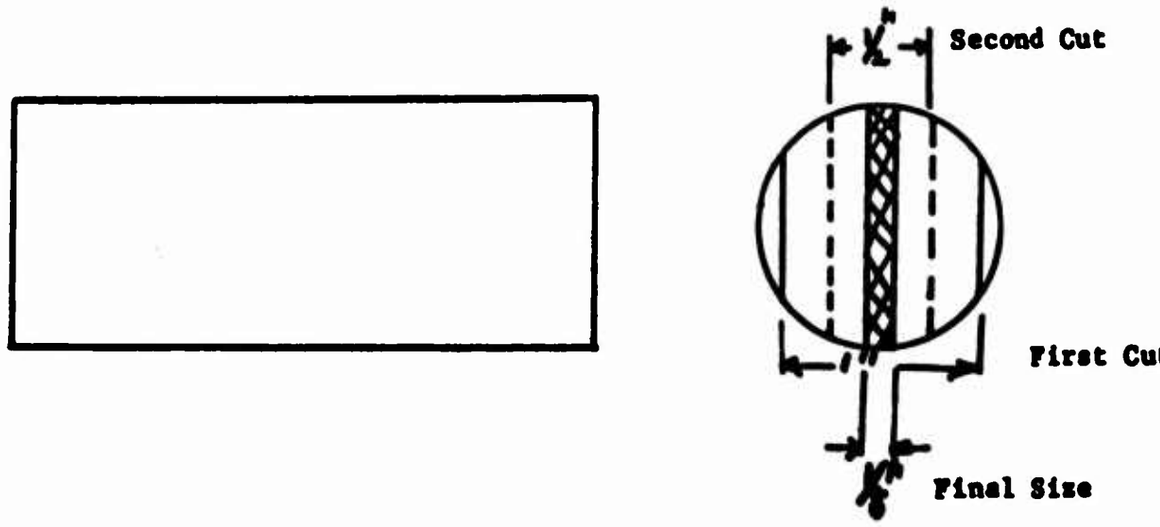

Figure 19. Typical Cuts Made on 10-mil Glass Fiber Specimen to Obtain a Specimen for Quantitative Photoelastic Stress Evaluation

The stress patterns of these cuts as shown under polarized light (quarter wave plates in the system) are found in Figures 20 through 22. Additional slices cut parallel to the fiber but perpendicular to the first cut might have further reduced the effect of heat during the cutting operation; however, this idea was rejected because such slices would have cut off the zero isochromatics reference points which are necessary for the quantitative analysis.

The pictures, of course, show some change in stress pattern between the first cut and the final cut. One has also to be very careful in evaluation of the fringe lines and remember that the fringe order increases with thickness of the specimen.

An elementary examination revealed that the stress near the center of the fiber for the first cut and the stress for the final cut turned out to be fairly close to each other in magnitude. On this basis, it was concluded that the original stress pattern was not greatly harmed by slicing.

It was decided to use the Budd Company reflection polarscope as shown in operation in Figure 23 to evaluate quantitatively the stresses in the slice from the cylindrical 10-mil glass fiber specimen.

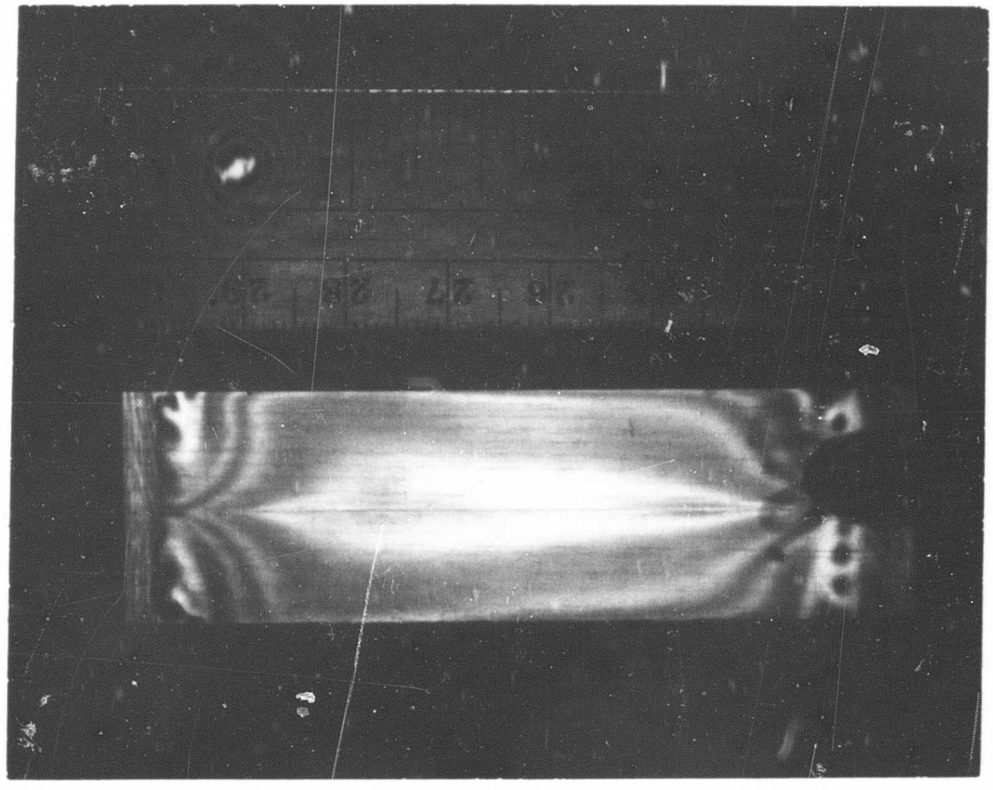

Figure 20. Glass Fiber (0.010-inch Diameter) in Epoxy Viewed under Polarized Light after Slicing the Cylinder to 1 inch Across Flat Areas

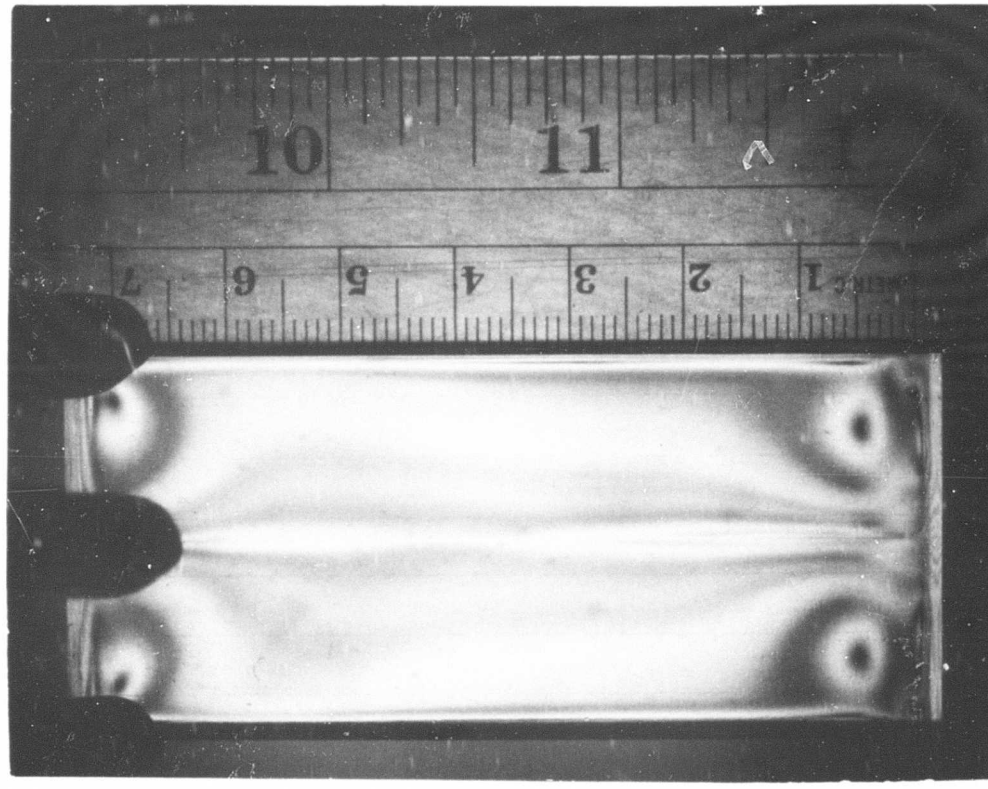

Figure 21. Glass Fiber (0.010-inch Diameter) in Epoxy Viewed under Polarized Light after Slicing the Cylinder to 1/2 inch Across Flat Areas (Second cut)

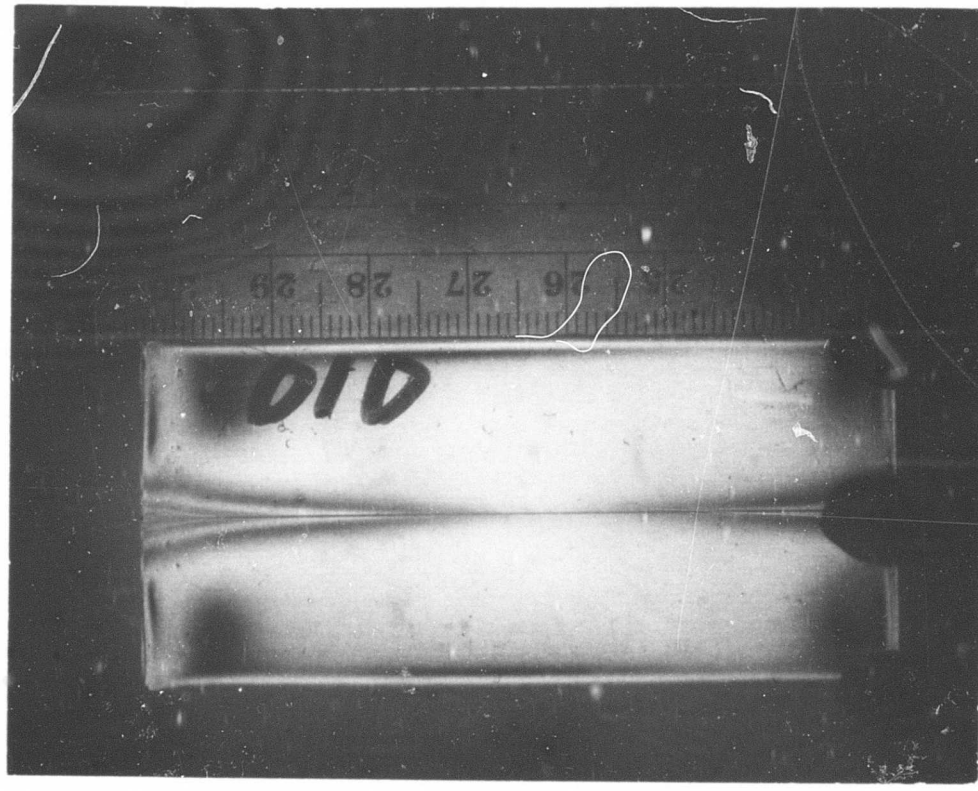

Figure 22. Glass Fiber (0.010-inch Diameter) in Epoxy Viewed under Polarized Light (Direct polarscope) where Distance Across Flats is 1/8 inch (Third cut)

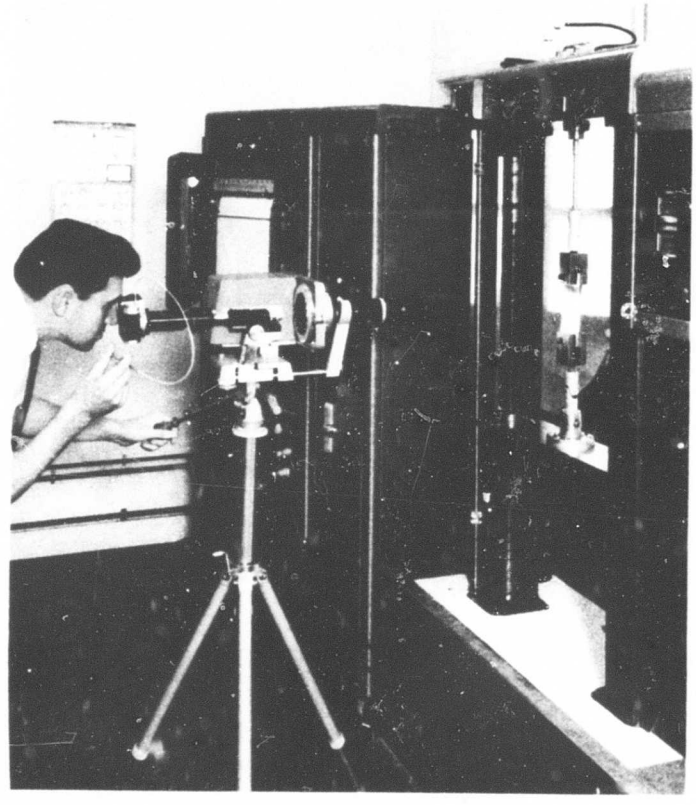

Figure 23. Budd Company Reflection Polarscope

EXPERIMENTAL ANALYSIS

The reflection polarscope operates by observing the fringes in a birefringence model coated on one side with a reflective coating. In effect, the reflection polarscope simply doubles the specimen thickness since the light-path thickness is doubled.

The first step in quantitative stress evaluation by photoelasticity is to determine the stress-optic coefficiency for the particular material of the model.

This is done by using a standard calculable stress distribution model and observing the fringes as this model is being loaded (this technique is discussed in detail in Reference 1).

For this case, a flat sheet of the same thickness as the final cut on the 10-mil glass fiber specimen was cast from the same resin and with the same cure cycle. A "dogbone" tensile specimen was then machined (under cooling) from this plate.

The test section of the machined dogbone was coated with an aluminum paint for reflection of the white light used in the Budd Company instrument.

The dogbone specimen was then placed in a tension testing machine and load was applied. As the load was increased, the "tint of passage" or fringe order was recorded. Several load and unload cycles were used in this process. In every case, the applied stress was below the elastic limit and conformed to Hooke's law.

A plot of the fringe order versus applied load gave the slope of the load-fringe order curve. The stress-optic coefficient was then computed as shown in Reference 1.

In the following, symbols and formulas used in photoelastic analysis are listed.

Difference in principal stresses;

$$\sigma_1 - \sigma_2 = \frac{Kn}{t} \quad \text{(Basic photoelastic equation)}$$

where

K = stress-optic coefficient in lb/in./order

n = fringe order

t = length of passage of the light vector

σ_1, σ_2 = stresses in 1 and 2 directions

For the tension specimen, let $\sigma_2 = 0$

$$\sigma_1 = \frac{P}{bh} \quad \text{(loaded direction)}$$

where

P = applied load

b = width of specimen at test section

h = thickness of specimen ;

then,

$$K = \frac{\sigma_1 t}{n}$$

$$= P/bh \ \frac{2h}{n}, \quad t = 2h \quad \text{(for reflection polarscope)}$$

P/n = slope of load vs fringe order curve

= 18.7 lb/in./order (as determined for this case)

$$K = \frac{2P}{bn} = \frac{2 \times 18.7}{0.5}$$

K = 74.8 lb/in./order for this type of resin

With the stress-optic coefficient determined, the 10-mil glass fiber slice was mounted so as to be viewed by the Budd instrument.

This picture under polarized light is shown in Figure 24. Small grease points were used to locate spots where the stress measurements were desired.

A plot of the difference in principal stresses at a radius of 0.10 inch from the fiber center along the fiber length is shown in Figure 25. The 0.10-inch radius was chosen for plotting, since this coincided with a station used in the theoretical analysis.

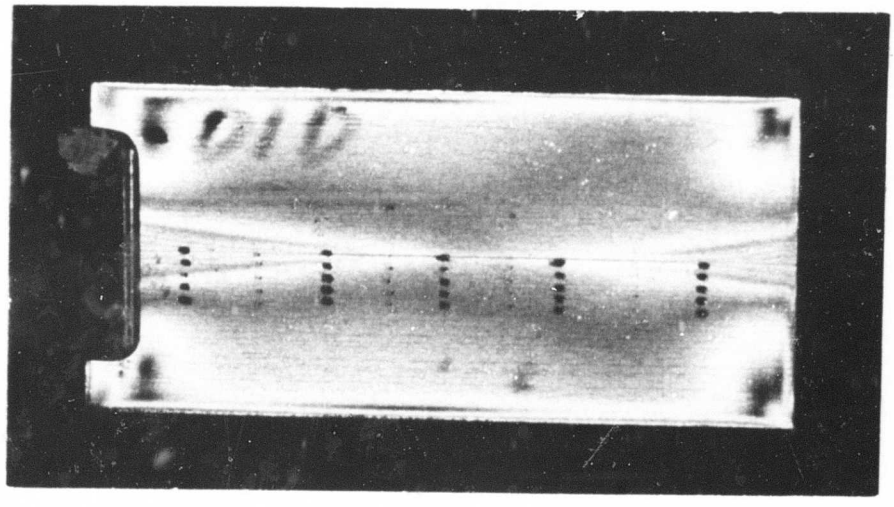

Unloaded

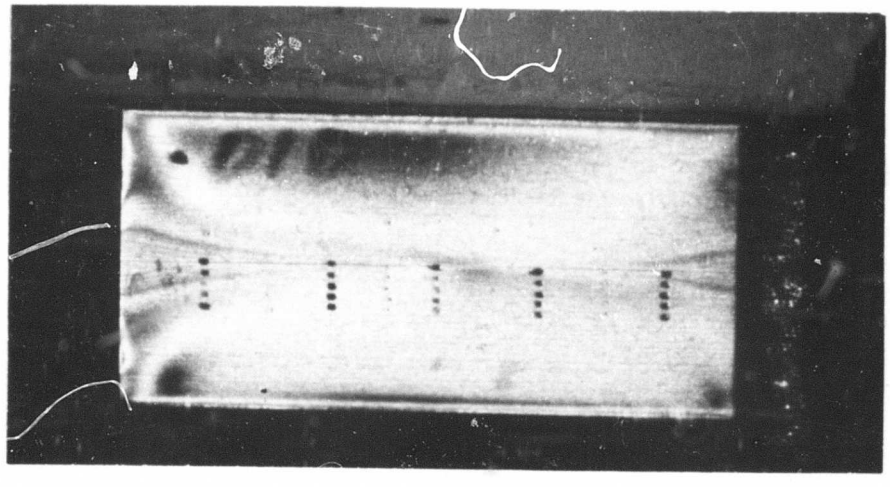

Loaded

Figure 24. Slice of 10-mil Glass Fiber in Epoxy Resin. Specimen under Reflection Polarscope (Quarter wave plate in system)

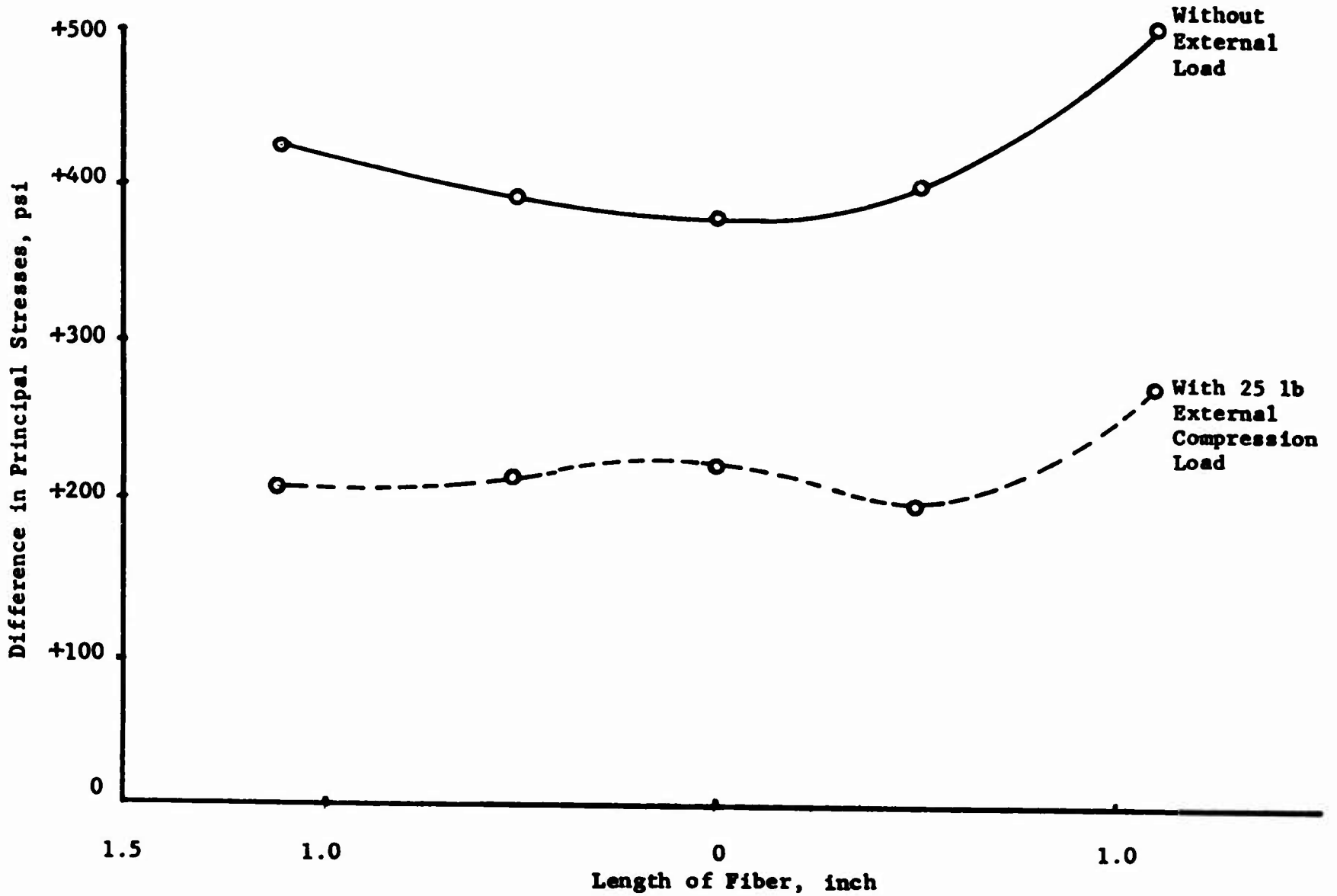

Figure 25. Magnitude of Difference in Principal Stresses (psi) at 0.10 inch Radius from Fiber Center in Resin versus Length of Fiber (inch)

The standard Tardy method was used to determine the fringe order at each point of interest; i.e., the polarizer and analyzer sections of the polarscope were oriented each time to bring an isoclinic or principal stress direction on each point. The analyzer then was adjusted to bring the lower observed fringe order to the point of interest. The fraction of this degree movement to 180° gave the fractional order to be added to the lower fringe for the final value.

The versatility of the Budd instrument allows an additional feature; i.e., to pass light obliquely into the specimen and thus to separate the magnitude of the stresses. This was done for the center fiber point and only for the specimen without external load. The principle of oblique incidence and separation of the principal stresses is discussed thoroughly in Reference 1. The plot of magnitudes of these stresses for the center point is shown in Figures 26 and 27.

The theoretical analysis has been extended to the case where the resin surrounding the fiber was subjected to a uniform compressive load in the direction of the length of the fiber.

It was desired to accomplish this same effect in the experimental work.

The loading scheme for this operation is shown in Figure 28.

A minute portion at both ends of the fiber was removed inside the resin so that, in effect, it was not loaded under a pressure application to the ends of the specimen. The load measurement was determined by the spring load cell attachment shown in Figure 28.

The results of this determination of principal stress difference under compressive load are shown also in Figure 25, and allow a direct comparison of the unloaded and loaded specimens.

Unfortunately, the mirror attachment for oblique incidence measurements could not be brought close enough to the specimen due to the interference of the load cell. Therefore, it was not possible to separate the stresses at the center point.

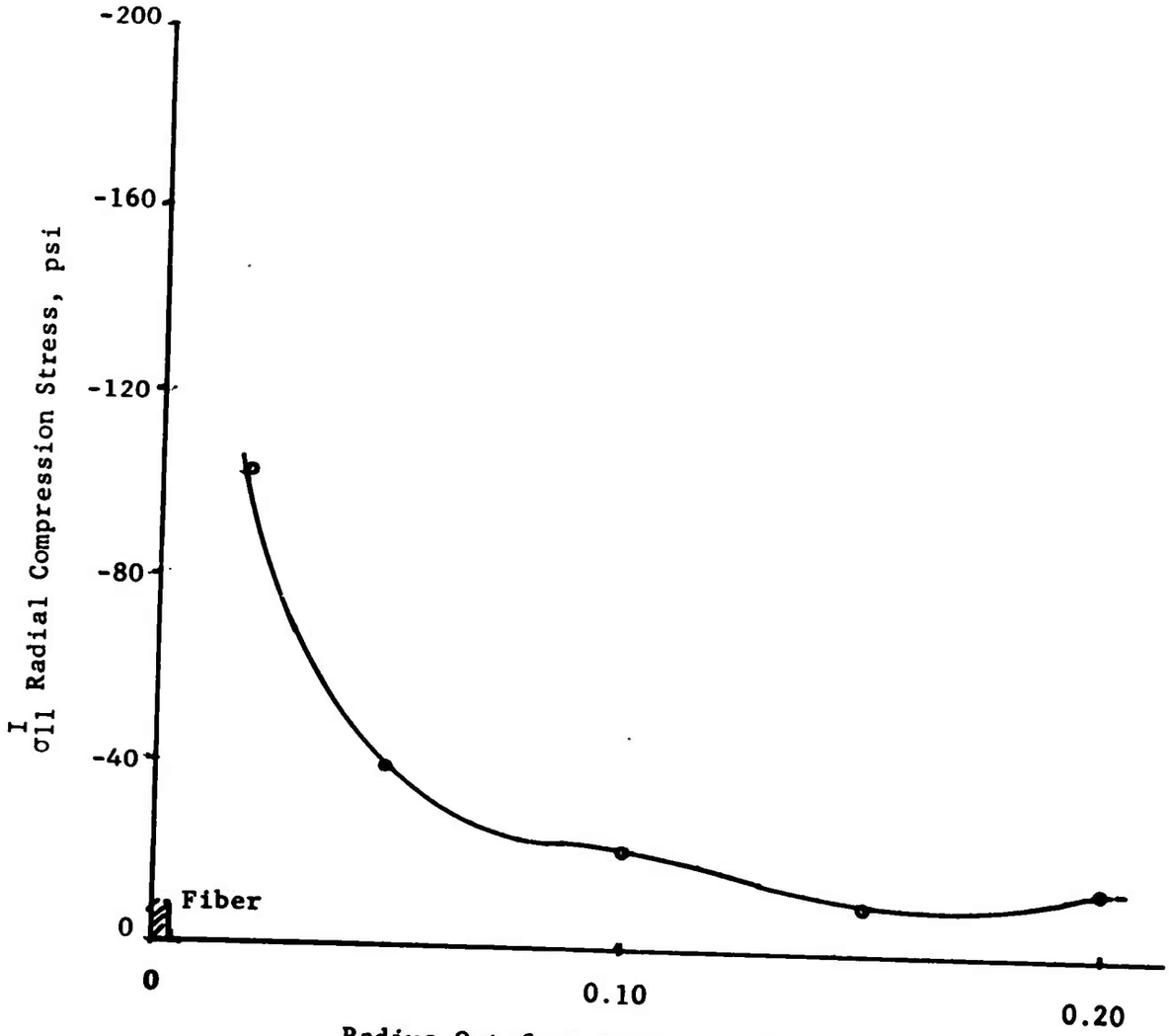

Figure 26. Radial Compressive Stresses $\left(\sigma_{11}^{I}\right)$ for Center Point of the Length of Fiber versus Radius (Without External Load)

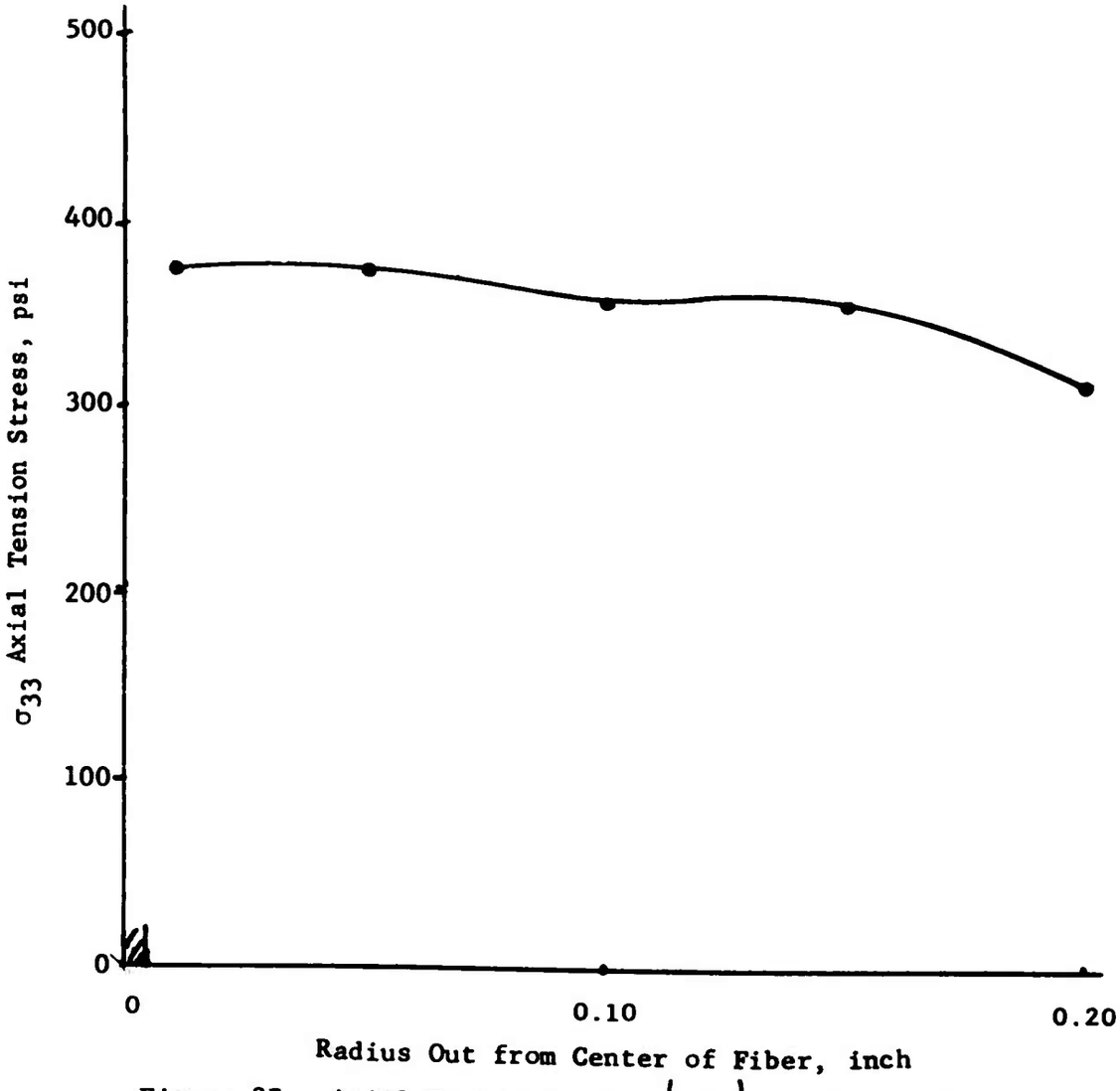

Figure 27. Axial Tension Stress (σ_{33}) for Center Point of the Length of Fiber versus Radius (Without External Load)

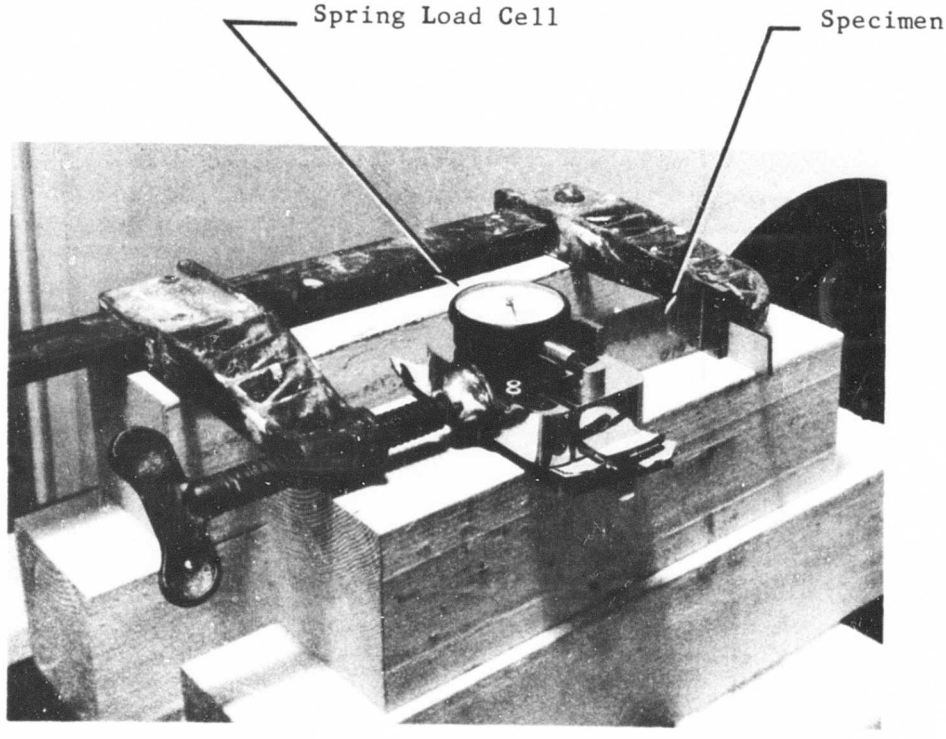

Figure 28. Compressive Loading System for the Single Glass Fiber Specimen (Fiber diameter - 0.010 inch)

MULTIFIBER MODEL

Glass rods 0.275 inch in diameter were assembled in a simulated cylinder consisting of a 19-fiber array and an epoxy resin of the same cycle which was used for the single-fiber specimen.

Figure 29 depicts the glass rods assembled just prior to the surrounding of the rods with resin.

Upon completion of the fabrication of the cylinder, a 1/8-inch-thick slice was cut from this specimen. This is shown in Figure 30 under polarized light (with quarter wave plate in the system).

It can be seen that the specimen shows the stresses in the resin between the rods to be symmetrical in nature.

The resin between a group of three rods within this specimen was selected for analysis (the selection was based upon uniformity of the distance between rods).

Figure 31 shows the magnitude of the difference in principal stresses along a line joining the center of the resin triangle to the interface of one of the glass rods.

A good comparison of these stress magnitudes was obtained with the analysis reported in Reference 2.

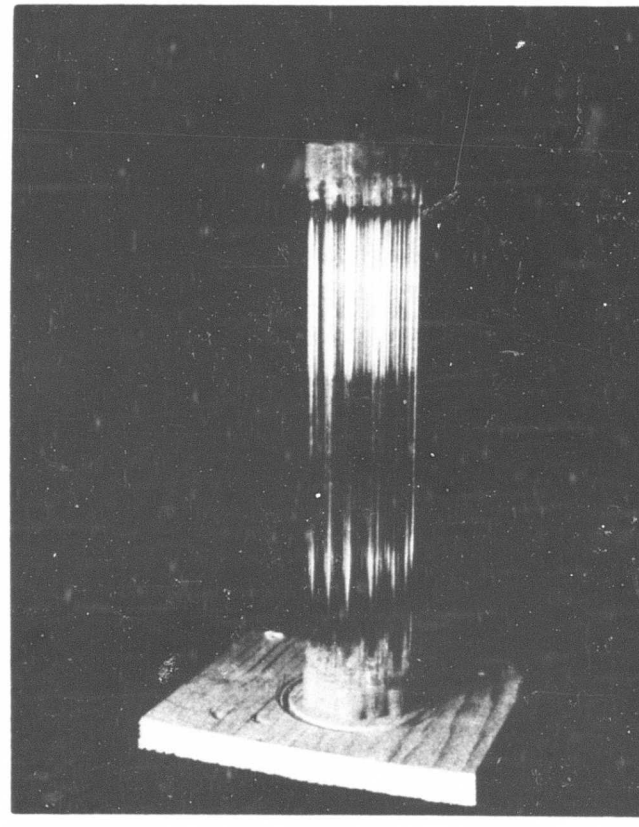

Figure 29. Assembly of Multifiber Glass Rod Specimen prior to Filling with Resin

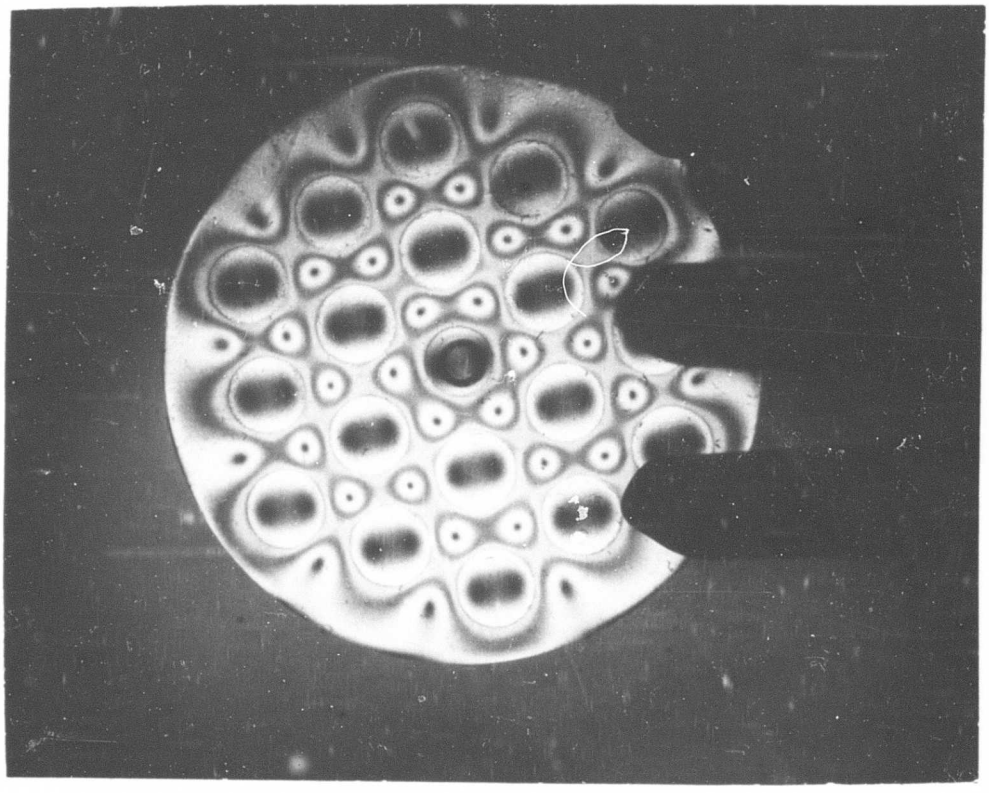

Figure 30. 1/8-inch-Thick Slice of 19-Rod Specimen as Viewed under Direct Polarscope Optic System

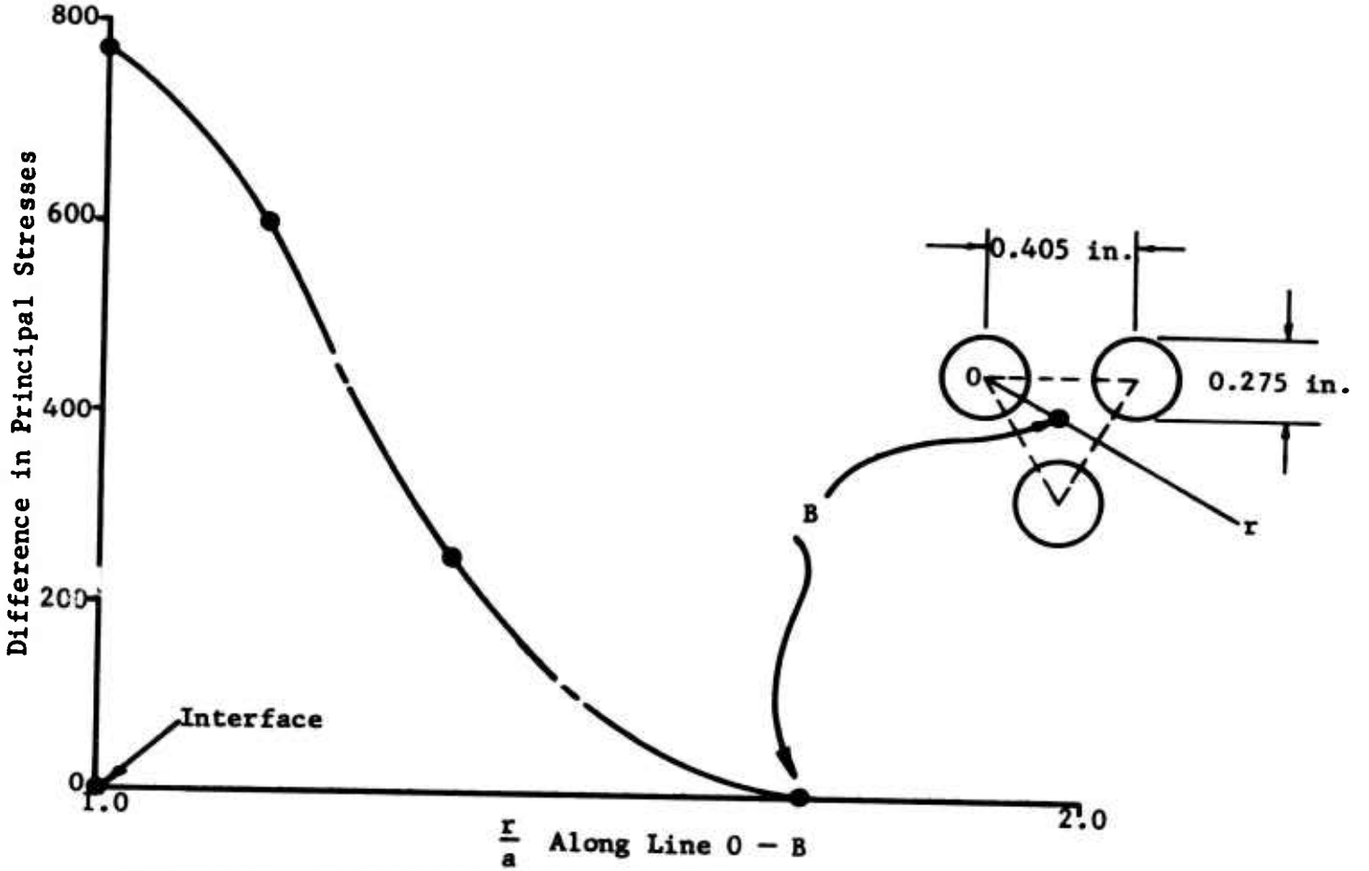

Figure 31. Difference in Principal Stresses Along Line 0 to B versus $\frac{r}{a}$

REFERENCES TO APPENDIX C

1. H. Hetenyi, Handbook of Experimental Stress Analysis, John Wiley & Sons, Inc., p. 688, June 1957

2. I. M. Daniel and A. J. Durelli, "Photoelastic Investigation of Residual Stresses in Glass-Plastic Composites" (paper presented at 16th Annual Meeting of the Society of the Plastics Industry, Inc., Chicago, Illinois, 1962)

BLANK PAGE

Unclassified

Security Classification

DOCUMENT CONTROL DATA - R&D

(Security classification of title, body of abstract and indexing annotation must be entered when the overall report is classified)

1. ORIGINATING ACTIVITY (Corporate author)	2a. REPORT SECURITY CLASSIFICATION
Whittaker Corporation Narmco Research & Development Division San Diego, California	Unclassified
	2b GROUP

3. REPORT TITLE

MICROMECHANICAL BEHAVIOR OF FIBER REINFORCED PLASTICS

4. DESCRIPTIVE NOTES (Type of report and inclusive dates)

Final Report (14 June 1965 through 14 May 1966)

5. AUTHOR(S) (Last name, first name, initial)

Haener, Juan

6. REPORT DATE	7a. TOTAL NO. OF PAGES	7b. NO. OF REFS
September 1966	126	9

8a. CONTRACT OR GRANT NO.	9a. ORIGINATOR'S REPORT NUMBER(S)
DA 44-177-AMC-320(T) b. PROJECT NO. 1P121401A14176 c. d.	USAAVLABS Technical Report 66-62 9b. OTHER REPORT NO(S) (Any other numbers that may be assigned this report)

10. AVAILABILITY/LIMITATION NOTICES

Distribution of this document is unlimited.

11. SUPPLEMENTARY NOTES	12. SPONSORING MILITARY ACTIVITY
	US Army Aviation Materiel Laboratories Fort Eustis, Virginia

13. ABSTRACT

The distribution of stresses in a unidirectionally oriented, multifiber composite as a result of process shrinkage and external loads has been analyzed after assuming continuity boundary conditions at the interface and certain hexagonal boundary conditions in the space between the reinforcements. Selected model specimens have been numerically analyzed by computer, and the results have been compared with photoelastic experimental studies.

DD FORM 1 JAN 64 1473

Unclassified

Security Classification

Unclassified

Security Classification

14. KEY WORDS	LINK A		LINK B		LINK C	
	ROLE	WT	ROLE	WT	ROLE	WT
Three-dimensional stress analysis Multifiber composites Use of potential functions Stress and displacement						

INSTRUCTIONS

1. ORIGINATING ACTIVITY: Enter the name and address of the contractor, subcontractor, grantee, Department of Defense activity or other organization *(corporate author)* issuing the report.

2a. REPORT SECURITY CLASSIFICATION: Enter the overall security classification of the report. Indicate whether "Restricted Data" is included. Marking is to be in accordance with appropriate security regulations.

2b. GROUP: Automatic downgrading is specified in DoD Directive 5200.10 and Armed Forces Industrial Manual. Enter the group number. Also, when applicable, show that optional markings have been used for Group 3 and Group 4 as authorized.

3. REPORT TITLE: Enter the complete report title in all capital letters. Titles in all cases should be unclassified. If a meaningful title cannot be selected without classification, show title classification in all capitals in parenthesis immediately following the title.

4. DESCRIPTIVE NOTES: If appropriate, enter the type of report, e.g., interim, progress, summary, annual, or final. Give the inclusive dates when a specific reporting period is covered.

5. AUTHOR(S): Enter the name(s) of author(s) as shown on or in the report. Enter last name, first name, middle initial. If military, show rank and branch of service. The name of the principal author is an absolute minimum requirement.

6. REPORT DATE: Enter the date of the report as day, month, year; or month, year. If more than one date appears on the report, use date of publication.

7a. TOTAL NUMBER OF PAGES: The total page count should follow normal pagination procedures, i.e., enter the number of pages containing information.

7b. NUMBER OF REFERENCES: Enter the total number of references cited in the report.

8a. CONTRACT OR GRANT NUMBER: If appropriate, enter the applicable number of the contract or grant under which the report was written.

8b, 8c, & 8d. PROJECT NUMBER: Enter the appropriate military department identification, such as project number, subproject number, system numbers, task number, etc.

9a. ORIGINATOR'S REPORT NUMBER(S): Enter the official report number by which the document will be identified and controlled by the originating activity. This number must be unique to this report.

9b. OTHER REPORT NUMBER(S): If the report has been assigned any other report numbers *(either by the originator or by the sponsor)*, also enter this number(s).

10. AVAILABILITY/LIMITATION NOTICES: Enter any limitations on further dissemination of the report, other than those imposed by security classification, using standard statements such as:

(1) "Qualified requesters may obtain copies of this report from DDC."

(2) "Foreign announcement and dissemination of this report by DDC is not authorized."

(3) "U. S. Government agencies may obtain copies of this report directly from DDC. Other qualified DDC users shall request through _____."

(4) "U. S. military agencies may obtain copies of this report directly from DDC. Other qualified users shall request through _____."

(5) "All distribution of this report is controlled. Qualified DDC users shall request through _____."

If the report has been furnished to the Office of Technical Services, Department of Commerce, for sale to the public, indicate this fact and enter the price, if known.

11. SUPPLEMENTARY NOTES: Use for additional explanatory notes.

12. SPONSORING MILITARY ACTIVITY: Enter the name of the departmental project office or laboratory sponsoring *(paying for)* the research and development. Include address.

13. ABSTRACT: Enter an abstract giving a brief and factual summary of the document indicative of the report, even though it may also appear elsewhere in the body of the technical report. If additional space is required, a continuation sheet shall be attached.

It is highly desirable that the abstract of classified reports be unclassified. Each paragraph of the abstract shall end with an indication of the military security classification of the information in the paragraph, represented as *(TS), (S), (C), or (U)*.

There is no limitation on the length of the abstract. However, the suggested length is from 150 to 225 words.

14. KEY WORDS: Key words are technically meaningful terms or short phrases that characterize a report and may be used as index entries for cataloging the report. Key words must be selected so that no security classification is required. Identifiers, such as equipment model designation, trade name, military project code name, geographic location, may be used as key words but will be followed by an indication of technical context. The assignment of links, rules, and weights is optional.